

**Inactivation of Pleiotropic Regulator 1  
reveals p53-dependent Control of Cell  
Proliferation and Apoptosis by the Pso4-  
complex**

Inaugural-Dissertation  
zur  
Erlangung des Doktorgrades  
der Mathematisch-Naturwissenschaftlichen Fakultät  
der Universität zu Köln

vorgelegt von  
André Kleinridders  
aus Krefeld  
Köln 2007

Berichterstatter: Prof. Dr. Jens Brüning  
Prof. Dr. Thomas Langer

Tag der mündlichen Prüfung: 09. Juli 2007

**Für Tina**

**„Darin besteht das Wesen der Wissenschaft. Zuerst denkt man an etwas, das wahr sein könnte. Dann sieht man nach, ob es der Fall ist und im allgemeinen ist es nicht der Fall.“**

Bertrand Russell (1872-1970), brit. Philosoph und Mathematiker, 1950  
Nobelpreis für Literatur



---

## Table of contents

Table of figures .....	IV
List of tables .....	VI
Abbreviations .....	VII
<b>1 Introduction .....</b>	<b>1</b>
1.1 PLRG-1, an evolutionary conserved component of the spliceosome	1
1.2 Regulation of pre-mRNA splicing .....	2
1.3 Role of PLRG-1 in DNA repair .....	6
1.4 DNA damage leads to cell cycle arrest .....	9
1.5 Regulation of apoptosis in DNA damage and repair .....	14
1.6 Involvement of the Bcl-2 family in the regulation of apoptosis .....	16
1.7 Objectives .....	19
<b>2 Materials and Methods .....</b>	<b>20</b>
2.1 Chemicals and antibodies .....	20
2.2 Molecular biology .....	22
2.2.1 Competent <i>E.coli</i> and isolation of plasmid DNA .....	22
2.2.2 Construction of targeting vectors .....	22
2.2.3 TA-cloning .....	24
2.2.4 Generation of gene replacement vectors.....	24
2.2.5 Isolation of genomic DNA .....	24
2.2.6 DNA electrophoresis.....	25
2.2.7 Pulsed-field gel electrophoresis .....	25
2.2.8 DNA sequencing .....	26
2.2.9 Quantification of DNA.....	26
2.2.10 PCR .....	26
2.2.11 RT-PCR and quantitative Real-Time PCR .....	29
2.2.12 DNA hybridization .....	31
2.2.13 Northern Blot and RNA hybridization.....	31
2.3 Cell culture .....	32
2.3.1 Primary embryonic fibroblast (EF) culture .....	32
2.3.2 Embryonic stem (ES) cell culture .....	33
2.3.3 HTN-Cre-mediated deletion <i>in vitro</i> .....	34
2.3.4 Cell cycle analysis .....	34
2.3.5 Cell cycle analysis using fluorescence-activated cell sorter (FACS) analysis.....	34
2.3.6 <sup>3</sup> H-thymidine incorporation .....	35

2.3.7 Analysis of apoptosis .....	35
2.3.8 DNA double-strand breaks after UV-treatment .....	36
2.3.9 Immunofluorescence .....	36
2.3.10 RNA interference (RNAi) .....	37
<b>2.4 Biochemistry .....</b>	<b>37</b>
2.4.1 Protein extraction from tissue.....	37
2.4.2 Protein extraction from cells .....	37
2.4.3 Nuclear and cytoplasmic protein extraction .....	38
2.4.4 Immunoprecipitation .....	38
2.4.5 Western Blot .....	39
2.4.6 Immunohistochemistry .....	40
2.5 Statistical methods .....	40
2.6 Animal Care .....	41
2.6.1 Mouse experiments.....	41
2.6.2 Mice .....	41
<b>3 Results.....</b>	<b>42</b>
3.1 Murine expression pattern of PLRG-1.....	43
3.2 Generation of a conventional PLRG-1 gene replacement vector.....	44
3.3 Analysis of PLRG-1 <sup>Δ/+</sup> mice.....	46
3.4 PLRG-1 <sup>Δ/Δ</sup> mice are embryonic lethal.....	47
3.5 Generation of a conditional PLRG-1 gene replacement vector .....	50
3.6 Inactivation of PLRG-1 in mouse embryonic fibroblasts blocks cell proliferation .....	53
3.7 PLRG-1 deficiency prevents S-phase entry.....	55
3.8 PLRG-1 deficiency increases p53 expression and induces apoptosis .....	57
3.9 No evidence for altered splicing in PLRG1-deficient MEFs .....	60
3.10 PLRG-1-deficient MEFs exhibit no spontaneously detectable DNA double-strand breaks.....	62
3.11 PLRG-1 deficiency results in enhanced γ-H2AX phosphorylation .	63
3.12 Conditional inactivation of PLRG-1 in heart and skeletal muscle ..	64
3.13 Conditional inactivation of PLRG-1 in heart results in dilated cardiomyopathy due to increased cardiomyocyte apoptosis.....	66
3.14 Conditional inactivation of PLRG-1 in the central nervous system of mice results in early postnatal lethality .....	68
3.15 Neuron-restricted PLRG-1 deficiency results in massive neuronal apoptosis.....	69
3.16 Interaction of the nuclear CDC5L-PLRG-1 complex with the p53 phosphatase WIP1 is disrupted in the absence of PLRG-1.....	71
3.17 Rescue of the apoptotic PLRG-1 phenotype by knockdown of p53	73
<b>4 Discussion .....</b>	<b>77</b>

---

4.1 Essential role for PLRG-1 in the development of the preimplantation murine embryo.....	77
4.2 Disruption of other splicing factors and their effects .....	78
4.3 Function of PLRG-1 orthologues .....	79
4.4 PLRG-1 in control of cell cycle and apoptosis.....	80
4.5 Impaired DNA damage repair as a consequence of PLRG-1 deficiency .....	83
4.6 Proposed model for PLRG-1, linking DNA repair, control of cell cycle progression and apoptosis via the Pso4-complex .....	85
<b>5 Summary .....</b>	<b>89</b>
<b>6 Zusammenfassung .....</b>	<b>90</b>
<b>7 Kurzzusammenfassung.....</b>	<b>91</b>
<b>8 References .....</b>	<b>92</b>
<b>9 Acknowledgements .....</b>	<b>115</b>
<b>10 Versicherung .....</b>	<b>116</b>
<b>11 Lebenslauf .....</b>	<b>117</b>

## Table of figures

Figure 1.1: Schematic representaion of splicing reaction.....	5
Figure 1.2: Schematic representation of the Pso4-complex in ICL repair....	8
Figure 1.3: Schematic representation of DNA damage checkpoint pathway.....	9
Figure 1.4: Schematic representation of the G <sub>1</sub> /S checkpoint.....	11
Figure 1.5: Apoptosis signalling in response to p53 activation.....	18
Figure 2.1: Schematic representation of semi-nested PCR method.....	28
Figure 3.1: Ubiquitous expression of PLRG-1.....	43
Figure 3.2: Conventional inactivation of the <i>PLRG-1</i> gene.....	46
Figure 3.3: Analysis of PLRG-1 <sup>Δ/+</sup> offspring.....	47
Figure 3.4: Identification of genotype using semi-nested PCR.....	49
Figure 3.5: Representative morphology of wild type and PLRG-1-deficient embryos at ED1.5.....	50
Figure 3.6: Conditional inactivation of the <i>PLRG-1</i> gene.....	52
Figure 3.7: Verification of PLRG-1 deletion in MEFs upon HTNC treatment.....	53
Figure 3.8: Growth rates and morphology of untreated or Cre-treated wild type and PLRG-1 <sup>flox/flox</sup> MEFs.....	55
Figure 3.9: FACS analysis of serum (FCS)-stimulated cell cycle progression in control and PLRG-1-deficient MEFs.....	56
Figure 3.10: <sup>3</sup> H-thymidine incorporation of wild type and PLRG-1-deficient MEFs.....	57
Figure 3.11: Western blot analysis of HTNC-treated wild type (WT) and PLRG-1 <sup>flox/flox</sup> MEF (KO).....	59
Figure 3.12: TUNEL analysis of wild type and PLRG-1-deficient MEFs.....	60
Figure 3.13: Splicing in PLRG-1-deficient MEFs is unaltered.....	61
Figure 3.14: Pulse-field gel electrophoresis of PLRG-1 <sup>flox/flox</sup> (control) and PLRG-1-deficient MEFs (KO).....	62
Figure 3.15: Analysis of γ-H2AX phosphorylation in untreated and HTNC-treated PLRG-1 <sup>flox/flox</sup> MEFs.....	63
Figure 3.16: Heart-restricted PLRG-1 deficiency in PLRG-1 <sup>□mus</sup> mice.....	65

---

Figure 3.17: Survival rate of control and PLRG-1 <sup>Δmus</sup> mice.....	65
Figure 3.18: Heart-phenotype of PLRG-1 <sup>Δmus</sup> mice.....	66
Figure 3.19: Histological analysis of control- and PLRG-1 <sup>Δmus</sup> -hearts at the age of 24 days.....	67
Figure 3.20: Western blot analysis of control (C) and PLRG-1 <sup>Δmus</sup> -(KO) hearts.....	68
Figure 3.21: Survival rate of control and PLRG-1 <sup>ΔCNS</sup> mice.....	69
Figure 3.22: Analysis of neuron-restricted recombination of the <i>PLRG-1</i> <sup>flox/flox</sup> allele.....	69
Figure 3.23: Immunohistochemical analysis of brains dissected from 3-day-old control and PLRG-1 <sup>ΔCNS</sup> mice.....	70
Figure 3.24: Western blot analysis of control (C) and PLRG-1 <sup>ΔCNS</sup> (KO) hearts.....	71
Figure 3.25: CDC5L and WIP1 fail to form complexes in the nucleus of PLRG-1-deficient MEFs.....	73
Figure 3.26: Rescue of the apoptotic PLRG-1 phenotype by knockdown of p53.....	74
Figure 4.1: Schematic representation of G1/S-phase progression and block.....	81
Figure 4.2: Proposed model for novel integration of pre-mRNA splicing components linking DNA repair, and control of cell cycle progression and apoptosis via CDC5L-PLRG-1 interaction.....	87

## List of tables

<b>Table 2.1: Chemicals.....</b>	<b>20</b>
<b>Table 2.2: Oligonucleotides used for generation of gene replacement vectors and probes for Southern and Northern Blot.....</b>	<b>22</b>
<b>Table 2.3: List of primers used for genotyping.....</b>	<b>28</b>
<b>Table 2.4: List of oligonucleotides used for amplification of cDNA.....</b>	<b>30</b>
<b>Table 2.5: List of probes used for quantitative Real-Time PCR.....</b>	<b>30</b>
<b>Table 2.6: Antibodies used for biochemical studies.....</b>	<b>39</b>
<b>Table 3.1: Genotype analysis of PLRG-1<sup>Δ/+</sup>-intercross offspring based on a semi-nested PCR approach.....</b>	<b>48</b>
<b>Table 3.2: Genotype analysis of mice obtained from breedings of PLRG-1<sup>flox/flox</sup> mice with PLRG-1<sup>flox/+</sup>MCKCre mice.....</b>	<b>64</b>
<b>Table 3.3: Genotype analysis of mice obtained from breedings of PLRG-1<sup>flox/flox</sup> mice with PLRG-1<sup>flox/+</sup>SynCre mice.....</b>	<b>68</b>

---

## Abbreviations

A	adenosine
aa	amino acid
AP	apurine / apyrimidine
BAC	bacterial artificial chromosome
bp	base pairs
BSA	bovine serum albumin
C	control
°C	temperature in degrees celsius
cDNA	complementary DNA
CO <sub>2</sub>	carbondioxide
cps	counts per second
Cre	<u>causes</u> <u>re</u> combination, recombinase from phage P1
C-terminal	carboxy-terminal
d	day/s
DEPC	diethylpyrocarbonate
DNA	desoxyribonucleic acid
dNTP	desoxyribonucleotide-triphosphate
DMEM	Dulbecco's modified Eagle medium
DMSO	Dimethyl sulfoxide
DTT	1,4-Dithio- DL-threitol
<i>E. coli</i>	<i>Escherichia coli</i>
ECL	enhanced chemiluminescence
ED	embryonic day
EDTA	ethylene-diaminetetraacetic acid
EF	embryonic fibroblasts
ES	embryonic stem cells
EtBr	ethidiumbromide
EtOH	ethanol
F	farad
FACS	fluorescence activated cell sorting
FCS	foetal calf serum

## Abbreviations

---

flox	lox P flanked
Flp	site-specific recombinase, product of yeast FLP1-gene
FRT	Flp recombination target
g	gram
G	guanosine
GANC	ganciclovir
G418	geneticin sulfate
h	hour/s
HCl	Hydrogenchlorid
HEPES	N-2-hydroxyethylpiperazine-N'-2-ethanesulfonic acid
HR	Homologous recombinant
HSV-tk	<i>Herpes simplex</i> virus-thymidine kinase
ICL	Interstrand crosslinks
LA	long arm of homology
LIF	leukaemia inhibitory factor
Kb	Kilobase pairs
KCl	potassium chloride
kD/kDa	kilodalton
loxP	recognition sequence for Cre (locus of <u>x</u> -ing over of phage <u>P</u> 1)
M	molar
MCK	Muscle creatinine kinase
MgCl <sub>2</sub>	magnesium chloride
min	minute
ml	milliliter
mM	millimolar
MMC	mitomycin C
µg	microgram
µl	microliter
µM	micromolar
NaCl	sodium chloride
NaF	sodium fluoride
NaOH	sodium hydroxide
Na <sub>3</sub> O <sub>4</sub> V	sodium orthovanadate



neo	neomycin resistance gene
N-terminal	amino-terminal
OD	optical density
OH	hydroxyl
PBS	Phosphate buffered saline
PCR	polymerase chain reaction
PFGE	pulsed-field gel electrophoresis
RNA	ribonucleic acid
rpm	revolutions per minute
RS	arginine/serine rich
RT	room temperature
s	second
SA	short arm of homology
SDS	sodium dodecyl sulfate
ss	single stranded
SSC	sodium chloride/ sodium citrate buffer
SYN	synapsin
T	thymidine
TAE	Tris-acetic acid-EDTA buffer
Taq	polymerase from <i>Thermus aquaticus</i>
TBE	Tris-acetic basic-EDTA buffer
T-DNA	transfer-DNA
TE	Tris-EDTA buffer
Tris	2-amino-2-(hydroxymethyl)-1,3-propandiole
TWEEN	polyoxyethylene-sorbitan-monolaureate
U	unit
UV	ultraviolet
V	volt
WT	wild type
Y	pyrimidine
5′	five prime end of DNA sequences
3′	three prime end of DNA sequences
Δ	knockout/PLRG-1-deleted allele



# 1 Introduction

## 1.1 PLRG-1, an evolutionary conserved component of the spliceosome

Mammalian Pleiotropic Regulator (PLRG-) 1 is an essential component of the spliceosome. PLRG-1 belongs to a highly conserved family of seven WD40 domain containing proteins in eukaryotes (Ajuh et al., 2000; Ajuh et al., 2001). Founding members of this WD40-repeat protein family, PRL1 and PRL2, were first identified by T-DNA tagging in *Arabidopsis thaliana* (Nemeth et al., 1998). Mutation of *Arabidopsis PRL1* confers hypersensitivity to glucose, sucrose and several plant hormones and results in transcriptional derepression of glucose and stress responsive genes (Nemeth et al., 1998). Whereas in plants the *PRL* genes are uniquely duplicated, in yeast, *C. elegans* and mammals there are only single orthologues of the Pleiotropic Regulator family which play important roles in the control of cellular homeostasis. siRNA-mediated knock-down of PLRG-1 (D1054.15) in *C. elegans* results in early embryonic lethality, whereas mutation of the yeast homologue YPL151c (Prp46) arrests cell proliferation causing a dual block in G<sub>1</sub>/S- and M-phase progression (Albers et al., 2003; Sonnichsen et al., 2005). Despite genetic studies of mutations, the exact regulatory function of PLRG-1 orthologues and the molecular mechanisms by which they integrate splicing and control cell proliferation so far remain elusive.

Human PLRG-1 has been initially identified as a subunit of spliceosomal complexes purified from HeLa nuclear extracts by coimmunoprecipitation with CDC5L (Ajuh et al., 2000). Later, it was observed that interaction between PLRG-1 and CDC5L is essential for pre-mRNA processing as peptides inhibiting complex formation of CDC5L with PLRG-1 efficiently block pre-mRNA splicing (Ajuh and Lamond, 2003). These studies also revealed that other proteins not directly implicated in regulation of pre-mRNA splicing, such as the cell cycle phosphatase PPM1D/WIP1, PP1- $\alpha$  and the DNA-dependent kinase (DDK)- $\alpha$  co-purified with the PLRG-1 containing CDC5L complex (Ajuh et al., 2000). These components also play a role in cell cycle regulation, apoptosis

and genome integrity. WIP1, a serine/threonine phosphatase, is a member of the PP2C family and was shown to be a negative regulator of p53 (Fiscella et al., 1997; Lu et al., 2004; Takekawa et al., 2000). PP1- $\alpha$  another serine/threonine phosphatase, plays an important role in the control of cell cycle progression and apoptosis by interacting with retinoblastoma protein (Liu et al., 1999) The other complex component, DNA-dependent kinase DDK- $\alpha$ , a serine/threonine kinase, is activated by DNA association and plays a role in processes such as DNA double-strand break repair, telomere maintenance and gene transcription (Boulton and Jackson, 1996; Boulton and Jackson, 1998; Smith and Jackson, 1999; Taccioli et al., 1998).

Recently, the CDC5L-PLRG-1 complex was demonstrated to interact with the WRN protein, which is deficient in Werner syndrome and required for processing of DNA interstrand crosslinks (Zhang et al., 2005). In addition to pre-mRNA splicing, the CDC5L-PLRG-1 complex is thus possibly involved in DNA repair. Another known component of the nuclear CDC5L-PLRG-1 complex is the mammalian homologue Pso4/PRP19, which is essential both for pre-mRNA-splicing and UV-radiation mediated crosslink repair (Mahajan and Mitchell, 2003). These findings strongly suggest that the Pso4-CDC5L-PLRG-1 complex integrates pre-mRNA splicing and DNA-repair.

### **1.2 Regulation of pre-mRNA splicing**

Most genes in eukaryotes are interrupted several times by intervening sequences, known as introns, which are transcribed into primary messenger RNA transcripts (pre-mRNA). For functional translation, these non-coding sequences have to be precisely excised, generating functional mRNAs. This task is performed by a ribonucleoprotein complex, called spliceosome. This complex consists of five small nuclear ribonucleoprotein (SnRNP) complexes U1, U2, U4, U5 and U6 and about 300 other non-snRNP proteins (Rappsilber et al., 2002; Zhou et al., 2002). The spliceosome orchestrates the precise excision of introns by several RNA-RNA, RNA-protein and protein-protein interactions. A key feature of correct splicing is the presence of a conserved 5' and 3' splice

site, a branch point region usually 20-40 nucleotides upstream of the 3' splice site and a polypyrimidine tract in the intron (Reed 1989; Smith et al., 1989; Stephens and Schneider 1992).

For many years it was thought that the spliceosome assembles in a stepwise manner. First, U1 snRNP binds to the 5' splice site, while the serine/arginine (SR) protein U2AF<sup>65</sup> binds the polypyrimidine tract and another SR protein U2AF<sup>35</sup> binds the 3' splice site (Merendino et al., 1999; Wu et al., 1999; Zamore et al., 1992; Zorio and Blumenthal, 1999). This RNA-protein complex is known as the E-complex (Michaud and Reed, 1991). Then, U2 snRNP binds weakly to the pre-mRNA using the integral associated U2 snRNP protein SF3b (Hastings and Krainer, 2001). Next, U2 snRNP binds to the branchpoint region forming the A-complex, a process dependent on ATP (Furmen and Glitz, 1995; Kramer, 1996). Subsequently, the U4/U6/U5 tri-snRNP complex adheres to the 5' splice site by interacting with Prp8 and the pre-mRNA in the presence of ATP, thereby generating the B-complex (Brown and Beggs, 1992; Umen and Guthrie, 1995; Umen and Guthrie, 1995). Exclusion of U1 and U4 snRNP leads to the active C-complex, which catalyzes the excision of introns (Fig. 1.1) (Jurica et al., 2004; Yean and Liu, 1991).

Recent findings suggest, that the spliceosome is partly preassembled (Nilsen 2002; Stevens et al., 2003). Upon complete assembly, the spliceosome undergoes dramatic conformational changes involving both its RNA and proteins prior to catalysis. These rearrangements result in the exclusion of two snRNPs, U1 and U4, and inclusion of new proteins, responsible for correct splicing reactions (Makarov et al., 2002; Staley and Guthrie, 1998) leading to the active complex.

The splicing reaction occurs in two steps by transesterification. First, the 2'OH group of the branchpoint adenosine performs a nucleophilic attack at the 5' splice site, destroying the phosphodiesterbond and thereby generating a 2'5'phosphodiester link (lariat structure in intron) between the adenosine of the branchpoint sequence and the 5' terminal intronic nucleotide. Second, the free 3'OH group of the 5' exon performs a nucleophilic attack at the 3' splice junction, thereby generating a new phosphodiesterbond between the 5' and 3' exon resulting in excision of the intronic sequence (Pasman and Garcia-Blanco, 2001).

PLRG-1 and CDC5L have both been shown to be involved in splicing reactions. These nuclear proteins are components of a large complex containing other splicing factors (Ajuh et al., 2000; Burns et al., 1999; Chen et al., 1999; McDonald et al., 1999; Neubauer et al., 1998). This conserved subspliceosomal complex is known as NTC (nineteen complex) in yeast and Prp19/CDC5L complex (Pso4-complex) in mammals (Ajuh et al., 2000; Makarova et al., 2002). Depletion of this complex leads to a block in splicing before the first transesterification step in splicing and lariat formation of the pre-mRNA (Makarova et al., 2002).

Although it was shown that both proteins are essential for splicing *per se* (Ajuh et al., 2001), mutation of CDC5L in yeast yielded in a G<sub>2</sub>/M block in part due to incorrect splicing of TUB1  $\alpha$ -tubulin gene (Burns et al., 2002). Mutation of Prp46p (PLRG-1 in mammals) in yeast also results in a G<sub>2</sub>/M block (Albers et al., 2003). These findings indicate that not only splicing factors are required for correct pre-mRNA splicing, but in addition they play an important role in cell cycle regulation.

Recent findings showed that the SR protein SF2/ASF is a proto-oncogene. Overexpression of SF2/ASF *in vitro* resulted in immortal rodent fibroblasts. In addition, SF2/ASF is upregulated in many tumors and knockdown of this SR protein inhibits tumor growth (Karni et al., 2007). Furthermore, it was shown that nuclear protein phosphatases, such as PP2C $\gamma$ , PP1, PP2A or WIP1, are components in spliceosomal assembly and catalysis (Fig 1.1) (Moorhead et al., 2007). These proteins also play functional roles in chromosome condensation (Trinkle-Mulcahy and Lamond, 2006; Vagnarelli et al., 2006), chromatid cohesion (Kitajima et al., 2006), TGF $\beta$  signalling (Duan et al., 2006; Knockaert et al., 2006; Lin et al., 2006) or in posttranslational control of p53 (Lu et al., 2005).

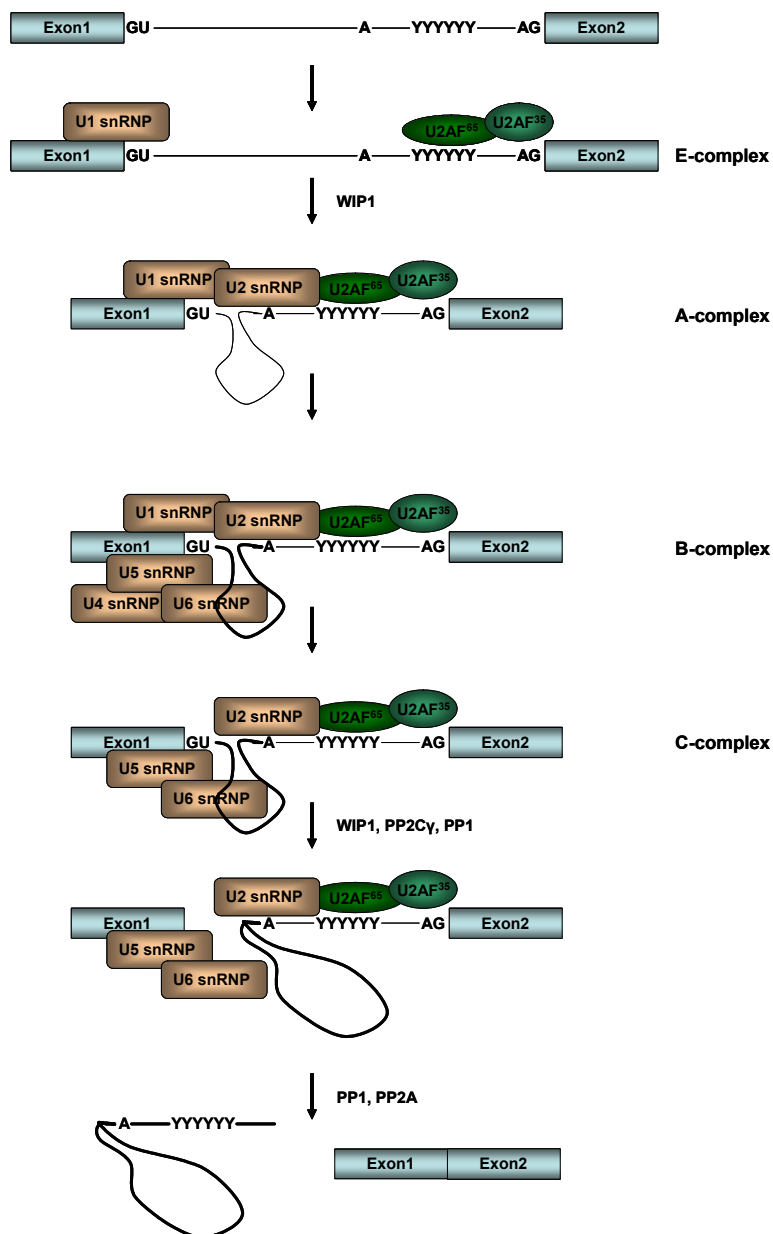


**Figure 1.1: Schematic representation of splicing reaction**

Nuclear protein phosphatases, which are involved in spliceosomal assembly and catalysis are depicted next to arrows. A represents the adenosine in the branchpoint region, YYYYYY the polypyrimidine tract, GU the 5' splice site and AG the 3' splice site. This scheme was composed based on information from: Hastings et al., 2001; Moorhead et al., 2007

In summary, splicing factors assembled in the spliceosome are not only required for correct pre-mRNA splicing. They also play important roles in other pathways, such as cell cycle progression, cytokine signalling or DNA damage response.

### 1.3 Role of PLRG-1 in DNA repair

DNA damage is a common cellular event that, if persistent, can lead to mutations, cancer, cell death or even the death of an entire organism. Several cellular responses enable the cell to either eliminate or to cope and survive with the damage or to activate programmed cell death, called apoptosis. These cellular responses include the removal of DNA damage, through repair and restoration of the integrity of the genome, activation of DNA damage checkpoints, leading to cell cycle arrest until damage is restored, transcriptional responses, which change the cellular profile, and apoptosis, when damage is not reparable and cells are severely dysregulated.

The term “DNA damage” comprises genome mutations, as for example in Down syndrome, and chromosomal mutations, such as translocation, deletion, insertion and inversion. Gene mutations are generated spontaneously or by external influences, such as ultraviolet (UV) radiation, inducing reactive oxygen species or leading to DNA base damages, here pyrimidine dimers or photoadducts. Other DNA damages are DNA backbone damages, including abasic sites and DNA single- and double-strand breaks. Abasic sites can develop spontaneously, due to base excision repair or formation of unstable base adducts (Memisoglu and Samson, 1998; Mol et al., 1999; Wilson, 1998). DNA single-strand breaks are caused by DNA damaging agents or as intermediates in nucleotide excision repair (Sancar 1996; Wood, 1997). DNA double-strand breaks are natural intermediates in recombination, but can also be generated by damaging agents, like ionizing radiation (Bonura et al., 1993; Natarajan et al., 1993; Priebe et al., 1994). Other agents, like mytomycin C or cisplatin, lead to interstrand or protein-DNA crosslinks (Jones and Yeung, 1990; Matsumoto et al., 1989; Stevnsner et al., 1993).

The cell relies on various DNA repair mechanisms that are activated in response to DNA damage, including direct repair, base excision repair, nucleotide excision repair, DNA double-strand break repair and repair of interstrand crosslinks.

Direct repair reverses photoadducts resulting from UV-irradiation by photolyases or O<sup>6</sup>-alkyl guanine appearance in DNA by transfer of the alkyl



group from the DNA to a cysteine in O<sup>6</sup>-alkylguanine-DNA alkyltransferase (Baer and Sancar, 1989; Gerson et al., 1987).

Base excision repair removes a damaged base by generating an apurin or apyrimidine (AP) site and subsequently filling the gap with an undamaged base. Alternatively, a long-patch pathway is used, where a complex consisting of RFC/PCNA-Pol  $\delta/\epsilon$  enables repair synthesis and nick translation, displacing several nucleotides (Frosina et al., 1996). The flap structure is then cleaved and the long-patch repair is ligated. Nucleotide excision repair is the major pathway for removing bulky adducts and uses a multiprotein complex to resolve DNA damage (Aboussekhra et al., 1995; Evans et al., 1997).

DNA double-strand breaks are repaired either by homologous recombination or nonhomologous end-joining (Takata et al., 1998). The advantage of homologous recombination is the full restoration of the lesion, without losing information, except in cases where the two duplexes are not exactly homologous and gene conversion may take place.

Nonhomologous end-joining is essential for V(D)J recombination and is thought to be the major pathway for DNA double-strand break repair induced by ionizing radiation (DiBiase et al., 2000; Grawunder et al., 1998; Wang et al., 2001). Crosslinks induce DNA double-strand breaks during replication both *in vivo* and *in vitro*, presumably due to replication fork collapse and nuclease attack (Bessho, 2003; McHugh et al., 2000; Rothfuss and Grompe, 2004). The major error free pathway involves incision of the crosslinked DNA by the nucleotide excision repair enzymes, followed by gap filling via recombination and involvement of RecA protein (Cole, 1973; Sladek et al., 1989). Another error-prone pathway involved in ICL repair, consists of the NER pathway, subsequently followed by DNA polymerase II-dependent DNA synthesis (Berardini et al., 1999; Jachymczyk et al., 1981).

The mismatch repair factor mutS $\beta$  recognizes the ICL by stimulation of PCNA. Subsequently, the WRN protein, RPA and the Pso4-complex are recruited to the point of DNA damage by an unknown mechanism (Zhang et al., 2005). This complex then unwinds the double-stranded DNA, forming single strands near to the interstrand crosslink. The unwound DNA represents a landmark for asymmetrical incisions that release the interstrand crosslink from one strand leading to a gap in the DNA. The heterodimer of the Ercc1 and Xpf

endonucleases produces the incision on both sides of the ICL (Kuraoka et al., 2000). The resulting gap is repaired by either translesion bypass or homologous recombination (Berardini et al., 1997; Berardini et al., 1999 McHugh et al., 2000;) (Fig. 1.2). The gap filling takes place in the following S-phase, where homologous recombination occurs, showing that replication and cell cycle progression are crucial for repairing ICL in mammals (Akkari et al., 2000).

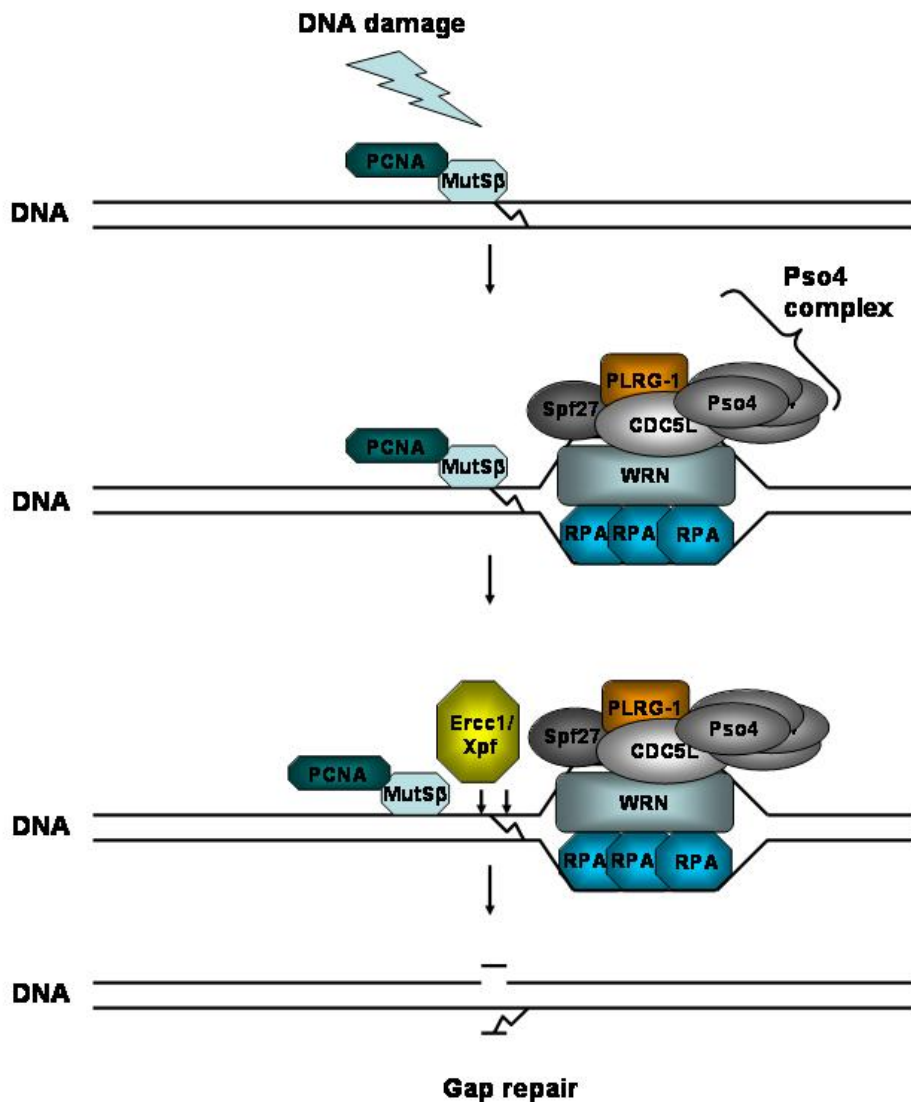


**Figure 1.2: Schematic representation of the Pso4-complex in ICL repair**

ICL is represented by the connection of the complementary DNA strands. The Pso4 complex consists of tetrameric Pso4, also known as Prp19, CDC5L, PLRG-1 and Spf27. This scheme was composed based on information from: Ohi et al., 2005 and Zhang et al., 2005

However, until now, it is not clear, whether DNA repair proteins participate directly in DNA damage checkpoint responses.

#### 1.4 DNA damage leads to cell cycle arrest

The G<sub>1</sub>/S, intra-S and G<sub>2</sub>/M DNA damage checkpoints are responsible for the delay or arrest of cell cycle progression in response to DNA damage. A common feature of these checkpoints is their signal transduction pathway (Fig. 1.3).

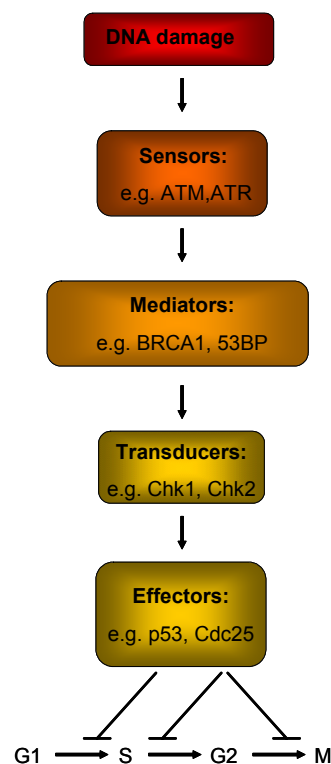


**Figure 1.3: Schematic representation of DNA damage checkpoint pathway**

Components of human DNA damage checkpoint protein are depicted here. DNA damage is detected by sensors, which activate with or without the help of mediators, transducers and effectors. The effectors themselves inhibit cell cycle progression until DNA damage is repaired or lead to apoptosis (for p53). Adapted from Sancar et al. 2004

However, the functions of different components of the DNA damage checkpoint pathway are not rigidly defined, as for example the protein *ataxia telangiectesia mutated* (ATM) can act as a sensor and as a signal transducer (Sancar et al., 2004).

DNA damage is recognized by two groups of proteins: the two phosphoinositide 3-kinase-like kinase (PIKK) family members ATM and ATR and the RFC/PCNA (clamp loader/polymerase clamp)-related Rad17-RFC/9-1-1 complex. ATM and ATR are serine/threonine kinases, whose activation leads to phosphorylation of proteins, such as Chk1, Chk2,

BRCA1 or p53 (Emili, 1998; Gardner et al., 1999; Sanchez et al., 1999; Vialard et al., 1998; Walworth et al., 1993). ATM is activated by DNA double-strand breaks, whereas ATR seems to be more important for DNA damage checkpoint response caused by UV irradiation or stalled replication forks (Guo et al., 2000; Liu et al., 2000; Matsuoka et al., 1998). Mediators like BRCA1 or 53 BP1 link the DNA damage sensors ATM, ATR with the transducers Chk1 and Chk2 (Schultz et al., 2000; Soulier and Lowndes, 1999; Sun et al., 1998; Wang et al., 2002). This signal cascade is required for correct DNA damage checkpoint response leading to a block in cell cycle transition. In mammals, DNA double-strand breaks are sensed by ATM transducing its signal to Chk2, whereas ATR activates Chk1 after UV irradiation (Hirao et al., 2000; Matsuoka et al., 2000; Zhao and Piwnica-Worms, 2001). ATM and ATR phosphorylate p53 at serine 15 leading to its stabilization and activation (Banin et al., 1998; Canman et al., 1998; Lakin et al., 1999). Chk1 and 2 themselves phosphorylate p53 and Cdc25 leading to a G<sub>1</sub>/S phase block (Lin et al., 1992; Mailand et al., 2000; Melchionna et al., 2000; Sanchez et al., 1997; Shieh et al., 2000; Zhao et al., 2002). Phosphorylation of Cdc25 results in binding to the 14-3-3 $\delta$  protein excluding Cdc25 from the nucleus and targeting it for degradation by the 26S proteasome (Mailand et al., 2000, Peng et al., 1997). Loss of nuclear Cdc25 results in Cdk2/CyclinE phosphorylation by Wee1 and Myt1 kinases leading to its inactivation (Coulonval et al., 2003; Mailand et al., 2000). This inactive complex is not able to activate Cdc45, thereby inhibiting replication initiation (Costanzo et al., 2003) (Fig. 1.4).

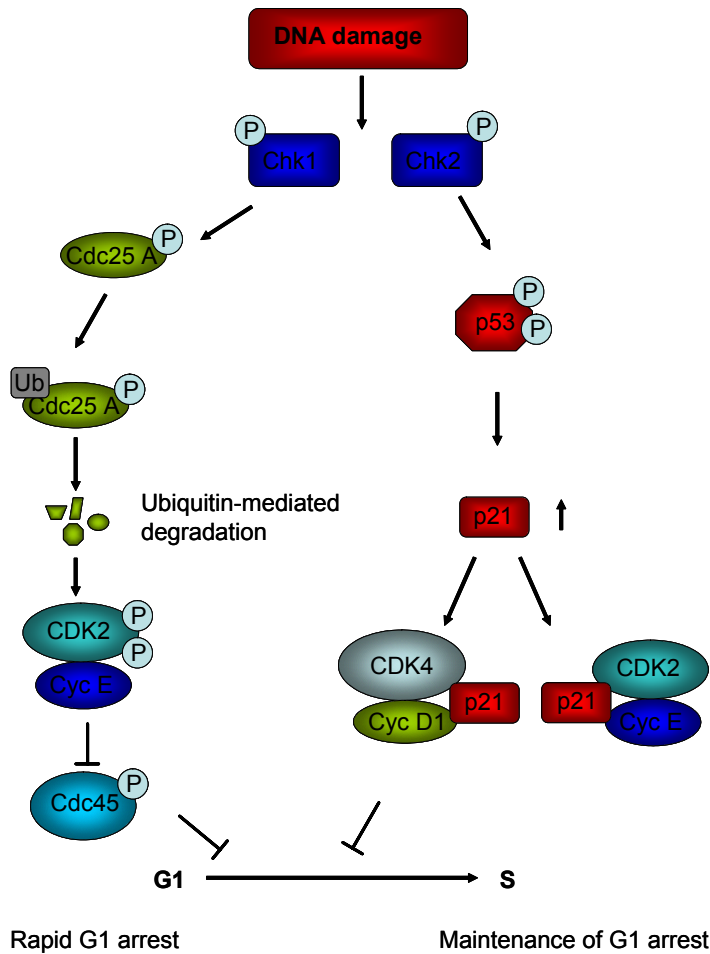


**Figure 1.4: Schematic representation of the G<sub>1</sub>/S checkpoint**

Due to DNA damage, Chk1 and 2 are phosphorylated and activated, leading to Cdc25A and p53 phosphorylation, respectively. On the one hand, Cdc25A phosphorylation leads to its nuclear exclusion and degradation, enabling the phosphorylation and inactivation of CDK2/Cyc E complex by Wee1 and Myt1 kinases. As a result, Cdc45 is not phosphorylated, blocking replication initiation. On the other hand phosphorylation of p53 stabilizes itself and enhances p21 expression, a CDK inhibitor. p21 binds and inhibits CDK4/Cyc D1 complex leading to hypophosphorylation of retinoblastoma protein (Rb, not shown). Rb binds and inhibits E2F, blocking transcription of genes responsible for G<sub>1</sub>/S-phase progression. Adapted from Sancar et al. 2004

The tumour suppressor p53 acts as a major player in a broad range of cellular stress responses. The functional signal transduction circuit of p53 consists of upstream mediators involving DNA damage, hypoxia, nucleotide depletion, aberrant growth signals, and chemotherapeutic drugs (Levine, 1997), whereas the regulatory circuit consists of p53 itself, Mdm2, p14<sup>Arf</sup> (in mouse p19<sup>Arf</sup>) and E2F-1, and downstream effectors including genes responsible for cell cycle arrest, such as p21 (el-Diary et al., 1994), inhibition of angiogenesis and metastasis (Kelly-Spratt et al., 2004; Zhang et al., 2000), apoptosis and DNA repair (Ford et al., 1997; Miyashita et al., 1995).

Two regulatory loops are essential for maintaining cellular p53 levels. On the one hand, Mdm2 forms a feedback loop with p53, in which p53 positively regulates Mdm2 by activating its transcription. Mdm2, in turn, negatively regulates p53 by promoting p53 ubiquitination and degradation (Honda et al.,

1997). On the other hand, E2F-1 activates p14<sup>Arf</sup> transcription, whereas p14<sup>Arf</sup> facilitates proteolytic degradation of E2F-1 (Mason et al., 2002). These loops are interconnected by p53 and p14<sup>Arf</sup>. p53 inhibits the transcription of p14<sup>Arf</sup>, whereas the latter p14<sup>Arf</sup> interacts with Mdm2, thereby inhibiting ubiquitination and degradation of p53. In turn, p53 inhibits the transcription of p14<sup>Arf</sup>. (Sancar et al., 2004)

In response to DNA damage, upstream activators of p53, such as ATM, ATR, Chk1 and Chk2 are activated, leading to phosphorylation of p53 and/or Mdm2 (Banin et al., 1998; Shieh et al., 2000). Phosphorylation of these proteins activates p53 through three distinct mechanisms: first by stabilizing p53 by disrupting the binding of Mdm2 to p53; second by enhancing p53 transactivation activity and third by promoting p53 shuttling into the nucleus (Jabbur et al., 2000; Sakaguchi et al., 1997; Unger et al., 1999; Zhang and Xions, 2001). Activated p53 itself activates or represses target genes (e.g. Mdm2) or interacts with other coactivator or transcription factors, such as CBP and Ets1, thereby activating or repressing the transcription of target genes (Alarcon et al., 1999; Lambert et al., 1998; Xu et al., 2002). In addition, p53 promotes apoptosis by activating pro-apoptotic genes, such as Bax, Bad or Apaf-1 (Jiang et al., 2006; Miyashtia et al., 1994; Moroni et al., 2001).

Another target of p53 is the serine/threonine phosphatase WIP1, which dephosphorylates and destabilizes p53 (Lu et al., 2005). WIP1 was found to attenuate UV-induced phosphorylation of p53 at Ser 46 by inactivating p38MAPK and thereby inhibiting apoptosis (Takekawa et al., 2000). Interestingly, over-expression of WIP1 is found in many tumours, including breast cancer (Bernards, 2004).

The intra-S-phase checkpoint is activated by DNA damage or stalled replication machinery occurring in the S-phase leading to a block in DNA replication. This checkpoint requires a large set of checkpoint proteins, such as ATM, the M/R/N complex, MDC1 and BRCA1 (Howlett et al., 2002; Mirzoeva and Petrini, 2001; Scully et al., 1997; Stewart et al., 2003). Due to spontaneous occurrence of DNA double-strand breaks, ATM, ATR and DNA-PK phosphorylate the histone variant H2AX at serine residue 139 (Burma et al., 2001; Park et al., 2003; Ward and Chen, 2001). The phosphorylated H2AX, called  $\gamma$ -H2AX, binds to MDC1, thereby establishing a large zone of modified

chromatin surrounding the DNA double-strand break (Goldberg et al., 2003). The interaction of both proteins enables the recruitment of other factors, such as Nbs1, Rad51 or BRCA1 to the DNA lesion leading to DNA damage repair (Lou et al., 2003; Stewart et al., 2003). These supramolecular structures at DNA double-strand breaks are termed 'foci'.

Similar to the G<sub>1</sub>/S checkpoint, an ATM-regulated pathway is responsible for Cdc25A regulation (Xiao et al., 2003). A second pathway depends on the phosphorylation of SMC1 by ATM resulting in DNA synthesis inhibition (Kim et al., 2002; Yazdi et al., 2002).

Activation of the G<sub>2</sub>/M checkpoint prevents cells progressing into mitosis, a process triggered by p53-mediated regulation of the Cyclin-dependent kinase Cdc2 (Winters et al., 1998). Cdc2 is activated through phosphorylation at threonine 161 by the CDK-activating kinase (CAK) and is bound to Cyclin B (Gu et al., 1992; Larochelle et al., 2007). During the G<sub>2</sub> phase, the Cdc2/Cyclin B complex is inactive when Cdc2 is phosphorylated on tyrosine 15 and threonine 14 by the protein kinases Wee1 and Myt1, respectively (Den Haese et al., 1995; Fattaey and Booker, 1997; Mueller et al., 1995). At the transition of G<sub>2</sub> into M phase, the phosphatase Cdc25 dephosphorylates Cdc2 (Lammer et al., 1998). In turn, the Cdc2/Cyclin B complex phosphorylates and further activates Cdc25, initiating a positive feedback loop (Hoffmann et al., 1993; Margolis et al., 2006). Activated Cdc2/Cyclin B complex leads to progression into mitosis (Li et al., 1997). p53 binds and inhibits CAK *in vitro*, thereby preventing the activation of Cdc2 at threonine 161 (Schneider et al., 1998).

The CDK inhibitor p21 inhibits CDK activity by binding directly to CDK/Cyclin complexes leading to a G<sub>2</sub>/M arrest (Dulic et al., 1998; Medema et al., 1998). Also, it interferes with the activating phosphorylation of Cdc2 by CAK, thus preventing phosphorylation at threonine 161 (Mandal et al., 1998). Another mechanism involving CDK2-mediated Cdc2 inhibition was shown in *Xenopus*. There, p21 inhibits CDK2 causing loss of Cdc2 activity (Guadagno and Newport, 1996).

Additionally, the p53 target gene *Gadd45* is able to dissociate the Cdc2/Cyclin B1 complex by binding to Cdc2 with its N-terminal part (Zhan et al., 1999).

Another mechanism for the G<sub>2</sub>/M arrest is the regulation of the subcellular localization of Cdc2. The p53 target gene *14-3-3δ* is responsible for nuclear exclusion of Cdc2 (Chan et al., 1999). It binds directly to the Cdc2/Cyclin B1 complex and sequesters it to the cytoplasm.

Furthermore, p53 induces transcription of target genes, such as *reprimin* (Ohki et al., 2000), *B99* (Utrera et al., 1998) and *MCG10* (Zhu and Chen 2000). All three proteins contribute to an arrest of cells in G<sub>2</sub> phase, but the precise mechanisms of the specific cell cycle arrest are still unknown.

Repression of topoisomerase II is another mechanism for the G<sub>2</sub>/M arrest by p53 (Sandri et al., 1996; Wang et al., 1997). During the G<sub>2</sub>/M transition, topoisomerase II is responsible for creating higher order compaction of chromatin and inhibition blocks cells in G<sub>2</sub>/M progression (Anderson and Roberge, 1996).

When cell cycle progression is impaired due to unreparable DNA damage, the cell induces programmed cell death.

### **1.5 Regulation of apoptosis in DNA damage and repair**

Programmed cell death, called apoptosis, is a crucial and conserved pathway in multicellular organisms (Kerr et al., 1972). The genetically programmed cell death ensures the proper elimination of dysregulated cells and maintains tissue homeostasis. Important roles for apoptosis in many diseases have been revealed in recent years. Lack of apoptosis may result in cancer, while excessive cell death leads to neurodegeneration (Landesman-Bollag et al., 1998; Zuscik et al., 2000). In contrast to necrosis, apoptosis requires energy, concerted action of a cascade of genes and does not lead to inflammation (Fadok et al., 1992; Shiraishi et al., 2001; Slee et al., 1999). Apoptotic cells shrink and condense, the cytoskeleton collapses, the nuclear envelope disassembles and the DNA is fragmented. Furthermore, apoptotic cells are characterized by cell membrane blebbing and phosphatidylserine exposure allowing macrophages to phagocytose them (Fadok et al., 1992).



The tight control of this pathway is essential for every metazoan, because dysregulated apoptosis results in the death of the organism. In mammalian cells, apoptosis is mediated by extrinsic (death-receptor-mediated) and intrinsic (mitochondria-mediated) signaling pathways (Du et al., 2000; Li et al., 2001; Liu et al., 1996; Scaffidi et al., 1998; Susin et al., 1999; Verhagen et al., 2000). However, damage or stress in many organelles such as nucleus or ER (besides mitochondria) may trigger apoptosis (Kaufman et al., 1999; Li et al., 2006; Patil and Walter, 2001; Rich et al., 2000; Zhou et al., 2001). These pathways converge onto a family of proteases, the caspases. Activation of caspase-family proteases is at the core of apoptotic cell death, representing a common point of intersection (Nunez et al., 1998). Common to these proteases is their expression as zymogens that possess a cysteine in their active site, which is responsible for cleaving their substrates after aspartate residues (Alnemri 1997). Caspases that participate in apoptosis can be divided into two major classes, the upstream `initiator` caspases group, consisting of caspases 2, 8, 9, 10 and 12 and the downstream `executor` caspases group including caspases 3, 6 and 7. Caspases collaborate in proteolytic cascades, whereas the activation of the caspases is dependent on the ability of certain procaspases to oligomerize and autoactivate themselves (Srinivasula et al., 1998; Van de Craen et al., 1999).

Procaspases either assemble at the plasma membrane (caspase 8) or reside in aggregates in the cytoplasm (caspase 9) (Fan et al., 2005). In the first case, binding of either FasL or TNF $\alpha$  to their respective `death` receptors leads to recruitment of procaspase 8 (initiator caspase) in the vicinity of the receptor through interaction with the adaptor molecule Fas-associated death domain (FADD). This results in formation of a `death-inducing signal complex` (DISC) and results in the dimerization and autoactivation of procaspase 8 (Kischkel et al., 1995; Medema et al., 1997). In turn, the active caspase 8 leads to activation of executor caspases such as caspase 3 (Woo et al., 1998). The mitochondria-mediated pathway for apoptosis is activated by a myriad stimuli, including growth factor deprivation, oxidant, DNA-damaging agents and others (Aoki et al., 1997; Cook et al., 1999; Lee et al., 2000; Madeo et al., 1999; Maroto and Perez-Polo, 1997; Sanz et al., 2000; Zhan et al., 1994; Zhan et al., 1999).

In the mitochondria-mediated pathway, procaspase 9 (initiator caspase) is recruited to a protein complex called the `apoptosome`, which consists of several Apaf-1 molecules. Oligomerization of Apaf-1 is induced by cytochrome c, that is released from the mitochondria (Srinivasula et al., 1998). The following recruitment of procaspase 9 leads to its activation (Srinivasula et al., 1998). This in turn cleaves and activates procaspase 3 (Li et al., 1997). Active caspase 3 will cleave specific vital substrates, such as poly (ADP-ribose) polymerase (PARP), PAK, certain isoforms of PKC and ICAD, resulting in the complete destruction of the cell associated with a typical DNA degradation pattern (`ladder pattern`) (Frutos et al., 1999; Sakahira et al., 1998 Tewari et al., 1995; Walter et al., 1998) .

Mitochondria can also participate in cell death pathways induced via TNF-family `death receptors`, through cross-talk mechanisms involving proteins, such as Bid, a pro-apoptotic member of the Bcl-2-family (Grinberg et al., 2005). In addition, caspase 8 cleaves and activates proteins from the Bcl-2 family, such as Bid, which catalyzes the permeabilization of the outer mitochondrial membrane, thus releasing cytochrome c and thereby facilitating the formation of the apoptosome (Kim et al., 2000; Korsmeyer et al., 2000 Li et al., 1998).

However, mitochondrial and death receptor pathway for caspase activation are fully capable of independent operation in most types of cells (Fulda et al., 2001).

### **1.6 Involvement of the Bcl-2 family in the regulation of apoptosis**

Apoptosis and caspase activation can be modulated by members of the Bcl-2 family. This protein family consists of anti- and pro-apoptotic members, which have the ability to prevent or force cells into undergoing apoptosis, through the modulation of mitochondrial release of cytochrome c and other apoptogenic proteins from this organelle (Liu et al., 1996; Scarlett and Murphy, 1997, Susin et al., 1999). It has been shown that the relative amounts of pro- and anti-apoptotic proteins determines the susceptibility of the cell to undergo

apoptosis (Oltvai et al., 1993; Wada et al., 1998). Members of the Bcl-2 family proteins are capable of physically interacting, forming homo- and heterodimers, and function as agonists or antagonists of each other (Gross et al., 1998; Mikhailov et al., 2001; Mikhailov et al., 2003). Pro-apoptotic members of the Bcl-2 family, such as Bax and Bak are capable of forming homo- and heterooligomers, thereby forming a pore, which lead to a limited permeabilization of the outer mitochondrial membrane and release of cytochrome c and apoptogenic factors, such as AIF, thereby leading to initiation of apoptosis (Jurgensmeyer et al., 1998; Kluck et al., 1999; Korsmeyer et al., 2000; Petit et al., 1998; Susin et al., 1998).

There exist at least 20 Bcl-2-related proteins in mammals and all of them possess at least one of four conserved motifs known as Bcl-2 homology domains (BH1 to BH4). Most anti-apoptotic Bcl-2 members contain BH1, BH2 and BH3 domains, whereas Bcl-2 and Bcl-x<sub>L</sub> possess all four domains (Kelekar and Thompson, 1998). BH1,2 and 3 domains are required for their dimerisation, being essential for pore formation (Mikhailov et al., 2003; Muchmore et al., 1996). The anti-apoptotic members located in the outer mitochondrial membrane inhibit apoptosis by preventing the opening of voltage-dependent anion channels (VDAC), which would lead to an influx of ions, followed by water influx and rupture of the outer mitochondrial membrane, releasing cytochrome c as a result (Narita et al., 1998; Shimizu et al., 1999).

The pro-apoptotic members can further be divided into two subfamilies, members which contain BH1 to BH3 domains, such as Bax, Bak and Bok, and members containing solely the BH3 domain, such as Bik, Hrk, Bim<sub>L</sub>, Noxa, Bad, Puma, Bmf and Bid (Adams and Cory, 1998; Reed et al., 1998). BH3-only proteins are expressed in many different cell types (Hsu et al., 1997; O'Reilly et al., 2000). They are primarily located in the cytoplasm and can relocalize to the outer mitochondrial membrane in response to an apoptotic stimulation, such as DNA damage, to induce cytochrome c release (Gross et al., 1998; Jurgensmeyer et al., 1998).

Pro-apoptotic members, such as Bax and Bak, are able to form homo- and oligomers, as well as heterodimers by binding through their BH 3 domain (Chittenden et al., 1995). This leads to the release of cytochrome c and

activation of caspase 8, initiating the caspase cascade leading to apoptosis (Mikhailov et al., 2003).

The BH3-only protein Bid is cleaved and activated by caspase 8, resulting in a tBid (Li et al., 1998). tBid itself can oligomerize with Bax or Bak forming large pores, thus releasing apoptogenic proteins, such as cytochrome c (Wei et al., 2000).

In response to DNA damage, members of the PIKK family ATM and ATR are activated leading to phosphorylation of Chk2, which in turn phosphorylates p53. This leads to enhanced expression of Bax or by Bax translocation to the mitochondria and reduced Bcl-2 expression (Miyashita et al., 1994; Miyashita and Reed, 1995; Thornborrow et al., 2002). This shifts the ratio between pro- and antiapoptotic Bcl-2 family members, leading to a pro-apoptotic signal. Furthermore, p53 can activate caspase 8, which results in cleavage of Bid to tBid. tBid translocates to the mitochondria and promotes Bak and Bax assembly generating a transition permeability pore. This leads to apoptosome formation (Haupt et al., 2003), further activation of the caspase cascade and apoptosis (Fig. 1.5).

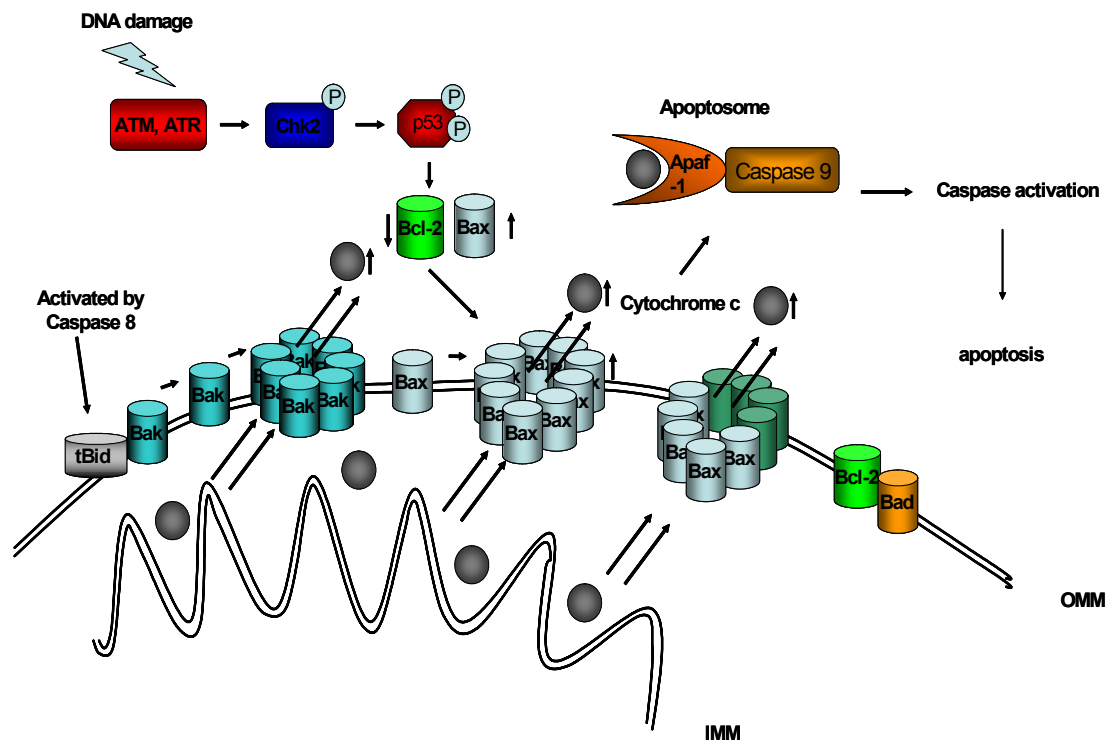


**Figure 1.5: Apoptosis signalling in response to p53 activation**

In response to DNA damage, p53 is activated, promoting the activation of Bax and inhibiting the transcription of Bcl-2. This shifts the ratio between pro- and antiapoptotic Bcl-2 family members leading to a pro-apoptotic signal further promoting apoptosis. IMM and OMM stands for inner and outer mitochondrial membrane.

## 1.7 Objectives

To elucidate the function of mammalian PLRG-1 *in vivo*, a conventional knockout of PLRG-1 in the mouse was generated using established gene targeting techniques. The targeting strategy resulted in a translational stop after 12 aminoacids ensuring the ablation of the protein. Due to embryonic lethality of the conventional knockout, another conditional gene targeting vector was generated, in which exon 3 was flanked by loxP sites. This construct was introduced into V6.5 ES cells and correctly targeted clones were injected into blastocysts, leading to successful generation of chimeras and germline transmission of the conditional *PLRG-1* allele ( $PLRG-1^{lox/+}$ ) onto following generations. Establishing homozygous loxP flanked mouse embryonic fibroblasts (MEF) enabled the functional characterization of PLRG-1 *in vitro* with the use of cell permeable Cre protein. The physiological role of PLRG-1 was defined by crossing mice carrying the conditional PLRG-1 allele with a muscle-specific and a neuron-specific Cre reporter mouse strain to selectively ablate PLRG-1 in these tissues.

## 2 Materials and Methods

### 2.1 Chemicals and antibodies

All chemicals used in this work are listed in table 2.1 and were mainly obtained from Sigma (Steinheim, Germany), Merck (Darmstadt, Germany) or Applichem (Darmstadt, Germany), if not otherwise stated.

Restriction enzymes were purchased from the following companies: Invitrogen (Karlsruhe, Germany), MBI Fermentas (St Leon-Rot, Germany), NEB (Schwalbach, Germany), Roche (Mannheim, Germany), and Takara (over Boehringer, Ingelheim, Germany).

Size markers for agarose gel electrophoresis were delivered from MBI Fermentas (Gene Ruler DNA Ladder Mix and  $\lambda$ HindIII Marker).

Size marker for Pulsed-field gel electrophoresis was delivered from NEB (Yeast chromosome PFG marker).

Size marker for SDS-PAGE gel electrophoresis was purchased from MBI Fermentas (Prestained Protein Ladder Mix).

**Table 2.1: Chemicals**

<b>Chemicals</b>	<b>Company</b>
Agarose	Peqlab, Erlangen, Germany
Agarose Ultra Pure	Invitrogen, Karlsruhe, Germany
Agarose Pulse Field Certified	Bio-Rad, München, Germany
$\beta$ -Mercaptoethanol	Merck, Darmstadt, Germany
Boric Acid	Applichem, Darmstadt, Germany
Bovine serum albumin (BSA)	Applichem, Darmstadt, Germany
Calciumchloride (CaCl <sub>2</sub> )	Merck, Darmstadt, Germany
Chloroform	Applichem, Darmstadt, Germany
Desoxy-ribonucleotid-triphosphates	Amersham, Freiburg, Germany
Dextran sulfate	Amersham, Uppsala, Sweden
Dimethylformamide (DMF)	Merck, Darmstadt, Germany
Dimethylsulfoxide (DMSO)	Sigma-Aldrich, Steinheim, Germany
Disodium hydrogen phosphate	Applichem, Darmstadt, Germany
Dithiothreitol (DTT)	Applichem, Darmstadt, Germany
Ethanol, abs.	Roth, Karlsruhe, Germany
Ethidium bromide	Applichem, Darmstadt, Germany
Ethylendiamine tetraacetate (EDTA)	Applichem, Darmstadt, Germany

<b>Chemicals</b>	<b>Company</b>
Fetal calf serum (FCS) for ES cells	PAA, Pasching, Austria
Fetal calf serum (FCS) for EF cells	Invitrogen, Karlsruhe, Germany
Gelatin, Type B	Sigma, Steinheim, Germany
Glacial acetic acid	Merck, Darmstadt, Germany
Glycerin	Applichem, Darmstadt, Germany
Hepes	Applichem, Darmstadt, Germany
Hydrochloric acid (37 %)	KMF Laborchemie, Lohmar, Germany
Imidazole	Applichem, Darmstadt, Germany
Isopropyl- $\beta$ -D-Thiogalacto-pyranoside (IPTG)	Biomol, Hamburg, Germany
Isopropanol (2-Propanol)	Roth, Karlsruhe, Germany
L (+)-Tartaric acid	Sigma, Steinheim, Germany
L-Arabinose	Sigma, Steinheim, Germany
L-Glutamine	Invitrogen, Karlsruhe, Germany
Luria-Bertani (LB) Agar	Sigma, Steinheim, Germany
Luria-Bertani (LB) Medium	Applichem, Darmstadt, Germany
Magnesiumchloride (MgCl <sub>2</sub> )	Merck, Darmstadt, Germany
Manganchlorid (MnCl <sub>2</sub> )	Merck, Darmstadt, Germany
Ni-NTA-agarose	Qiagen, Hilden, Germany
Nitrogen (liquid) (N <sub>2</sub> )	Linde, Pullach, Germany
N-Lauroylsarcosine	Sigma, Steinheim, Germany
Non essentiell aminoacids (NEAA)	Invitrogen, Karlsruhe, Germany
$\alpha$ -P <sup>32</sup> -CTP	Amersham, Freiburg, Germany
Orange G	Chroma Gesellschaft Schmidt & Co, Stuttgart, Germany
Phenol/Chloroforme/Isoamylalkohol	Applichem, Darmstadt, Germany
Potassium chloride	Merck, Darmstadt, Germany
Potassium hydroxide	Merck, Darmstadt, Germany
Proteinase K	Roche, Switzerland
Roswell Park Memorial Institute medium (RPMI)	PAA, Pasching, Austria
Salmon sperm DNA	Biomol, Hamburg, Germany
Sodiumacetate (NaOAc)	Applichem, Darmstadt, Germany
Sodiumchloride	Applichem, Darmstadt, Germany
Sodium-Citrate	Merck, Darmstadt, Germany
Sodiumdodecylsulfat (SDS)	Applichem, Darmstadt, Germany
Sodiumhydroxide	Applichem, Darmstadt, Germany
Sodiumpyruvate	Invitrogen, Karlsruhe, Germany
Spermidin	Sigma, Steinheim, Germany
Trishydroxymethylaminomethan (Tris)	Applichem, Darmstadt, Germany

## 2.2 Molecular biology

Standard methods in molecular biology were performed according to protocols published in Sambrook *et al.* (1989)

### 2.2.1 Competent *E.coli* and isolation of plasmid DNA

Competent *Escherichia coli* DH5 $\alpha$  cells were prepared according to the protocol of Inoue *et al.* (1990) and used for heat shock transformations.

Plasmid DNA was isolated from transformed *E.coli* using an alkaline lysis method (E.Z.N.A.<sup>®</sup> Plasmid Miniprep Kit 1, Peqlab, Erlangen, Germany) according to the protocol of Zhou *et al.* (1990).

### 2.2.2 Construction of targeting vectors

All constructs used for vector generation were confirmed by sequencing. Primers used for the generation of targeting vectors are listed in table 2.2.

**Table 2.2: Oligonucleotides used for generation of gene replacement vectors and probes for Southern and Northern Blot**

Name	Sequence (5'-3')	Purpose
P1	GTA GAC TAA ACG GCG GCG ACA TG	Used for amplification of the short arm of homology for the conventional PLRG-1 targeting vector
P2	GTG TGT GTA CAG AAT GCA TCT GTA CC	Used for amplification of the short arm of homology for the conventional PLRG-1 targeting vector
P_long1_5	GGC CGG CCA GGT CTT AAA GGT GCA TAC TCA CAG GAC	Used for amplification of the long arm of homology for the conventional PLRG-1 targeting vector



<b>Name</b>	<b>Sequence (5'-3')</b>	<b>Purpose</b>
P_long6_3	CTC GAG GCA TCA ATG TCA CCA AAC CTG TAG CAC T	Used for amplification of the long arm of homology for the conventional PLRG-1 targeting vector
KA5	CGG CCG CGT AGA CTA AAC GGC GGC GAC ATG	Used for amplification of the short arm of homology for the conditional PLRG-1 targeting vector
KA3	CCG CGG TCA AGG GTC CAA GTG AAT TAA AGA C	Used for amplification of the short arm of homology for the conditional PLRG-1 targeting vector
flExon3_5	GGC GCG CCG GTC TCA TCC AAA AAG GTT TTG TGT	Used for amplification of the loxP flanked exon 3
flExon3_3	GGC CGG CCG AAT CAA CTT GAG TTT TCC CTG TAG	Used for amplification of the loxP flanked exon 3
LA5	CTC GAG CTA GCC TGT GGG GAG ACC ATC T	Used for amplification of the long arm of homology for the conditional PLRG-1 targeting vector
LA3	GTT TAA ACA AAC ACC CTC TCA CGA GTG GGG	Used for amplification of the long arm of homology for the conditional PLRG-1 targeting vector
SB5A	CAT TGC TGT ATC GGC GGT ACG TTT	Used for amplification of probe A
SB3A	CTT GGT GCT CCT TAC TTG GAG GTT	Used for amplification of probe A
Neo5	TGA ATG AAC TGC AGG ACG AGG CA	Used for amplification of neo probe
Neo3	GCC GCC AAG CTC TTC AGC AAT AT	Used for amplification of neo probe
PLRGN5	CAT CAG TAC AGT GCG TGG TGT GA	Used for amplification of PLRG-1 northern probe
PLRGN3	CTA AAA TCG CTT TCT CTT GAT AAT TTC	Used for amplification of PLRG-1 northern probe

### 2.2.3 TA-cloning

All PCR products used for gene replacement vectors were first introduced into the TOPO cloning vector (Invitrogen, Germany) using the TA-overhangs generated by PCR following the manufacturer's protocols followed by sequencing.

### 2.2.4 Generation of gene replacement vectors

All PCR products used for gene replacement vectors were cut out of the TOPO cloning vector containing the short arm of homology, long arm of homology and loxP flanked exon3, respectively, using the appropriate restriction endonucleases. Cloning was performed according to protocols published in Sambrook *et al.* (1989) and ligation of DNA fragments using the NEB T4-ligase according to the manufacturer's protocol.

### 2.2.5 Isolation of genomic DNA

Mouse tail biopsies or cultured cells were incubated overnight at 56°C in lysis buffer (10 mM Tris-HCl [pH 8]; 10 mM EDTA; 150 mM NaCl; 0.2% SDS; 400 mg/ml proteinase K) on a thermomixer. DNA was precipitated by adding an equal volume of isopropanol, mixed and pelleted by centrifugation. The pellet was washed in 70% EtOH, dried, and resuspended in TE-buffer (10 mM Tris-HCl [pH 8]; 1 mM EDTA) plus RNaseI (50 µg/ml). When used for Southern Blotting, DNA was resuspended in TE containing 50 µg/ml RNase A.

Total DNA from ES cells grown in 96-well tissue culture dishes was extracted according to the protocol of Pasparakis and Kollias (1995).

For the preparation of DNA from mouse tissue, 100 mg tissue was incubated overnight at 56°C in tissue lysis buffer (0.1 M Tris-HCl, [pH 8.5]; 5 mM EDTA; 0.2% SDS; 0.2 M NaCl; 1 g/ml proteinase K) on a thermomixer.

Debris was pelleted and the supernatant was mixed with an equal volume of phenol-chloroform followed by centrifugation. The upper, aqueous phase was transferred to a fresh tube and mixed with an equal volume of chloroform and centrifuged. Finally the upper phase was mixed with an equal volume of isopropanol and centrifuged to precipitate the DNA. The pellet was washed in 70% EtOH, dried and resuspended in TE-buffer.

### **2.2.6 DNA electrophoresis**

DNA fragments were separated by size using electrophoresis in agarose gels (0.7% - 2%; 1xTAE; 0.5 mg/ml ethidiumbromide (Sambrook *et al.*, 1989)). When desired, DNA fragments were excised using a scalpel, and eluted from agarose gel slices using the QIAEX II kit (QIAGEN, Hilden, Germany) following the manufacturer's protocol.

### **2.2.7 Pulsed-field gel electrophoresis**

Pulsed-field gel electrophoresis (PFGE) provides the possibility to separate DNA ranging in size from a few kilobase pairs up to 10 megabase pairs. Because of the large size of these molecules, cell lysis has to occur in agarose embedded plugs. This prevents shearing of the DNA which could lead to diminished quality of the PFGE separations. To generate agarose embedded plugs, the CHEF Genomic DNA Plug Kit from Bio-Rad was used according to manufacturer's protocol.  $10^6$  mouse embryonic fibroblasts were embedded in 100  $\mu$ l agarose plugs and used for PFGE using the CHEF-DR II system from Bio-Rad. A 1% agarose gel (Pulse Field Certified Agarose, Bio-Rad, München, Germany) was run at 6 V/cm<sup>2</sup> using pulse times of 70 s for 15 h, followed by 120 s for additional 11 h in 0.5% TBE buffer containing 50 mM Tris-HCl, 50 mM boric acid and 1 mM EDTA. After running, the gel was stained with EtBr to visualize the DNA.

### 2.2.8 DNA sequencing

DNA was sequenced using the 'Big Dye termination Cycle Sequencing Kit' (Applied Biosystems, Foster City, USA), which is a PCR-based modification of the original Sanger protocol (Sanger et al., 1977). The DNA fragments were analysed automatically using the ABI373A and ABI377 systems (Applied Biosystems, Foster City, USA).

### 2.2.9 Quantification of DNA

The concentration of nucleic acids was determined by measuring the absorption of the sample at 260 nm and 280 nm in a spectrophotometer. An  $OD_{260}$  of 1 corresponds to approximately 50  $\mu\text{g/ml}$  for double stranded DNA. Purity of nucleic acids was estimated by calculating the ratio  $OD_{260}/OD_{280}$ . Pure nucleic acids show a ratio  $OD_{260}/OD_{280}$  of 2. Protein contaminations decrease this value. Samples with a quotient between 1.8 and 2 are pure enough for DNA quantification.

Residual glass milk from the QIAEX II kit interferes with UV absorption, hence, for estimating the concentration of DNA fragments extracted from agarose gels, a small sample of the DNA was again subjected to electrophoresis, and the concentration was compared to the band intensity of a standard marker.

### 2.2.10 PCR

The Polymerase Chain reaction (PCR) was used for *in vitro* amplification of DNA fragments, e.g. for generation of targeting vectors, detecting the presence of targeted alleles or generating fragments for sequencing (Saiki et al., 1985; Saiki et al., 1986). Reactions were performed in Thermocycler iCycler

PCR machine from Bio-Rad or in Peltier Thermal Cycler PTC-200 from MJ Research.

Genotyping of cells and mice was performed in a total volume of 25  $\mu$ l containing 250 ng DNA, 25 pmol of each primer, 25  $\mu$ M dNTP's, 1.5 mM MgCl<sub>2</sub>, 0.75 U *Thermus aquaticus* (Taq) Polymerase (homemade), 10 mM Tris-HCl pH 8.3, 50 mM KCl. PCR started with an initial denaturation at 94°C for 5 min, followed by 30-35 repeating cycles of denaturation at 94°C for 30 s, annealing at 54-57°C for 30 s, elongation at 72°C for 1 min and a final extension step of 10 min at 72°C.

Genotyping of blastocysts, 2-cell stage embryos and fertilized oocytes was performed using a semi-nested PCR (Fig. 2.1). The first PCR generates a large amount of specific DNA fragments using primers for the wildtype (W5.1, W3.2) and the targeted allele (W5.1, 1.2 rev1). These products are used in the second PCR as template. Here, the PCR was performed by using a different internal 5' primer (W5.2) and the same 3' primers (W3.2, 1.2 rev1). This technique allows the analysis of a single cell, so the first PCR reaction contained one blastocyste, morula or fertilized oocyte, 25 pmol of each primer, 23.5  $\mu$ l ddH<sub>2</sub>O and 25  $\mu$ l of a mastermix obtained from Roche. The PCR started with an initial denaturation at 94°C for 2 min, followed by 25 repeating cycles of denaturation at 94°C for 15 s, annealing at 54°C for 30 s, elongation at 72°C for 1 min followed by another round of additional 35 repeating cycles of denaturation at 94°C for 20 s, annealing at 54°C for 30 s, elongation at 72°C for 1.5 min and a final extension step of 10 min at 72°C. 2  $\mu$ l of the first PCR were used as template for the second PCR, containing 25 pmol of each primer, 22  $\mu$ l ddH<sub>2</sub>O and 25  $\mu$ l mastermix. This second PCR started with an initial denaturation at 94°C for 2 min, followed by 15 repeating cycles of denaturation at 94°C for 15 s, annealing at 54°C for 30 s, elongation at 72°C for 1 min and additional 25 repeating cycles of denaturation at 94°C for 20 s, annealing at 54°C for 30 s, elongation at 72°C for 1.5 min and a final extension step of 10 min at 72°C.

Amplification of DNA fragments for targeting vectors was performed using the High Fidelity Kit from Roche according to the manufacturer's guidelines. Primers used for genotyping are listed in table 2.3.

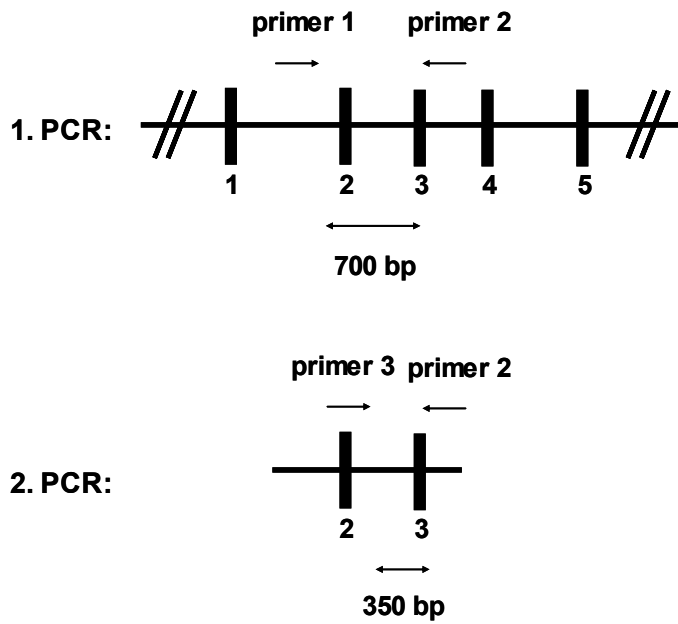


**Figure 2.1: Schematic representation of semi-nested PCR method**

Genomic DNA serves as a DNA template for the first PCR. The PCR product of the first PCR serves as a DNA template for the second PCR.

Note: Primer names and sizes of bands are fictitious.

**Table 2.3: List of primers used for genotyping**

Name	Sequence(5'-3')	T <sub>Ann.</sub> °C	Location	direction
W5.1	GCC AGA CAG GAG CTT TCT CAT	54	Intron 1	sense
W5.2	CCT TCT CCA TAT TTA GCG TGG	54	Intron 1	sense
W3.1	CCT CTC TTC ATC CAA AGG CAC	54	Boundary Exon2/Intron2	antisense
W3.2	TCT CTC TGC ACC CTT CTG TTA	54	Intron 2	antisense
1,2rev1	CCT ACC GGT GGA TGT GGA ATG TG	55	PGK promotor of neo <sup>r</sup>	antisense
Flp5	GAC AAG CGT TAG TAG GCA CAT	61	N-terminal part of FLP cDNA	sense
Flp3	GAG AAG AAC GGC ATA GTG CGT	61	C-terminal part of FLP cDNA	antisense
LA2	TGT TAT GTG CAG TGC CTT TCT	55	Intron 1	sense
Seq4	GTC CTC TGT CCA AGC ATA TTT G	55	Intron 3	antisense
MCK5	GTT CTT AAG TCT GAA CCC GG	60	MCK promotor	sense

Name	Sequence(5'-3')	T <sub>Ann.</sub> °C	Location	direction
MCK3	GTC TGG ATG ACA TCG TCC AG	60	N-terminal part of MCK	antisense
Cre_intern_rev	ATG TTT AGC TGG CCC AAA TGT	60	N-terminal part of Cre	antisense
Syn5	TTC CCG CAG AAC CTG AAG ATG TTC G	59	N-terminal part of SYNCre cDNA	sense
Syn3	GGG TGT TAT AAG CAA TCC CCA GAA ATG C	59	C-terminal part of SYNCre cDNA	antisense
Lox5	TGT GAT GGT GGC CGT ATT GAT	54	(Intron3) Between Exon3 and 3'loxP site	sense
Lox3	CTG TTC CAG CTG TTC TTC ACA	54	Intron3	antisense

Sequences of oligonucleotides are shown in 5'-3' direction. Direction is designated "sense", if the primer orientation coincides with transcriptional direction, and "anti-sense" vice versa.

### 2.2.11 RT-PCR and quantitative Real-Time PCR

RNA from mouse embryonic fibroblasts was isolated using the RNeasy mini kit (QIAGEN, Hilden, Germany) according to the manufacturer's protocol. DNase treatment of RNA was performed prior to RT-PCR using the RQ1 Rnase-Free Dnase I endonuclease according to the manufacturer's guidelines (Promega, Mannheim, Germany). 200 ng total RNA per reaction was used for cDNA synthesis using the One step RT qPCR Master Mix from Eurogentec. 1 µl of cDNA was used for PCR with exon spanning primers (Tab. 2.4)

Quantitative Real-Time PCR was performed using the qPCR Mastermix Plus without UNG kit from Eurogentec with a TaqMan Principles ABI Prism 7700 Sequence Detection System. Relative expression of mRNAs was determined using standard curves based on MEF cDNA. Samples were

adjusted for total RNA content by TBP RNA quantitative PCR. Calculations were performed by a comparative method ( $2^{-\delta\delta CT}$ ). Used samples for quantitative Real-Time PCR are listed in Tab. 2.5.

**Table 2.4: List of oligonucleotides used for amplification of cDNA**

<b>Name</b>	<b>Sequence(5'-3')</b>	<b>T<sub>Ann.</sub> °C</b>	<b>Location</b>	<b>direction</b>
5CycD1	CTT GAC TGC CGA GAA GTT GTG	54	Exon 2	sense
3CycD1	AAG TGT TCG ATG AAA TCG TGG	54	Exon 3	antisense
5CycE1	CTG GGA TGA TAA TTC AGC ATG	54	Exon 5	sense
3CycE1	AAA GTG CTC ATC TCT CAG GTA	54	Exon 6	antisense
p53-5RT	AGT CAC AGC ACA TGA CGG AGG	54	Exon 5	sense
p53-3RT	TGC CTG TCT TCC AGA TAC TCG	54	Exon 6	antisense

Sequences of oligonucleotides are shown in 5'-3'direction. Direction is designated "sense", if the primer orientation coincides with transcriptional direction, and "anti-sense" vice versa.

**Table 2.5: List of probes used for quantitative Real-Time PCR**

<b>Gene name</b>	<b>Abbreviation</b>	<b>Order number</b>
DNA-damage inducible transcript 3	Ddit 3	Mm00492097_m1
Forkhead box 1	Foxo 1	Mm00490672_m1
Forkhead box 3a	Foxo 3a	Mm00490673_m1
Notch1	Notch1	Mm00435245_m1
Transforming growth factor beta 1	TGF- $\beta$ 1	Mm00441724_m1
Tubulin alpha 1	Tuba 1	Mm00846967_g1



### 2.2.12 DNA hybridization

10 µg of genomic DNA were digested overnight using 100 U of the appropriate restriction enzyme and separated on a 0.8% agarose gel. DNA was subsequently transferred and immobilized on a nylon membrane (Hybond-N+, Amersham) using an alkaline capillary transfer (Chomczynski and Qasba 1984). To crosslink the DNA with the membrane, membranes were baked at 80°C for 30 min, equilibrated in 2xSSC (Sambrook et al., 1989) and prehybridized at 65°C for 2-4 h in hybridization solution (1M NaCl, 1% SDS, 10% dextran sulfate, 50 mM Tris-HCl pH 7.5, 250 µg/ml sonicated salmon sperm DNA). Probes were labeled with  $\alpha^{32}\text{P}$ -dCTP using the Ladderman<sup>TM</sup> DNA Labeling Kit (TaKaRa, Otsu, Japan) according to the manufacturer's guidelines. Hybridization of the probe was performed overnight at 65°C. The membranes were washed several times with 2xSSC/0.1% SDS at 65°C until radioactive signals determined with a handheld Geiger counter reached 50 cps. Subsequently, the membrane was sealed in a plastic bag and exposed to an X-ray film (BioMAX MS; Kodak) overnight at -80°C. Films were developed in an automatic developer. Alternatively, membranes were exposed to a phosphorimager screen (Fuji, Fuji, Japan) and analyzed on a Bio-Imaging Analyser (Fuji Bias 1000; Fuji, Japan).

The following probes were used:

1. A *PLRG-1* 5' probe was PCR amplified from a *PLRG-1* BAC using primers SB5A and SB3A resulting in a 498bp fragment.
2. A *Neomycine resistance gene* probe was PCR amplified from pGK12 vector using primers Neo5 and Neo3 resulting in a 510bp fragment.

### 2.2.13 Northern Blot and RNA hybridization

RNA blots from mouse adult tissue (N1334447-BC) and different embryo stages (R1011-SG) were purchased from BioCat. Blots were hybridized with a radiolabeled *PLRG-1* probe.

The membrane was prehybridized at 68°C for 2 h in prehybridization solution (Express Hyb, Stratagene, Heidelberg, Germany). A probe was labeled

with  $\alpha^{32}\text{P}$ -dCTP using the Ladderman<sup>TM</sup> DNA Labeling Kit (TaKaRa, Otsu, Japan) according to the manufacturer's guidelines. Hybridization of the probe was performed overnight in hybridization solution (Express Hyb, Stratagene, Heidelberg, Germany) containing 100  $\mu\text{g}/\text{ml}$  salmon sperm DNA. After hybridization, membranes were washed several times in  $2\times\text{SSC}/0.1\%$  SDS until radioactive signals reached 50 cps. Membranes were sealed in plastic bags and exposed to an X-ray film (BioMAX MS; Kodak) overnight at  $-80^\circ\text{C}$ .

The following probe was used:

1. A *PLRG-1* 5' probe was PCR amplified from bl/6 mouse tail DNA using primer PLRGN5 and PLRGN3 resulting in a fragment of 753bp.

## 2.3 Cell culture

### 2.3.1 Primary embryonic fibroblast (EF) culture

Primary EF cells were obtained from mouse embryos at day 13.5 day p.c.

Mice of the desired genotypes were mated and pregnancy was verified by the occurrence of vaginal plugs. 13.5 days after mating, the pregnant mice were sacrificed by cervical dislocation. The mouse was disinfected using Bacillol (Bode Chemie, Hamburg, Germany), the abdomen opened and the uterus containing the embryos dissected. The embryos and placentae were placed in PBS containing 10% Beta-Isodona (Bode Chemie, Hamburg, Germany) and after removal of the placenta embryos were transferred into PBS/7,5% Beta-Isodona. Heart, liver and brain were removed and the residual tissue was placed in PBS, strained through a sterile nylon sieve and washed with EF-medium (Dulbecco's modified Eagle's medium (DMEM) containing stable glutamine (Glutamax), 10% FCS, 4500 mg/l glucose, and 1xnon-essential amino acids). The cells were pelleted, resuspended in medium, plated on a 10 cm tissue culture dish (Falcon, Bedford, USA) and grown at  $37^\circ\text{C}$  in an atmosphere of 10%  $\text{CO}_2$ . Primary EF cells were used only up to passage 20.

### 2.3.2 Embryonic stem (ES) cell culture

For all transfections V6.5 (129Sv x C57BL/6) Embryonic stem cells (Eggan et al., 2002) were used. ES cells were grown at 37°C in an atmosphere of 10% CO<sub>2</sub> in Dulbecco's modified Eagle's medium (DMEM) containing 15% fetal calf serum (FCS), 4500mg/l glucose, 1xnon-essential amino acids, 2 mM glutamine, 1 mM Na-pyruvat, 0.01 mM β-mercaptoethanol, and 1.3 ml leukemia inhibitory factor. Cells were grown on mitotically inactivated feeder cells, which had been treated with mitomycin C (10 µg/ml for 2 h) and washed extensively with PBS before seeding with ES cells

ES cell colonies were trypsinized before they reached confluency or after three days. Therefore, cells were washed with PBS and treated with trypsin (0.05 % trypsin, 0.02 % EDTA in PBS; Gibco, Karlsruhe, Germany) for 3 min at 37°C. Trypsin was stopped by adding an equal amount of ES-medium containing FCS to the cells and centrifugation. ES cells were passaged to fresh plates, transfected or frozen (in 90% FCS, 10% DMSO at -80°C, transfer to liquid nitrogen the next day).

For transfection,  $1 \times 10^7$  ES cells were mixed with 40 µg DNA in 800 µl transfection buffer (RPMI w/o phenol red, Gibco, Karlsruhe, Germany) in a prechilled electroporation cuvette. For electroporation 500 µF and 240 V at 23°C as standard conditions were used. ES cells were allowed to recover for 5 min on ice prior to seeding on 4x10 cm tissue culture dishes containing an embryonic feeder cell layer.

48 h after transfection, positive selection started using 250 µg/ml G418 (Gibco, Karlsruhe, Germany). Negative selection against HSV-*tk* containing random integrants started at day five by adding  $2 \times 10^{-6}$  M gancyclovir (Cymeven, Syntex, Aachen, Germany) to the medium. On day 9 and 10 after transfection, double resistant colonies were picked from the culture dishes using yellow pipette tips and seeded into EF-containing 96-well tissue culture dishes for recovery and expansion. 3 days after picking the clones, cell samples were frozen, and in parallel expanded for DNA extraction.

### **2.3.3 HTN-Cre-mediated deletion *in vitro***

Fibroblasts were treated with His-TAT-NLS-Cre (HTNC) to delete loxP-flanked gene segments, which was purified according to Peitz et. 2002

$3 \times 10^6$  cells were plated on a 15 cm cell culture dish. After 4 h, cells were washed twice with PBS and incubated with 5  $\mu$ M HTN-Cre dissolved in DMEM/PBS. 16 h later, cells were washed with PBS and passaged for the respective experiments.

### **2.3.4 Cell cycle analysis**

HTNC-treated fibroblasts were grown to confluence, washed twice with PBS, serum deprived for 48 h, left untreated or stimulated with 10% FCS for 2, 4, 6, and 8 h, respectively. Cells were trypsinized and counted using an improved Neubauer Haemocytometer.  $10^6$  cells were lysed in 500  $\mu$ l 2xSDS sample buffer containing 125 mM Tris-HCl [pH 6.8], 5% SDS, 43.5% glycerol, 100 mM DTT, and 0.02% bromophenol blue and used for immunoblotting.

### **2.3.5 Cell cycle analysis using fluorescence-activated cell sorter (FACS) analysis**

$10^6$  HTNC-treated fibroblasts were cultured in the absence of serum for 24 h and left untreated or stimulated with 10% FCS for 24 h. Cells were collected by trypsin digestion and fixed in ice-cold 70% EtOH in PBS for at least 2 h. After the removal of ethanol, cells were washed once with PBS, and incubated with 500  $\mu$ l propidium iodide (PI) staining solution containing 0.1% Triton X-100 (Sigma), 200  $\mu$ g/ml DNase-free RNase A (Sigma), and 20  $\mu$ g/ml Propidium Iodide (Sigma) in PBS. 25000 cells were analyzed by FACS (FACSCalibur, Becton-Dickinson Biosciences Immunocytometry Systems) and

the proportion of cells in the G<sub>0</sub>/G<sub>1</sub>, G<sub>2</sub>/M, and S phase was assessed using the CellQuest software (Becton Dickinson, Mountain View, USA).

### 2.3.6 <sup>3</sup>H-thymidine incorporation

HTNC-treated fibroblasts were trypsinized and counted using a Neubauer Haemocytometer. 10<sup>4</sup> cells were seeded per well (200 µl/well → 5x10<sup>4</sup>/ml) onto a 96-well tissue culture dish and serum deprived overnight. The following day medium was removed and cells were washed once with PBS. Fresh MEF or starving medium containing 5 µCi/ml <sup>3</sup>H-thymidine was added to the. MEFs were incubated with 100 µl of these prepared media for 0, 16 and 24 h. Thereafter, cells were washed with PBS and trypsinized. MEFs were harvested and fixed onto self aligning glass fiber filters (Packard Instrument Company, Downers Grove, USA ) using the Packard Harvester Filtermate 196 harvester (Packard Instrument Company, Downers Grove, USA) and air-drying of filters. Incorporated <sup>3</sup>H-thymidine was measured using liquid scintillation counter (Packard Topcount microplate scintillation counter). Counts per minute were used as the readout for proliferation. Calculating the quotient of serum added and serum deprived <sup>3</sup>H-thymidine containing medium resulted in proliferative capacity. For all experiments 48 wells were used for each condition, to receive low standard abbreviations.

### 2.3.7 Analysis of apoptosis

To assess apoptosis, a TUNEL assay (DeadEnd™ Fluorometric TUNEL System, Promega) was used. HTNC-treated fibroblasts were cultivated on glass coverslips in a 6-well plate for 3 days after Cre-treatment. Thereafter, cells were fixed in 4% formaldehyde for 25 min at 4°C and washed twice in PBS. TUNEL assays were performed according to the manufacturer's guidelines. Percentage

of apoptotic cells was calculated as TUNEL-positive cells per DAPI-stained nuclei.

### **2.3.8 DNA double-strand breaks after UV-treatment**

To determine the occurrence of DNA double-strand breaks,  $10^6$  HTNC-treated mouse embryonic fibroblasts were left either untreated or broadband UV irradiated for 2 min using a UV transilluminator (Gel Doc EQ System, München, Germany). Non- and UV-irradiated cells were cultivated for additional 24 h, harvested, agarose embedded (CHEF Genomic DNA Plug Kit, Bio-Rad, München, Germany) and analyzed by PFGE.

### **2.3.9 Immunofluorescence**

HTNC-treated fibroblasts were cultivated on glass coverslips in a 6-well plate for 2 days after Cre-treatment. Thereafter, cells were fixed in 4% paraformaldehyde for 10 min at RT and washed 3 times with PBS. Cells were permeabilized with 0.5% Triton X-100 and additionally washed another 3 times with PBS. Subsequently, fixed and permeabilized fibroblasts were blocked with 0.5% BSA in PBS for 45 min at RT. Samples were incubated for 1 hour at RT with an 1:500  $\gamma$ -H2AX antibody (JBW 301, Millipore, Billerica, USA) dilution in 0.5% BSA/PBS. Following, samples were washed 4 times with PBS, incubated for 45 min at RT with an 1:3000 Alexa-Fluor 555 antibody (Invitrogen, Carlsbad, USA) dilution in 0.5% BSA/PBS and kept in dark. Cells were stained with DAPI in Vectashield to visualize nuclei. Percentage of  $\gamma$ -H2AX positive cells was calculated per DAPI-stained nuclei.

### **2.3.10 RNA interference (RNAi)**

RNAi-mediated knockdown of endogenous PLRG-1 and p53 was performed using Lipofection. PLRG-1 siRNA was purchased from Ambion (16704) and p53 siRNA was purchased from Santa Cruz (sc-44219, sc-29436). si-CONTROL from Dharmacon (D-001210-01) was used as control siRNA. These siRNA duplexes (25 nM) were introduced into MEFs using Lipofectamine 2000 (Invitrogen, Germany) following the manufacturer's guidelines. 48 h after transfection, cells were harvested and used for TUNEL assay and immunoblotting.

## **2.4 Biochemistry**

### **2.4.1 Protein extraction from tissue**

100-500 mg tissue were dissolved in 1 ml lysis buffer containing 50 mM HEPES [pH 7.4], 1% Triton X-100, 0.1% SDS, 100 mM NaF, 10 mM Na<sub>3</sub>O<sub>4</sub>V, 250 mM EDTA, 50 mM NaCl, 10 µg/ml aprotinin, 2 mM benzamidin, 348 µg/ml PMSF, and homogenized using a Ultra Thurrax homogenizer. Protein extracts were centrifuged for 45 min at 4°C to separate supernatants from debris. Protein concentration was measured using a photometer and the Christian-Warburg formula. 10 µg/µl protein stock solution was prepared in 1xSDS sample buffer and heated at 95°C for 5 min. 100µg protein were used for immunoblotting. Protein solutions were always stored at -80°C.

### **2.4.2 Protein extraction from cells**

Collected samples of cells were directly lysed in 2xSDS sample buffer containing 125 mM Tris-HCl [pH 6.8], 5% SDS, 43.5% glycerol, 100 mM DTT,

and 0.02% bromophenol blue and heated at 95°C for 5 min. Lysates of  $5 \times 10^4$  cells were loaded and fractionated on 10-15% SDS-PAGE gels. Alternatively,  $5 \times 10^5$  cells were lysed in 250  $\mu$ l 2xSDS sample buffer and heated at 95°C for 5 min. Protein extracts were directly used for SDS-PAGE gel electrophoresis or frozen at -80°C.

### 2.4.3 Nuclear and cytoplasmic protein extraction

Embryonic fibroblasts were washed with PBS.  $10^6$  cells were resuspended in 15  $\mu$ l hypotonic buffer A containing 10 mM HEPES [pH 7.6], 10 mM KCl, 2 mM  $MgCl_2$ , 0.5 mM DTT, 0.1 mM EDTA, and 1 tablet of Proteinase Inhibitor (Complete mini, Roche, Germany) and incubated for 10 min at 4°C. NP40 were added to a final concentration of 1% and incubated at 4°C for 1 min. Cells were immediately collected by centrifugation at 13000rpm at 4°C for 1 min. The supernatant contained the cytoplasmic fraction. The pellet was washed with buffer A and resuspended in 10  $\mu$ l high salt buffer B containing 50 mM HEPES [pH 7.8], 50 mM KCl, 300 mM NaCl, 0.5 mM DTT, 0.1 mM EDTA, 10% glycerol, and 1 tablet of Proteinase Inhibitor (Complete mini, Roche, Germany). The pellet was incubated at 4°C on a full speed shaker for 1 h. After incubation, the suspension was centrifuged at 13000 rpm at 4°C for 1 h. The supernatant contained the nuclear fraction.

### 2.4.4 Immunoprecipitation

150  $\mu$ g nuclear proteins were incubated with 2  $\mu$ g of anti-WIP1 or anti-insulin receptor (negative control) antibody at 4°C on a rotator for 1 h. Then, 100  $\mu$ l of Protein A-Sepharose (100 mg/ml, Amersham, Freiburg, Germany) were added and incubated overnight. The suspension was washed 5 times with high salt buffer B, 50  $\mu$ l 2xSDS loading buffer was added, and samples were



incubated for 5 min at 95°C. The samples were separated on SDS-PAGE gels, and processed for western blot analysis.

#### 2.4.5 Western Blot

Proteins were fractionated on 10-15% SDS-PAGE gels (Laemmli, 1970) and semi-dry blotted onto a PVDF-membrane for 30 min to 1 h using a current of 200 mA. Unspecific binding sites were blocked with 1% blocking solution in 1x TBS (20mM Tris [pH 7.6], 0.14 M NaCl) (Amersham, Freiburg, Germany) for 1 h at RT and incubated with appropriate primary antibodies at 4°C overnight (table 2.6). Membranes were washed 4 times for 10 min with TBS-T (1x TBS, 0,1% Tween 20), incubated with respective secondary antibodies, which were coupled to horseradish peroxidase (HRP), at RT for 1 h. Membranes were washed again 4 times for 10 min with TBS-T and signals were detected using the ECL kit (Amersham, Freiburg, Germany).

**Table 2.6: Antibodies used for biochemical studies**

Specificity	Order number	Company
AKT	9272	Cell signaling
$\beta$ -Actin	1616	Sigma
Bax	N-20, sc 493	Santa Cruz
Bcl-2	N-19, sc 492	Santa Cruz
CDC5L	612362	BD Transduction Laboratories
cleaved Caspase 3	9661	Cell Signaling
Cyclin D1	sc 718	Santa Cruz
Cyclin E	C-19, sc 198	Santa Cruz
IR- $\beta$	C-19, sc 711	Santa Cruz
Lamin A/C	N-18, sc 6215	Santa Cruz
p21	C-19, sc 397	Santa Cruz
p44/42 MAP kinases	9102	Cell Signaling

<b>Specificity</b>	<b>Order number</b>	<b>Company</b>
pp44/42 MAP kinases	9106	Cell Signaling
p53	FL-393, sc 6243	Santa Cruz
p-S15-p53	GTX 21431	Gene Tex
PLRG-1	selfmade	Received from Dr. Paul Ajuh
WIP1	H-300, sc 20712	Santa Cruz

Secondary antibodies were peroxidase-coupled goat anti-rabbit IgG (whole molecule), anti-goat/sheep IgG (whole molecule) (Sigma), and anti-mouse IgG (whole molecule) (Amersham).

### **2.4.6 Immunohistochemistry**

Brains were dissected from 2 to 3 day old mice and snap frozen in tissue-freezing medium (Jung Tissue Freezing Medium; Leica Microsystems, Germany). Sections were performed using a cryostat. Brain slices were either stained with H&E or used for TUNEL assays following manufacturer's guidelines.

Hearts were dissected from 3 week old mice, frozen in tissue-freezing medium (Jung Tissue Freezing Medium; Leica Microsystems, Germany) and sectioned on a cryostat. Sections were either stained with H&E or processed for TUNEL assays.

### **2.5 Statistical methods**

Data was analyzed for statistical significance using a two-tailed unpaired student's T-Test.

## 2.6 Animal Care

Care of all animal was within institutional animal care committee guidelines. All animal procedures were conducted in compliance with protocols and approved by local government authorities (Bezirksregierung Köln, Cologne, Germany) and were in accordance with NIH guidelines. Mice were housed in groups of 3 to 5 at 22–24°C using a 12 h light/dark cycle.

### 2.6.1 Mouse experiments

General handling and breeding of mice was performed according to Hogan (Hogan et al., 1987) and Silver (Silver, 1995).

### 2.6.2 Mice

C57BL/6 and CB20 mouse strains were ordered from Charles River, Taconic or Jackson Laboratories. Flp deleter mice (Rodriguez et al., 2000) were obtained from our animal facility. PLRG-1<sup>Δ/+</sup> mice were intercrossed to receive homozygous PLRG-1<sup>Δ/Δ</sup> mice. MCKCre mice (Brüning et al., 1998) were mated with PLRG-1<sup>flox/flox</sup> mice, and a breeding colony was maintained by mating PLRG-1<sup>flox/flox</sup> with PLRG-1<sup>flox/+</sup>MCKCre mice. SynCre mice (Zhu et al., 2001) were mated with PLRG-1<sup>flox/flox</sup> mice, and a breeding colony was maintained by mating PLRG-1<sup>flox/flox</sup> with PLRG-1<sup>flox/+</sup>SynCre mice. The SynCre was always transmitted from females, as the transgene has previously been demonstrated to result in germline deletion if transmitted via male germ cells (Rempe et al., 2006).

### 3 Results

The protein pleiotropic regulator PLRG-1 was identified as a spliceosomal component *in vitro*, but its functional role *in vivo* until now has not been examined. To elucidate the function of PLRG-1 *in vivo*, we generated a gene replacement vector to inactivate the murine *PLRG-1* gene. The resulting heterozygous PLRG-1<sup>Δ/+</sup> mice exhibited no apparent phenotype, but analysis of the offspring from PLRG-1<sup>Δ/+</sup> intercrosses at postnatal day 21 indicated an absence of PLRG-1<sup>Δ/Δ</sup> mice. Detailed inspection of litters at different stages of embryogenesis revealed that homozygous PLRG-1-deficient early embryos were only detectable until embryonic day 1.5.

To determine whether early embryonic lethality caused by the PLRG-1 mutation is due to a general cell cycle defect also manifested in somatic cells, a second gene replacement vector for conditional Cre-loxP-mediated inactivation of PLRG-1 was generated. This allowed a functional characterization of PLRG-1 *in vivo*, circumventing embryonic lethality and enabling analysis of PLRG-1 deletion in a tissue specific manner. In addition, a line of embryonic fibroblasts, homozygous for the loxP-flanked allele of PLRG-1, was established for *in vitro* studies. In these cells, deletion of PLRG-1 is achieved through HTN-Cre application.

To obtain mice lacking PLRG-1 specifically in skeletal muscle and heart, PLRG-1<sup>flox/+</sup> mice were crossed with mice expressing a Cre recombinase under control of the muscle specific creatinine kinase (MCK)-promoter (Bruning et al., 1998). Double-heterozygous PLRG-1<sup>flox/+</sup>MCKCre mice were crossed with PLRG-1<sup>flox/flox</sup> mice to obtain PLRG-1<sup>flox/flox</sup>MCKCre offspring, i.e. mice lacking PLRG-1 expression in skeletal muscle and heart (PLRG-1<sup>Δmus</sup>)

PLRG-1 was also inactivated in the central nervous system (CNS) by intercrossing PLRG-1<sup>flox/flox</sup> mice with mice expressing a Cre recombinase under control of the synapsin promoter (Zhu et al., 2001). PLRG-1<sup>flox/flox</sup> mice were crossed with double-heterozygous PLRG-1<sup>flox/+</sup>SynCre mice to obtain PLRG-1<sup>ΔCNS</sup> mice with neuron-restricted PLRG-1 deficiency.

Analysis of different mouse lines with distinct tissue specific PLRG-1 ablation and studies with homozygous loxP-flanked mouse embryonic fibroblasts enabled the gain of novel insights into the function of PLRG-1 *in vivo* and *in vitro*.

### 3.1 Murine expression pattern of PLRG-1

In order to determine the expression pattern of the pleiotropic regulator gene 1 (PLRG-1) in C57BL/6 wild type mice, Northern Blot analysis was performed using a PLRG-1 cDNA probe. This analysis revealed the ubiquitous expression of PLRG-1 in all tested organs of adult mice with highest levels in thymus, testis, kidney, brain and spleen (Fig. 3.1A).

In addition, a murine embryo stage Northern blot, containing RNA from embryos of day 4.5 to 18.5, was performed, revealing that PLRG-1 is expressed throughout all phases of mouse embryonic development, showing a peak of steady-state mRNA levels between embryonic days (ED) 10.5 and 14.5 (Fig. 3.1B).

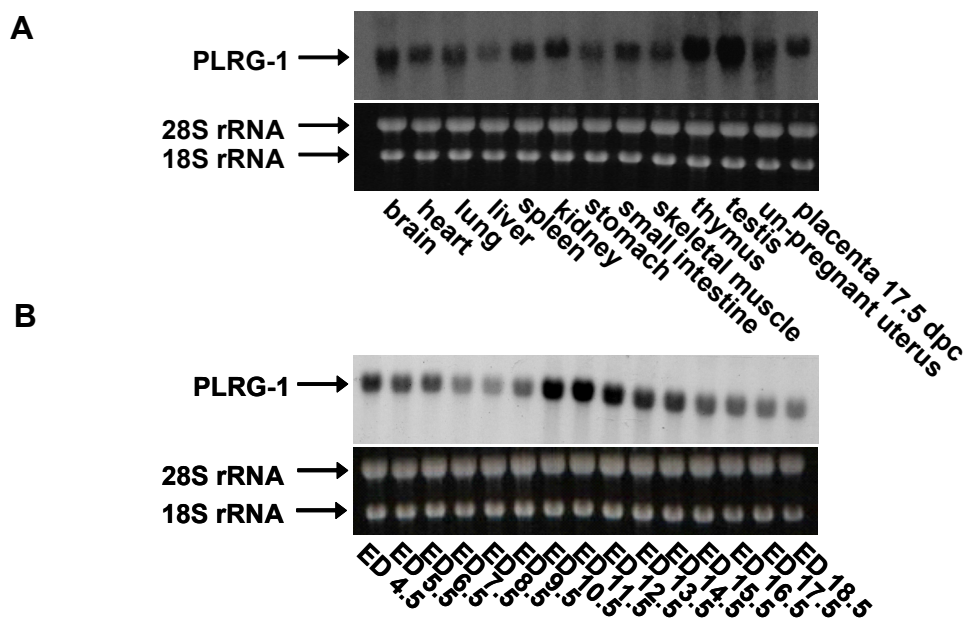


**Figure 3.1: Ubiquitous expression of PLRG-1**

Northern RNA hybridization analysis of PLRG-1 expression in mice.

(A) Expression analysis of PLRG-1 in tissues from adult mice.

(B) Expression of PLRG-1 in the developing mouse embryo. (ED: embryonic day).

Upper panels show hybridization of the PLRG-1 probe, the lower panels display the corresponding 18S and 28S RNA as loading controls.

### 3.2 Generation of a conventional *PLRG-1* gene replacement vector

The murine gene coding for *PLRG-1* comprises 15 exons and spans 17kb of genomic DNA. The C-terminal part of the protein consists of a conserved WD-40 domain of 7 WD-40 repeats. The WD-40 domain is part of many components of multiprotein-complexes and is responsible for protein-protein interactions. The N-terminal part of *PLRG-1* is not conserved across different species and contains no known motifs.

To disrupt the *PLRG-1* gene using conventional gene targeting techniques, a neomycin resistance cassette was inserted into the second exon of the murine *PLRG-1* gene (Fig. 3.2A). This insertion caused a frame shift and a subsequent translational stop of the protein after 12 amino acids. The *PLRG-1* targeting vector was generated using the pGK12 vector (Artemis Pharmaceuticals, Köln, Germany), which contains a PGK neomycine resistance cassette, as a positive selection marker, and the *Herpes Simplex virus thymidine kinase* (TK) gene, as a negative selection marker.

The 1.2 kb short arm of homology comprising exon 1, intron1 and the first 27 bp of exon 2 was amplified from C57BL/6J BAC DNA via PCR. The BAC (RP23-333D8) was constructed in the laboratory of Kazutoyo Osoegawa and Minako Tateno from pooled tissues derived from three female C57BL/6J mice (Osoegawa et al., 2000). The oligonucleotides P1 and P2, used for this PCR, harboured restriction sites allowing a direct cloning into *NotI* and *BamHI* sites of the the pGK12 vector after an intermediate subcloning into the TOPO cloning vector (Invitrogen, Karlsruhe, Germany). After a control digest and sequencing, the fragments were cloned into the respective restriction sites of the pGK12 vector.

The long arm of homology containing the exons 4 to 6 was PCR amplified from C57BL/6J BAC DNA via PCR using the oligonucleotides P\_long1\_5 and P\_long6\_3, adding restriction sites for *FseI* and *XhoI* to the amplified fragment, which was then processed as described above and cloned into the pGK12 vector containing the short arm of homology.

For verification of correct clones an additional control digest was performed, and homology arms were sequenced. The sequences of used oligonucleotides are depicted in table 2.2.

Prior to electroporation of murine V6.5 ES (129Sv x C57BL/6) cells, 30 µg of vector DNA was linearized with *NotI*. Successfully electroporated ES cells were double selected with G418 and ganciclovir. After selection, 300 clones were isolated as single, undifferentiated colonies and grown for 3 days. All clones were analysed by Southern Blot analysis or partly used for freezing at -80°C.

The probes used for Southern Blot analysis were PCR amplified from mouse DNA using the primers SB5A and B (probe A), and Neo5 and 3 (probe B). *BamHI* digestion of the genomic DNA derived from the selected clones and hybridization of probe A was used to determine 5' integration of correctly targeted clones. *BglI* digest and hybridization of probe B verified single and correct 3' integration of the construct. Out of 300 clones, one homologous recombinant that showed successful insertion of the neo cassette in exon 2 of the PLRG-1 gene could be detected. Hybridization with probe A yielded a recombinant band of 2.6 kb in addition to the 7.8 kb wild type band. Using probe B, a specific band of 9 kb was visible, confirming the homologous recombination (Fig 3.2B).

Homologous recombinant ES cells were injected into C57BL/6 blastocysts, which subsequently were transferred into a pseudo-pregnant foster mouse. Resulting 80-90% chimeric mice were crossed to C57BL/6 mice in order to receive PLRG-1<sup>Δ/+</sup> mice.

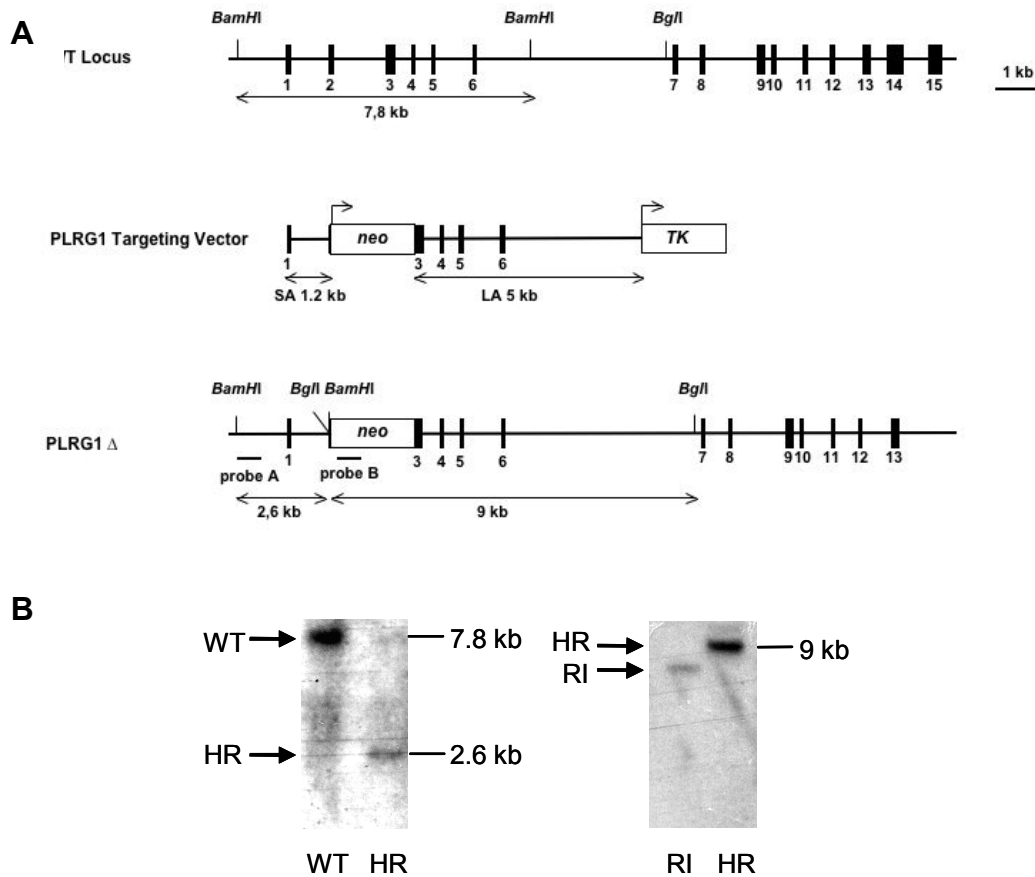


**Figure 3.2: Conventional inactivation of the *PLRG-1* gene**

(A) Schematic representation of the *PLRG-1* gene replacement vector and its respective localization within the murine *PLRG-1* locus.

(B) Verification of *PLRG-1* gene replacement. Left panel: Southern blot analysis of ES cell clones hybridized with the probe A depicted in A. Right panel: Southern blot analysis of the same clones hybridized with probe B corresponding to the neomycin-resistance gene to verify single copy integration.

WT stands for wild type and the respective band, RI for random integrant, HR for homologous recombinant and the respective band

### 3.3 Analysis of *PLRG-1* <sup>$\Delta$ /+</sup> mice

*PLRG-1* <sup>$\Delta$ /+</sup> mice were viable and did not exhibit any significant differences in size or body weight (Fig 3.3A). The slightly elevated weight of *PLRG-1* <sup>$\Delta$ /+</sup> females was attributed to the mixed background of this mouse strain. Western Blot analysis of different mouse adult tissues revealed no difference in expression of *PLRG-1* in all tested organs (Fig. 3.3B).



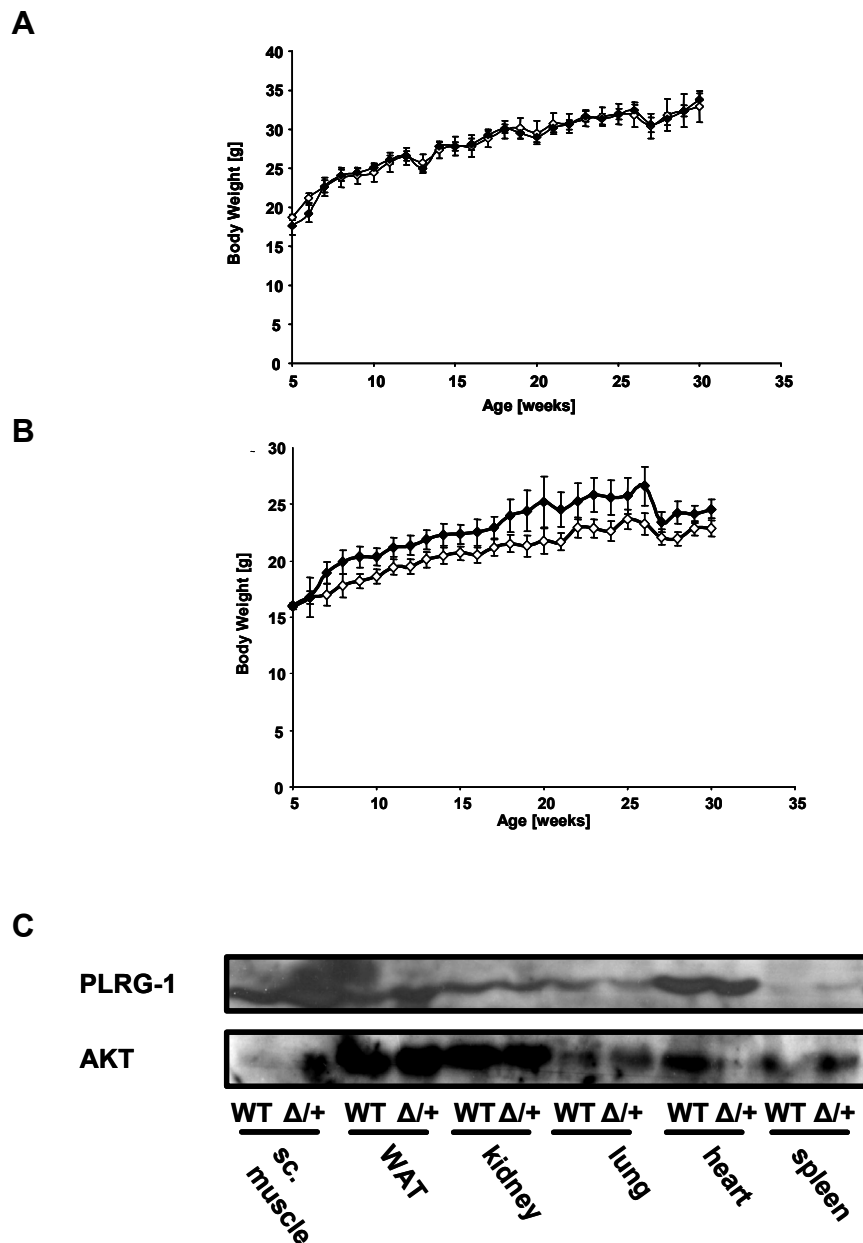


**Figure 3.3: Analysis of PLRG-1 <sup>$\Delta/+$</sup>  offspring**

(A) Body weight of PLRG-1 <sup>$\Delta/+$</sup>  (n=14) and wild type males (n=10)

(B) Body weight of PLRG-1 <sup>$\Delta/+$</sup>  (n=18) and wild type females (n=16)

(C) Expression analysis of PLRG-1 in PLRG-1 <sup>$\Delta/+$</sup>  and wild type mice. Anti-AKT was used to control for loading. Open squares: wt; filled squares: PLRG-1 <sup>$\Delta/+$</sup>

### 3.4 PLRG-1 <sup>$\Delta/\Delta$</sup> mice are embryonic lethal

To generate PLRG-1 <sup>$\Delta/\Delta$</sup>  mice, PLRG-1 <sup>$\Delta/+$</sup>  mice were intercrossed. The first analysis of offspring at postnatal day 21 indicated the absence of PLRG-

## Results

---

1<sup>Δ/Δ</sup> mice (Table 3.1). Due to this fact, the genotype of animals was monitored from birth, showing a lack of PLRG-1<sup>Δ/Δ</sup> mice in all inspected litters (Tab.3.1).

In order to define the time point at which PLRG-1<sup>Δ/Δ</sup> mice die, different embryonic stages were investigated, ranging from embryonic day (ED) 0.5 to 18.5. Genotyping of embryos was performed using a semi-nested PCR enabling the amplification of DNA fragments from single cells. A three primer strategy in the first PCR was applied using oligonucleotides in front of exon 2 (W5.1), 3' of exon 2 (W3.2) and 5' of the neomycine resistance cassette (1.2 rev1) (Fig. 3.4A). The PCR product was divided to be used as a template in a second PCR reaction, in order to detect the wild type allele and the deleted *PLRG-1* allele. Both PCR reactions depend on the same antisense oligonucleotides, whereas the sense oligonucleotide of the second PCR was designed to anneal 70bp downstream of exon 2 (W5.2) (Fig. 3.4A). This method enabled the identification of different genotypes (Fig. 3.4B).

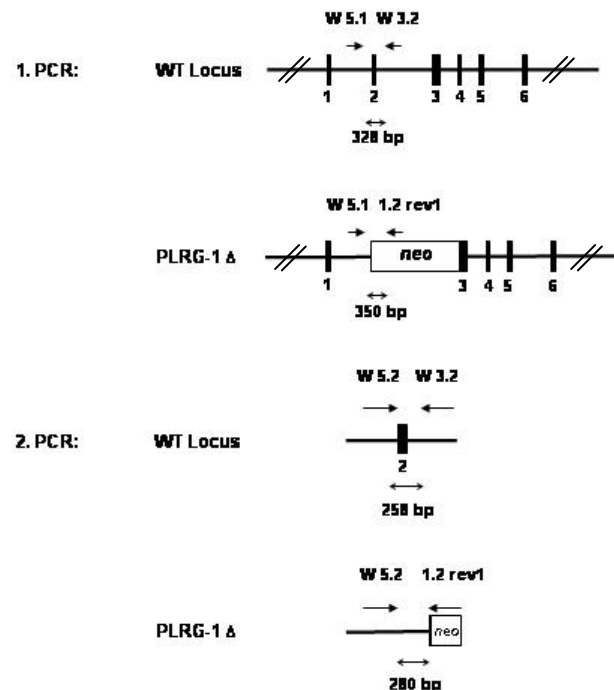
Detailed inspection of litters at these different stages of embryogenesis revealed that homozygous PLRG-1-deficient embryos were viable until embryonic day 1.5 (Table 3.1 and Fig. 3.4B).

**Table 3.1: Genotype analysis of PLRG-1<sup>Δ/+</sup>-intercross offspring based on a semi-nested PCR approach**

PLRG-1 <sup>Δ/+</sup> x PLRG-1 <sup>Δ/+</sup>	+/+	Δ/+	Δ/Δ	Total
E 0.5	3	11	3	17
E1.5	6	15	9	30
E2.5	3	10	0	13
E3.5	11	15	0	26
E12.5	3	15	0	18
E18.5	15	32	0	47
P21	33	58	0	91

Homozygous PLRG-1-deficient early embryos are only detectable up to embryonic day (ED) 1.5.

A



B

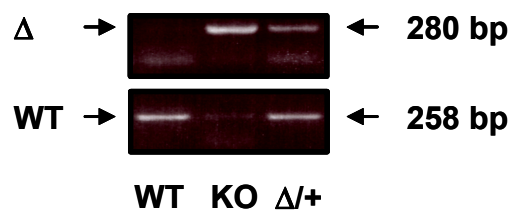


**Figure 3.4: Identification of genotype using semi-nested PCR**

(A) Schematic representation of semi-nested PCR strategy.

(B) Semi-nested PCR of ED 1.5 old embryos displaying all possible combinations of genotypes, such as wild type,  $\Delta$ /+ (PLRG-1 $\Delta$ /+) and KO (PLRG-1 $\Delta$ / $\Delta$ )

$\Delta$  stands for the deleted allele

Although I could identify PLRG-1-deficient embryos up to ED 1.5, microscopical inspection revealed their substantial degradation (Fig. 3.5). In contrast, wild type embryos exhibited a normal two-cell stage morphogenesis at ED 1.5 (Fig. 3.5).

These results indicate that PLRG-1 plays a crucial role during early embryogenesis at the stage of the first cell division.

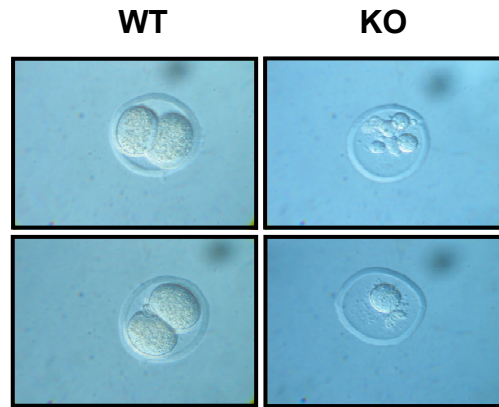


**Figure 3.5: Representative morphology of wild type and PLRG-1-deficient embryos at ED1.5**

Wild type embryos show normal two-cell stadium, whereas knockout embryos are degenerated, showing failed division and fragmented nuclei. Shown are representative pictures of 9 embryos of each genotype analyzed.

### 3.5 Generation of a conditional PLRG-1 gene replacement vector

As embryonic death of PLRG-1-deficient embryos does not permit any further analysis, I decided to inactivate the *PLRG-1* gene conditionally. The targeting vector introduced loxP sites upstream and downstream of exon 3, and deletion of exon 3 by Cre-mediated recombination was predicted to cause a frame-shift mutation resulting in a translational stop after 59 amino acids (Fig. 3.6A).

The pGK12 vector was used and the cloning steps were performed as described for the conventional targeting strategy. To introduce the 2.5 kb short arm of homology consisting of exon 1, intron 1 and the first 27 bp of exon 2 amplified from C57BL/6 BAC DNA via PCR. For this purpose the primers KA5 and KA3 were used containing restriction sites for *NotI* and *SacII*, respectively. For amplification of the loxP-flanked exon 3, oligonucleotides flExon3\_5 and flExon3\_3 harbouring *AscI* and *FseI* restriction sites were used. The fragment was digested with the respective restriction enzymes and cloned into the pGK12 vector already containing the short arm of homology. The 5 kb long arm of homology consisting of a 5 kb fragment including genomic DNA from exons 4 to 6 was PCR-amplified with the primers LA5 and LA3, containing restriction sites for *XhoI* and *PmeI*. The long arm of homology was introduced with the

respective restriction enzymes into the pGK12 vector already containing the short arm of homology and the loxP-flanked exon 3. The sequences of used oligonucleotides are depicted in table 2.1. All PCR products were subcloned and verified by sequencing and restriction digest analysis. V6.5 (129Sv x C57BL/6) ES cells were electroporated with 30 µg of *NotI* linearized targeting vector and double selected with G418 and ganciclovir (as described in materials and methods). 450 clones were isolated and analyzed by Southern Blot using the same probes described for the conventional targeting vector (Fig. 3.6A and B). Probe A was used to determine 5' integration of correctly targeted clones after *BamHI* digestion, resulting in a recombinant band of 4.4 kb besides the 7.8 kb wild type band. *BglI* digest and use of probe B verified single and 3' integration of the construct through a 5.8 kb band. To confirm the cointegration of the external 3' loxP site, a PCR was performed using oligonucleotides Lox5 and Lox3 (Fig. 3.6C). Four homologous recombinant clones containing the external loxP site could be identified. Injection of one homologous ES cell clone into BL/6 blastocysts yielded in high-grade chimeras transmitting the conditional *PLRG-1* allele (*PLRG-1<sup>lox/+</sup>*) through germline. Intercrosses of *PLRG-1<sup>lox/+</sup>* mice generated *PLRG-1<sup>lox/lox</sup>* mice according to the expected Mendelian ratios.

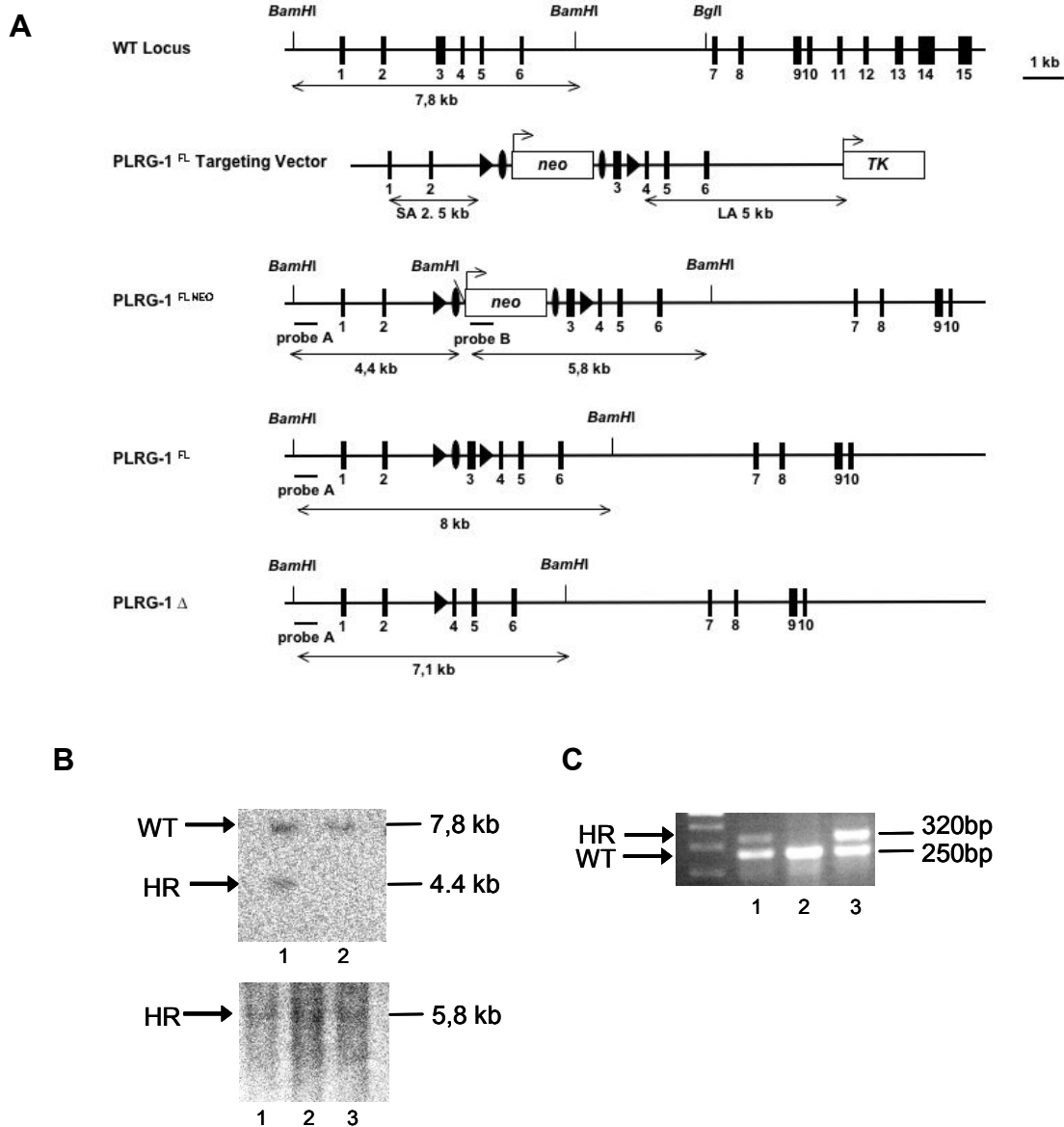


**Figure 3.6: Conditional inactivation of the *PLRG-1* gene**

(A) Schematic representation of the targeting strategy to introduce loxP sites (triangles) into the *PLRG-1* locus.

(B) Southern Blot analysis of ES cell clones after electroporation with the targeting construct shown in A. Blots were hybridized with the probes depicted in A. Upper panel: Homologous recombinant (1) displaying a 4.4kb band beside the 7.8kb wild type band using a *Bam*HI digest and probe A specific for *PLRG-1*. Lower panel: The 5.8 kb band indicates single integration of the targeting vector using *Bam*HI digested DNA and probe B hybridizing to the neomycin resistance gene (1).

(C) PCR analysis with primers flanking the 3'-loxP site confirming co-integration of this loxP site. The 250bp band indicates the wild type (wt) locus, whereas the 320bp band displays the correct integration of the external loxP site (1 and 3).

### 3.6 Inactivation of PLRG-1 in mouse embryonic fibroblasts blocks cell proliferation

For *in vitro* experiments, mouse embryonic fibroblasts (MEF) from wild type and PLRG-1<sup>flx/flx</sup> embryos were generated and treated with recombinant, cell permeable Cre protein (HTNC) (Peitz et al., 2002). Cre-treatment resulted in efficient removal of exon 3 from the PLRG-1<sup>flx/flx</sup> locus as verified by PCR using oligonucleotides LA2 and Seq4, yielding a 1.7 kb band for wild type and a 1 kb band for PLRG-1<sup>flx/flx</sup> MEF treated with HTNC (Fig. 3.7A and B). MEFs carrying the resulting *PLRG-1* mutant locus lacked detectable PLRG-1 protein expression as verified by Western Blot analysis (Fig. 3.7C).

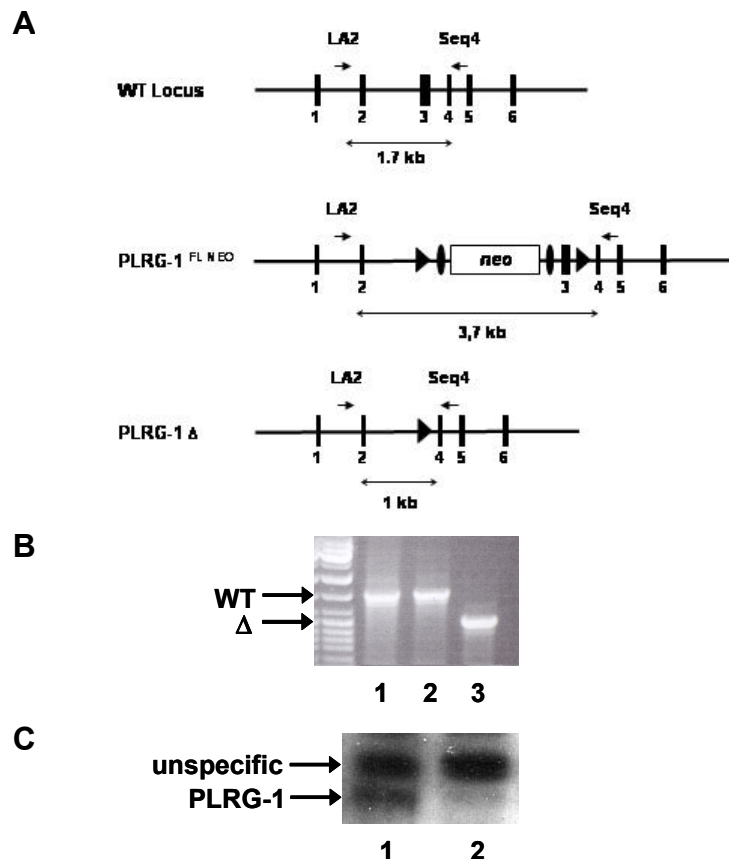


**Figure 3.7: Verification of PLRG-1 deletion in MEFs upon HTNC treatment**

(A) Schematic representation of PCR primer locations

(B) PCR analysis of wild-type (lanes 1 and 2) and PLRG-1<sup>flx/flx</sup> MEF (lane 3, Δ) after treatment with cell permeable Cre-protein using primers LA2 and Seq 4.

(C) Western Blot analysis of wild type (lane 1) and PLRG-1<sup>flx/flx</sup> MEFs (lane 2) after HTNC treatment.

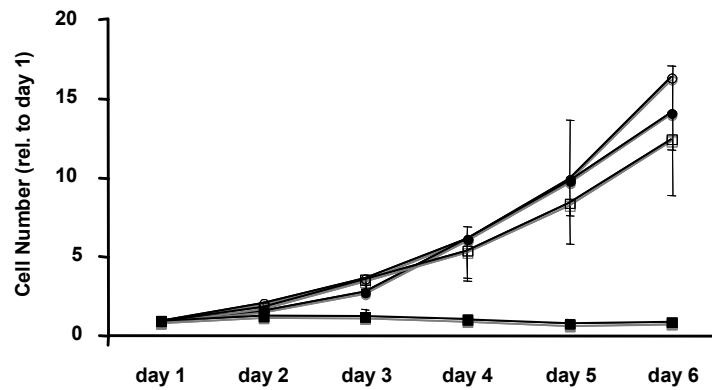
As the conventional PLRG-1 knockout in mice resulted in a defect in cell division during embryogenesis, the growth rate of wild type and PLRG-1<sup>flox/flox</sup> MEFs was determined in the absence or presence of HTNC treatment. Cells were incubated overnight in serum free DMEM with or without HTNC, thereafter re-exposed to medium supplemented with fetal calf serum and were counted every day using a Neubauer Hemocytometer.

Cre-treatment of PLRG-1<sup>flox/flox</sup> MEFs resulted in an immediate growth arrest of these cells, while having no effect on wild type MEF proliferation compared to untreated wild type and PLRG-1<sup>flox/flox</sup> MEFs (Fig. 3.8A). Also, PLRG-1-deficiency in MEFs resulted in a larger cell size, potentially due to a block in G<sub>0</sub>/G<sub>1</sub>- or in G<sub>2</sub>/M-phase (Fig. 3.8B).

This phenotype is similar to the phenotype observed in conventional PLRG-1 knockout mice, in which the PLRG-1 mutation resulted in a failure to execute the first cell division during embryogenesis, emphasizing the assumption that PLRG-1 is essential for cell proliferation.



A



B

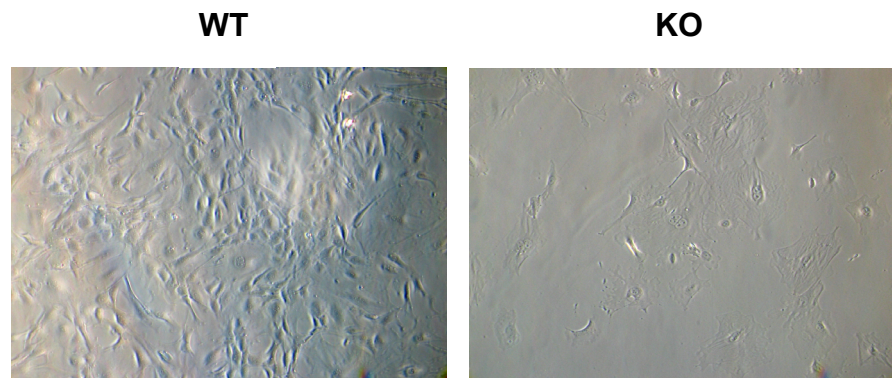


**Figure 3.8: Growth rates and morphology of untreated or Cre-treated wild type and PLRG-1<sup>flox/flox</sup> MEFs**

(A) Circles: WT MEFs; squares: PLRG-1<sup>flox/flox</sup> MEFs; open symbols: -Cre; closed symbols: +Cre. Data represent mean  $\pm$  SEM of three independent experiments, each performed in duplicate

(B) MEFs were treated with cell-permeable HTN-Cre and microphotographed after 48h incubation.

### 3.7 PLRG-1 deficiency prevents S-phase entry

To define the precise role of PLRG-1 during cell proliferation, analysis of serum stimulated cell cycle progression in wild type and PLRG-1-deficient MEFs by fluorescence activated cell sorting (FACS) was performed. Using propidiumiodide (PI) as an intercalating dye for DNA, it is possible to distinguish between G<sub>0</sub>/G<sub>1</sub>-, S- and G<sub>2</sub>/M-phase. The first peak in a FACS histogram

represents the G<sub>0</sub>/G<sub>1</sub>-phase, in which cells contain the normal 2n DNA content. The following S-Phase is relatively short with a duration of approximately 2 to 4 hours. It contains an intermediate DNA content and is depicted in a histogram as the phase between the two peaks. The second peak displays the G<sub>2</sub>/M-phase, which is characterized by the double 4n DNA content after S-phase and is the last phase before entering mitosis and cytokinesis. Here again cells grow until they receive the signal to progress into mitosis. To perform this experiment, cells have to be synchronized by serum depletion for 24 – 48 h resulting in resting cells in G<sub>0</sub>/G<sub>1</sub> phase. After addition of serum, cells will progress simultaneously into cell cycle allowing the distinction between the different cell cycle phases.

While serum stimulation resulted in G<sub>1</sub>- to S-phase progression in wild type cells in both absence and presence of recombinant Cre protein, the S-phase entry was blocked in PLRG-1<sup>fllox/fllox</sup> MEF after HTNC treatment (Fig. 3.9).

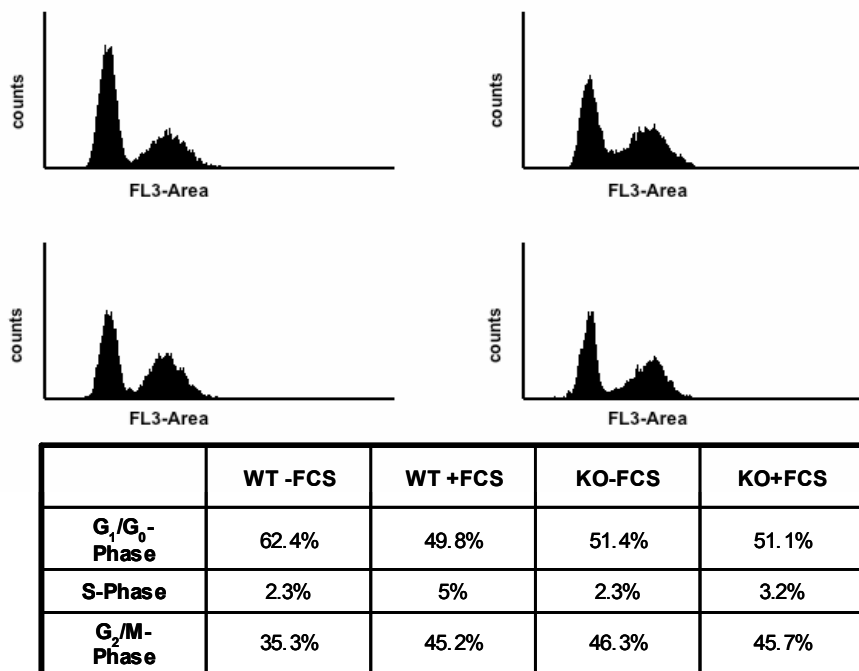


**Figure 3.9: FACS analysis of serum (FCS)-stimulated cell cycle progression in control and PLRG-1-deficient MEFs**

Different cell cycle phases of wild-type and PLRG-1-deficient MEFs before serum stimulation (-FCS: left) and 24 h after serum stimulation (+FCS: right). Distribution of cell cycle phases obtained from three independent experiments are summarized in the table.

To confirm the observed block in cell cycle as revealed by FACS analysis, a  $^3\text{H}$ -thymidine incorporation assay was performed. This method determines the ability to replicate DNA by measuring the incorporation of  $^3\text{H}$ -thymidine into newly synthesized DNA. Therefore, cells were again synchronized by serum deprivation to start in the  $G_0/G_1$ -phase and were then stimulated with 10% FCS to initiate cell cycle progression. The  $^3\text{H}$ -thymidine content of wild type and PLRG-1<sup>fl $\alpha$ /fl $\alpha$</sup>  MEFs treated with HTNC protein was measured at 0, 16 and 24 h after FCS stimulation. PLRG-1-deficient MEFs did not incorporate  $^3\text{H}$ -thymidine at any time point, which confirmed the disability to progress into the S-phase (Fig. 3.10), demonstrating that PLRG-1 is required for serum-stimulated  $G_1/S$ -phase transition in murine cells.

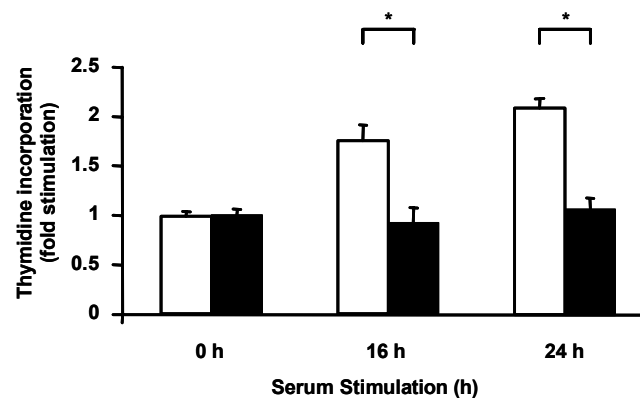


**Figure 3.10:  $^3\text{H}$ -thymidine incorporation of wild type and PLRG-1-deficient MEFs**  
 $^3\text{H}$ -thymidine incorporation was measured after 0, 16, and 24 h of serum stimulation in wild-type (open bars) and PLRG-1-deficient (closed bars) MEFs. Values represent mean  $\pm$  SEM values from three independent experiments ( $*p < 0.05$ ).

### 3.8 PLRG-1 deficiency increases p53 expression and induces apoptosis

To investigate the molecular mechanism by which PLRG-1 ablation prevents cells from entering the S-phase, the early regulatory steps of  $G_1/S$  transition were examined using biochemical approaches. Wild type and PLRG-1<sup>fl $\alpha$ /fl $\alpha$</sup>  MEFs were treated with cell permeant Cre-protein to delete PLRG-1, serum deprived for 48 h to synchronize MEFs in  $G_0/G_1$ -phase and subsequently stimulated with 10% FCS to progress into cell cycle. Cells were harvested,

lysed and cellular proteins were separated by SDS-PAGE, transferred onto PVDF membranes to determine expression and phosphorylation of proteins responsible for G<sub>1</sub>/S-phase progression, such as Erk1 and Erk2 MAP kinases, which are key mediators of proliferative signalling by Western Blot analysis. In addition, proteins, which are expressed as a result of Erk1 or Erk2 activation, such as Cyclin D1 and Cyclin E, were also analyzed.

During G<sub>1</sub>- to S-phase progression, Cyclin D1 binds CDK4 and allows for the hyperphosphorylation of Retinoblastoma (Rb) protein, leading to a release of the transcription factor E2F. E2F is responsible for transcription of proteins involved in DNA replication and cell cycle progression, such as MCM proteins and Cyclin E. Cyclin E, in turn, activates more CyclinD1/CDK4 complexes, thereby promoting the G<sub>1</sub>-S-phase progression.

Expression and activation status of other proteins involved in a G<sub>1</sub>/S-phase block, namely p53, stabilized S15-phosphorylated p53 and CDK inhibitor p21, were also determined.

Examination of the regulatory steps of G<sub>1</sub>/S transition revealed an unaltered biphasic activation of MAP kinases Erk1 and Erk2 in both wild type and PLRG-1-deficient MEFs upon serum stimulation (Fig. 3.11) (Balmanno and Cook, 1999). In contrast, serum stimulated Cyclin D1 expression was dramatically reduced in PLRG-1-deficient MEFs compared to wild type cells (Fig. 3.11). The mutant cells also displayed significantly lower Cyclin E expression (Fig. 3.11). Concomitantly, expression of p53, and also, during later time points of serum stimulation, of CDK inhibitor p21 were increased in the absence of PLRG-1 (Fig. 3.11).

The activity of p53 is tightly controlled via posttranslational modification, in particular through stabilization by phosphorylation (Nakagawa et al., 1999; She et al., 2000; Vega et al., 2004). Therefore, the phosphorylation state of p53 was analyzed by immunoblotting using an antibody recognizing phosphorylated p53 at serine 15. During the course of serum stimulation, remarkably higher levels of p53 phosphorylation at serine 15 were observed in PLRG-1-deficient cells compared to wild type cells (Fig. 3.11). Taken together, the elevated levels of phosphorylated p53 protein correlate with the block of S-phase transition and the increase of CDK-inhibitor p21 levels in MEF cells lacking PLRG-1.

Since continuously elevated p53 levels are known to induce apoptosis (M. Schuler, 1997), I directly addressed whether apoptosis is increased in PLRG-1-deficient MEFs. Therefore, TUNEL assays were performed, which revealed a dramatic induction of apoptosis in PLRG-1-deficient MEFs compared to wild type controls (Fig. 3.12). PLRG-1-deficient MEFs exhibited approximately 7%, whereas wild type cells displayed 0.5% of apoptotic cells (Fig. 3.12).

To further characterize p53-induced apoptosis, expression of p53 targets and downstream effectors of apoptosis was determined. Caspase 3, an aspartate-specific cysteine protease, is a key executor of apoptosis and is typically activated by proteolytic processing. It triggers apoptosis by cleavage of different cytosolic and nuclear substrates, such as poly (ADP-ribose) polymerase (PARP) and ICAD. Consistent with the detection of enhanced apoptosis, cleavage of caspase 3 was also dramatically increased, as assessed by Western Blot (Fig. 3.12). This was paralleled by increased levels of the pro-apoptotic Bax protein, its gene being a well-characterized target of p53, along with a slight decrease in the level of anti-apoptotic Bcl-2-protein in PLRG-1-deficient MEFs (Fig. 3.12).

In summary, these experiments indicate that PLRG-1 deficiency blocks G<sub>1</sub>/S-phase transition and stimulates apoptosis, possibly as a consequence of increased p53 phosphorylation and stabilization

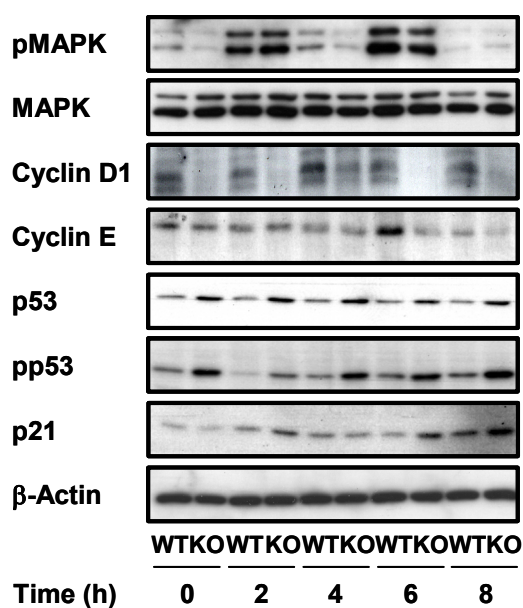


**Figure 3.11: Western blot analysis of HTNC-treated wild type (WT) and PLRG-1<sup>flox/flox</sup> MEF (KO)**

HTNC-treated control and PLRG-1<sup>flox/flox</sup>-fibroblasts were serum deprived for 48 h and then stimulated with 10% FCS for 2, 4, 6, 8 h, respectively. Expression of MAPK, Cyclin D1, Cyclin E, p53, and p21 as well as phosphorylation of MAPK and S-15 phosphorylation of p53 were analyzed by western blot. Anti-β-actin served as a loading control.

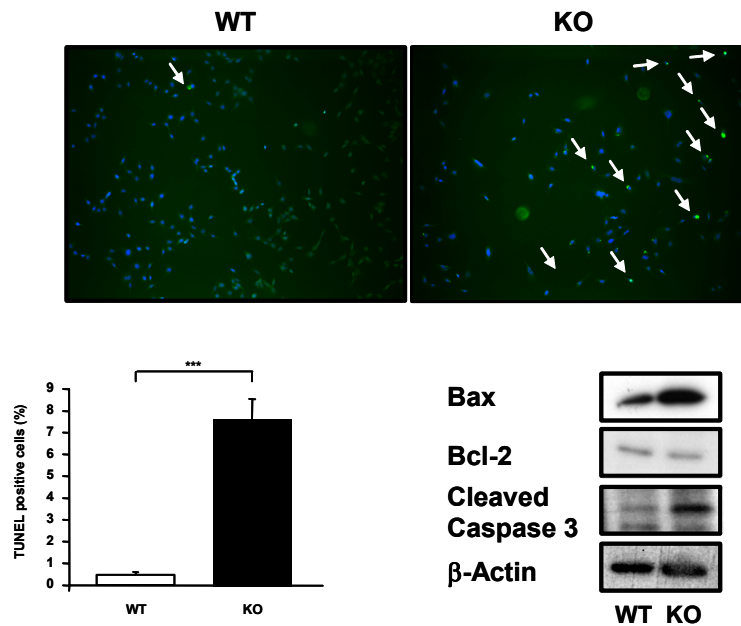


**Figure 3.12: TUNEL analysis of wild type and PLRG-1-deficient MEFs**

Upper panel: Photomicrograph of TUNEL-stained wild type and PLRG-1-deficient MEFs. TUNEL-positive cells are marked by white arrows. Lower left panel: Percentage of apoptotic cells in wild type and PLRG-1-deficient MEFs. Values represent mean  $\pm$  SEM from three independent experiments (\*\* $p < 0.001$ ). Lower right panel: Expression of Bax, Bcl-2, and active cleaved Caspase 3 of wild type and PLRG-1-deficient MEFs. Anti- $\beta$ -actin was used to control for equal loading.

### 3.9 No evidence for altered splicing in PLRG1-deficient MEFs

As PLRG-1 has been initially identified as a component of the spliceosome and as peptides interfering with the PLRG-1/CDC5L interaction inhibit pre-mRNA-splicing *in vitro*, the question was addressed, whether PLRG-1 deletion results in pre-mRNA accumulation and a reduction of mRNA. Therefore, RNA from untreated and HTNC-treated PLRG-1<sup>flox/flox</sup> MEFs was isolated 48 h after Cre-treatment. RNA was DnaseI digested and used for RT PCR. Following, PCR using exon spanning primers for Cyclin D1 (5CycD1, 3CycD1), Cyclin E1 (5CycE1, 3 CycE1) and p53 (p53-5RT, p53-3RT) were performed, to investigate splicing defects of these genes. DNA was used as positive control for detectability of unspliced products, i.e. pre-mRNA. PLRG-1-deficient MEFs did not show aberrant splicing of these genes displaying correct spliced products as observed in untreated PLRG-1<sup>flox/flox</sup> MEFs (Fig 3.13 A and

B). Thereby, reduced Cyclin D1 and E1 expression in PLRG1-deficient MEFs shown in serum stimulated cell cycle progression was not due to aberrant splicing of these genes.

For further validation quantitative Real-time PCR was performed using probes for genes involved in ER stress (Ddit 3), transcriptional and cell cycle regulation (Foxo 1, Foxo 3a), Notch signalling (Notch 1), inflammation (TGF- $\beta$ 1) and cytoskeletal formation (Tuba 1). No difference in expression of these genes was observed, except for  $\alpha$ -tubulin, which was 1.5 fold increased in PLRG1-deficient MEFs (Fig. 3.13 C). This was consistent with the findings in PLRG1-deficient MEFs, which display an increased cell size

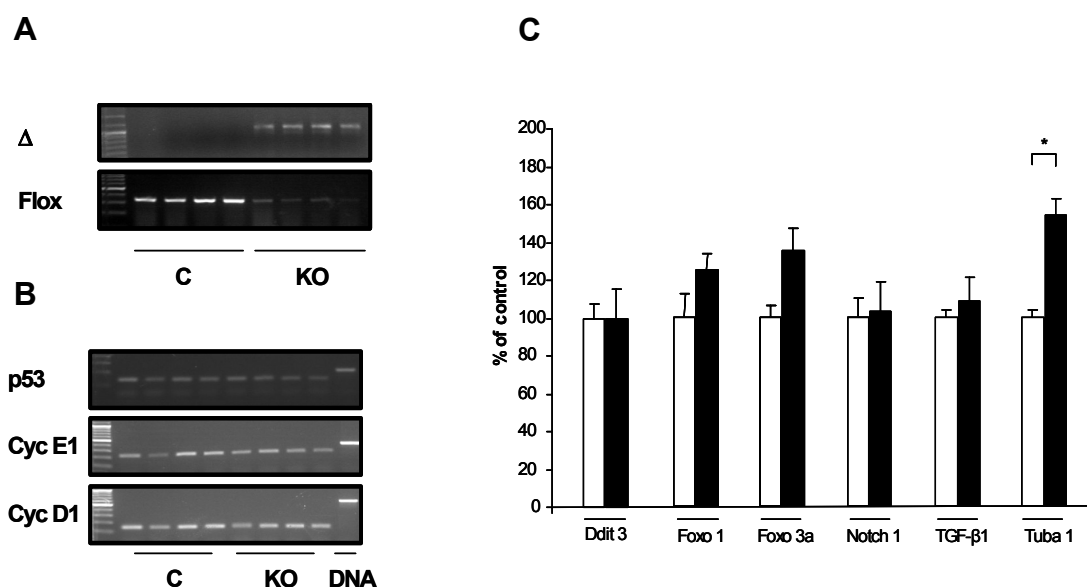


**Figure 3.13: Splicing in PLRG-1-deficient MEFs is unaltered**

(A) PCR analysis of untreated (C) and HTNC treated PLRG-1<sup>flox/flox</sup> MEF (KO) using primers lox3 and lox5 for the loxP flanked allele and LA2 and Seq 4 for the deleted allele

(B) PCR analysis based on cDNA and exon spanning primers. Control and KO samples show no aberrant splicing. DNA represents the unspliced variant of Cyclin D1, Cyclin E1 and p53

(C) Expression analysis of PLRG-1<sup>flox/flox</sup> (open bars) and PLRG-1-deficient (closed bars) MEFs of Ddit 3, Foxo 1, Foxo 3a, Notch 1, TGF- $\beta$ 1 and Tuba 1 using quantitative Real-time PCR. Samples were adjusted for total RNA content by TBP RNA quantitative PCR

Flox stands for PCR product of the loxP flanked allele,  $\Delta$  for PCR product of the deleted allele.

Taken together, these results indicate, that PLRG1-deficient MEFs did not suffer from general alteration in pre-mRNA-splicing, as proposed for yeast or mammals using an adeno-pre-mRNA vector for splicing assays.

### 3.10 PLRG-1-deficient MEFs exhibit no spontaneously detectable DNA double-strand breaks

Since p53 phosphorylation and accumulation represents a response to DNA damage and as it was recently demonstrated, that PLRG-1 is a component of the Pso4-complex, which uncouples DNA interstrand crosslinks, thus ensuring genomic integrity, I next directly addressed whether PLRG-1 deficiency results in spontaneously detectable DNA double-strand breaks.

Therefore, PLRG-1<sup>flox/flox</sup> MEFs left untreated or treated with cell permeable Cre. 48 h after HTNC treatment, MEFs left either unirradiated or were UV irradiated for 2 min to induce genomic instability, namely DNA double-strand breaks. 24 h after UV-irradiation, cells were harvested, agarose embedded, lysed and used for pulse-field gel electrophoresis. Fragmented DNA was released into the gel and visualized using EtBr staining, whereas highmolecular and unfragmented DNA remained in the agarose plugs. Untreated and HTNC-treated MEFs showed no difference in DNA release into the gel, indicating that PLRG-1 deficiency per se did not cause DNA double-strand breaks, whereas UV-irradiated cells displayed DNA fragmentation, resulting in DNA release into the pulse-field gel to similar extend in PLRG-1<sup>flox/flox</sup> and deficient MEFs (Fig. 3.14).

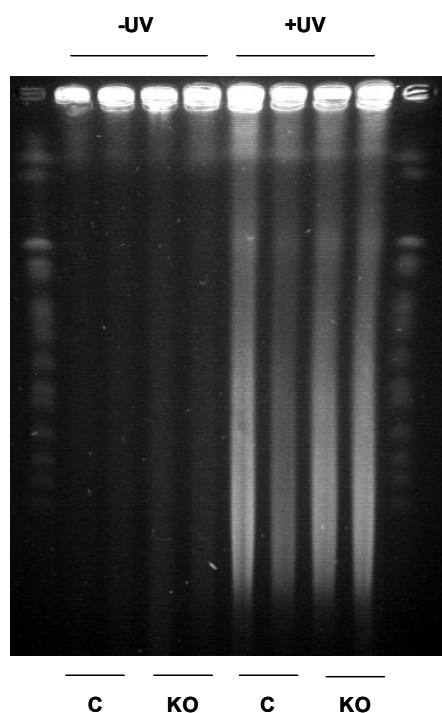


**Figure 3.14: Pulse-field gel electrophoresis of PLRG-1<sup>flox/flox</sup> (control) and PLRG-1-deficient MEFs (KO)**

PLRG-1<sup>flox/flox</sup> MEFs left untreated or treated with HTNC. As control for DNA fragmentation, cells were UV treated. The gel shows two control versus two KO samples.



In summary, these experiments indicate that PLRG-1 deficiency does not enhance genomic instability, by promoting occurrence of spontaneous DNA double-strand breaks.

### 3.11 PLRG-1 deficiency results in enhanced $\gamma$ -H2AX phosphorylation

As a consequence of stalled replication forks or DNA double-strand breaks spontaneously occurring during DNA replication, the phosphorylation of  $\gamma$ -H2AX was investigated using immunofluorescence.  $\gamma$ -H2AX represents a variant of histone proteins, which are phosphorylated by members of the PIKK-family, such as ATM and ATR, thereby recruited to stalled replication forks or DNA lesions.

Therefore PLRG-1-deficient MEFs were investigated in terms of  $\gamma$ -H2AX phosphorylation. PLRG-1<sup>flox/flox</sup> MEFs left untreated or treated with cell permeant Cre protein. 48 h after HTNC treatment, cells were fixed and stained with phospho-S139- $\gamma$ -H2AX antibody. PLRG-1-deficient MEFs showed enhanced  $\gamma$ -H2AX phosphorylation compared to untreated PLRG-1<sup>flox/flox</sup> MEFs displaying an increase in  $\gamma$ -H2AX foci (Fig. 3.15A). About 90% of PLRG-1-deficient MEFs were  $\gamma$ -H2AX positive compared to 10% of untreated MEFs (Fig. 3.15B) These data indicate that PLRG-1 deficiency results in increment of  $\gamma$ -H2AX foci as a result of stalled replication forks, rather than DNA double-strand breaks as shown in figure 3.14 using PFGE.

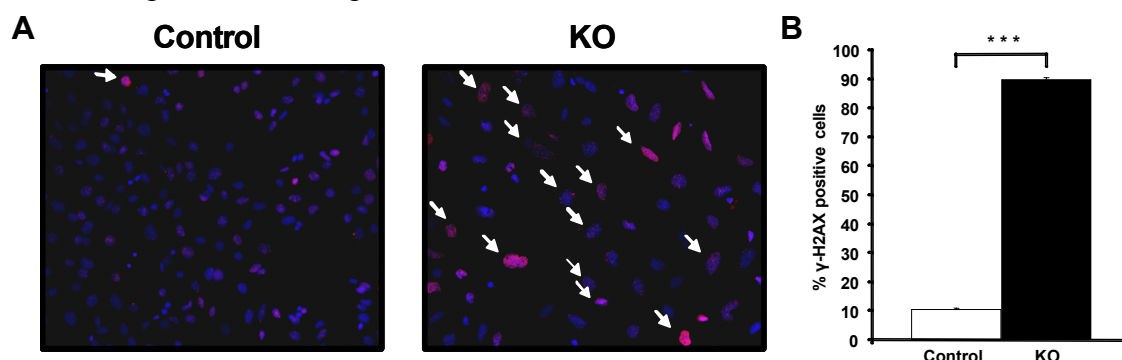


**Figure 3.15: Analysis of  $\gamma$ -H2AX phosphorylation in untreated and HTNC-treated PLRG-1<sup>flox/flox</sup> MEFs**

(A) Photomicrograph of phospho-S139- $\gamma$ -H2AX -stained PLRG-1<sup>flox/flox</sup> (Control) and PLRG-1-deficient MEFs (KO). Representative S139- $\gamma$ -H2AX-positive cells are marked by white arrows. (B) Percentage of  $\gamma$ -H2AX positive cells in control and PLRG-1-deficient MEFs. Values represent mean  $\pm$  SEM from three independent experiments (\*\* $p < 0.001$ )

### 3.12 Conditional inactivation of PLRG-1 in heart and skeletal muscle

To examine developmental regulatory effects of PLRG-1 *in vivo*, mice with conditional tissue-specific inactivation of the *PLRG-1* gene were generated. To obtain mice lacking PLRG-1 specifically in skeletal muscle and heart, PLRG-1<sup>flox/+</sup> mice were crossed with mice expressing the Cre recombinase under the control of the muscle-specific creatinine kinase (MCK) promoter (Brüning et al., 1998). Double-heterozygous PLRG-1<sup>flox/+</sup>MCKCre mice were crossed with PLRG-1<sup>flox/flox</sup> mice to obtain PLRG-1<sup>flox/flox</sup>MCKCre offspring lacking PLRG-1 expression in skeletal muscle and heart (PLRG-1<sup>Δmus</sup>). As in the case of conventional PLRG-1-deficient knockout mice, the analysis of offspring from these breedings at postnatal day 28 revealed the absence of PLRG-1<sup>Δmus</sup> mice, indicating that PLRG-1 deficiency also in skeletal muscle and heart results in early lethality (Table 3.2).

**Table 3.2: Genotype analysis of mice obtained from breedings of PLRG-1<sup>flox/flox</sup> mice with PLRG-1<sup>flox/+</sup>MCKCre mice**

	PLRG-1 <sup>flox/+</sup>	PLRG-1 <sup>flox/flox</sup>	PLRG-1 <sup>flox/+</sup> MCKCre	PLRG-1 <sup>Δmus</sup>	Total
P1	18	16	28	20	82
P28	10	19	16	0	45

However, in contrast to the conventional knockout mice, PLRG-1<sup>Δmus</sup> mice were detected at the expected Mendelian frequency at birth (Table 3.2) leading to the assumption that during early lifespan a defect in heart and skeletal muscle occurs due to PLRG-1 deficiency. To confirm heart- and muscle-specific recombination of the *PLRG-1* gene in PLRG-1<sup>Δmus</sup> mice, genomic DNA was extracted from individual tissues of PLRG-1<sup>flox/flox</sup> and PLRG-1<sup>Δmus</sup> mice at postnatal day 5 and subjected to PCR analysis using the oligonucleotides LA2 and Seq4 as shown in figure 3.7. Surprisingly, only in heart successful recombination could be detected (Figure 3.16). Presumably, expression and activity of MCKCre in skeletal muscle is initiated during later stages of murine development. Deletion efficiency in heart was not 100%, as can be concluded

from the appearance of a PCR product for the floxed allele besides the band for the deleted allele. It is possible that full Cre expression and activity in heart cannot be reached before failure of the organ.

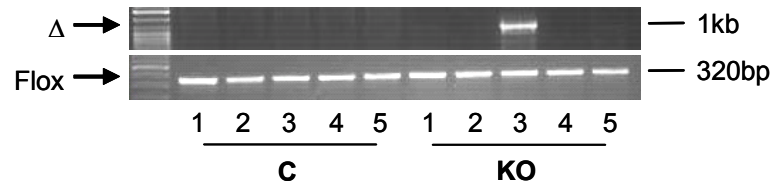


**Figure 3.16: Heart-restricted PLRG-1 deficiency in PLRG-1<sup>Δmus</sup> mice**

PCR analysis of genomic DNA isolated from different organs of 5d old PLRG-1<sup>flox/flox</sup> and PLRG-1<sup>Δmus</sup> mice. The panel shows the specific deletion of PLRG-1 in the heart using primers flanking exon 3. Excision of exon 3 is indicated by PCR amplification of a 1 kb DNA fragment ( $\Delta$ ). PCR analysis with primers flanking the 3'-loxP site was used as loading control (Flox) (1: brain, 2: skeletal muscle, 3: heart, 4: liver, 5: spleen).

Close postnatal monitoring of the litters revealed that, while 80% of control mice survived the first 28 days of life, the survival rate of PLRG-1<sup>Δmus</sup> mice was dramatically reduced to 5% during the same period (Fig. 3.17). The premature death of control animals displays normal values for animals kept under standard animal care in the animal facility.

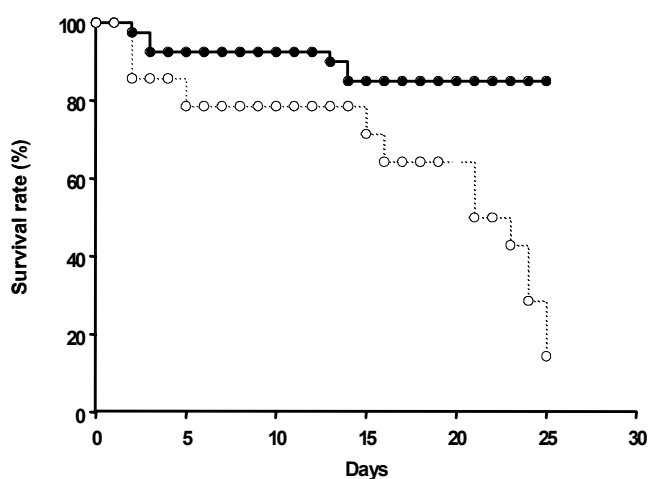


**Figure 3.17: Survival rate of control and PLRG-1<sup>Δmus</sup> mice**

Survival rate of control (closed circles) and PLRG-1<sup>Δmus</sup> (open circles) mice (n = 40 control (PLRG-1<sup>flox/flox</sup>, PLRG-1<sup>flox/+</sup> and wild type), n = 14 PLRG-1<sup>Δmus</sup>).

### 3.13 Conditional inactivation of PLRG-1 in heart results in dilated cardiomyopathy due to increased cardiomyocyte apoptosis

Because Cre-mediated recombination was only detectable in heart, heart function in mice surviving up to postnatal days 24 to 26 was investigated. Opening of the thorax revealed an increase in heart size in PLRG-1<sup>Δmus</sup> mice (Fig 3.18A) Consistent with this observation, quantitative assessment of heart mass revealed an increase in heart weight of PLRG-1<sup>Δmus</sup> mutant compared to control mice (PLRG-1<sup>flox/flox</sup>) (Fig. 3.18B)

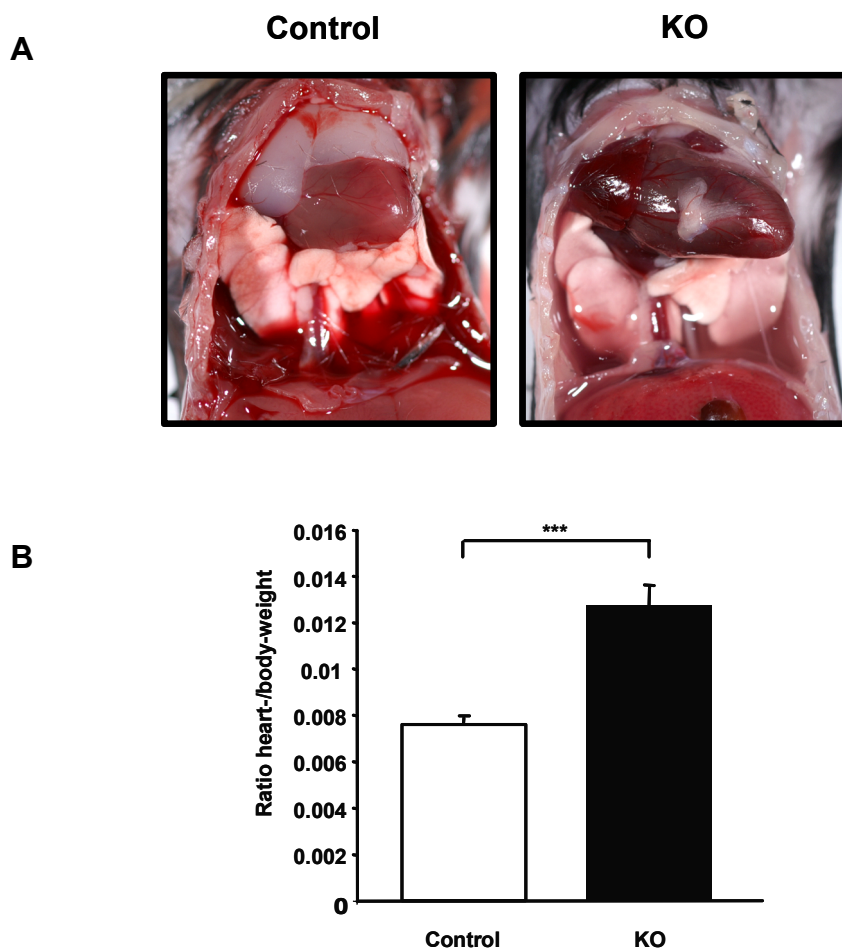


**Figure 3.18: Heart-phenotype of PLRG-1<sup>Δmus</sup> mice**  
(A) Autopsy of postnatal day 24 control (PLRG-1<sup>flox/flox</sup>) and PLRG-1<sup>Δmus</sup> (KO) mice. Note the enlarged heart for PLRG-1<sup>Δmus</sup> compared to control.  
(B) Relative heart/body weight ratio in control and PLRG-1<sup>Δmus</sup> mice. Data represent the mean ± SEM of seven control and six PLRG-1<sup>Δmus</sup> mice (\*\**p* < 0.001).

Haematoxylin / Eosin staining and histological analysis of hearts at postnatal day 24 demonstrated severe thinning of both ventricle walls and

massive dilatation of both left and right ventricle in hearts derived from PLRG-1<sup>Δmus</sup>, reflecting the pathology of severe dilated cardiomyopathy (Fig. 3.19).

Taking into account the results obtained from the analysis of PLRG-1-deficient MEFs, the question arose, whether the heart dilation was due to increased apoptosis of cardiomyocytes. In fact, TUNEL staining of explanted heart tissue revealed an increase in apoptotic cardiomyocytes in the PLRG-1<sup>Δmus</sup> mice compared to control mice (Fig. 3.19).

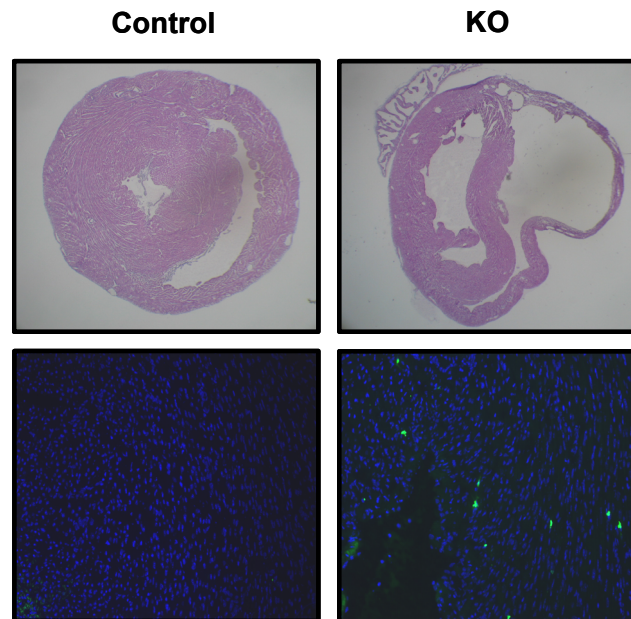


**Figure 3.19: Histological analysis of control- and PLRG-1<sup>Δmus</sup>-hearts at the age of 24 days**

The upper panel shows H&E stained control and PLRG-1<sup>Δmus</sup> hearts. The lower panel shows TUNEL stained heart sections, revealing increased cardiomyocyte apoptosis in PLRG-1<sup>Δmus</sup> hearts.

Western blot analysis of protein extracts from hearts of control and PLRG-1<sup>Δmus</sup> mice showed increased Bax and decreased Bcl-2 expression (Fig. 3.20). Consistent with the previous findings in PLRG-1-deficient MEFs, hearts of PLRG-1<sup>Δmus</sup> mice also showed higher levels of phosphorylated p53 (Fig. 3.20). Taken together, these results establish the underlying molecular basis of PLRG-1<sup>Δmus</sup> pathology, which is characterized by dilated cardiomyopathy due to increased cardiomyocyte apoptosis in the presence of enhanced p53 phosphorylation along with increased Bax and decreased Bcl-2 expression. The data also demonstrate that the PLRG-1-dependent pathway regulating

apoptosis, as determined for PLRG-1-deficient MEFs, is also functional in tissues of postnatal mice.

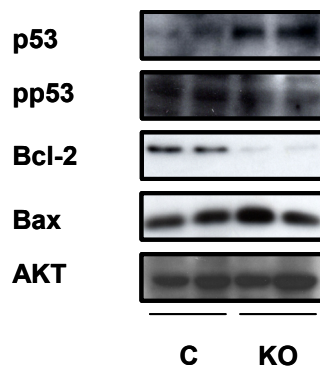


**Figure 3.20: Western blot analysis of control (C) and PLRG-1<sup>Δmus</sup>-(KO) hearts**  
 Expression of total cellular protein extracts of p53, S15-phospho-p53 (pp53), Bcl-2 and Bax was analyzed by western blotting. Anti-AKT was used to control for equal loading.

### 3.14 Conditional inactivation of PLRG-1 in the central nervous system of mice results in early postnatal lethality

To investigate whether the observed phenotype of PLRG-1 deficiency represents a more general phenomenon, PLRG-1 was also inactivated in another predicted non-mitotic organ, i.e. the post-mitotic neurons in the central nervous system (CNS), by intercrossing PLRG-1<sup>flox/flox</sup> mice with mice expressing the Cre recombinase under control of the Synapsin promoter (Zhu et al., 2001). The Cre transgene was always transferred maternally due to an undesired germline activity in males (Rempe et al., 2006). PLRG-1<sup>flox/flox</sup> mice were crossed with PLRG-1<sup>flox/+</sup>SynCre mice to obtain PLRG-1<sup>ΔCNS</sup> mice with neuron-restricted PLRG-1 deficiency. These mice also revealed early lethality as no PLRG-1<sup>ΔCNS</sup> mice reached the age of weaning (Table 3.3).

**Table 3.3: Genotype analysis of mice obtained from breedings of PLRG-1<sup>flox/flox</sup> mice with PLRG-1<sup>flox/+</sup>SynCre mice**

	PLRG-1 <sup>flox/+</sup>	PLRG-1 <sup>flox/flox</sup>	PLRG-1 <sup>flox/+</sup> SynCre	PLRG-1 <sup>ΔCNS</sup>	Total
P1	11	13	18	13	55
P21	8	8	13	0	29

Monitoring of the litters directly after birth showed an even more dramatic phenotype of  $PLRG-1^{\Delta CNS}$  mice than  $PLRG-1^{\Delta mus}$  mice.  $PLRG-1^{\Delta CNS}$  mice had survival rates of only 25% at postnatal day 3, while control mice showed an 88% survival rate, representing normal surviving variations of mouse populations in standard animal facilities. On postnatal day 9 no surviving  $PLRG-1^{\Delta CNS}$  mice were observed, indicating again the important role  $PLRG-1$  plays in the developing mouse (Fig. 3.21).

PCR analysis of genomic DNA derived from 3 day old control and  $PLRG-1^{\Delta CNS}$  mice at postnatal day 3 using oligonucleotides LA2 and Seq4, confirmed CNS-restricted recombination of the  $PLRG-1$  gene in  $PLRG-1^{\Delta CNS}$  mice (Fig. 3.22). Again, deletion was not complete, since full Cre expression and activity would require longer survival.

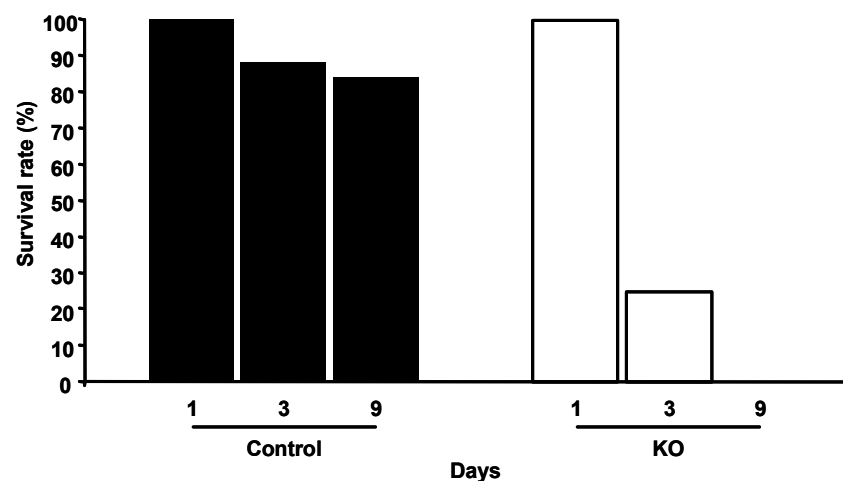


**Figure 3.21: Survival rate of control and  $PLRG-1^{\Delta CNS}$  mice**  
Survival rate of control ( $n = 25$  ( $PLRG-1^{flox/flox}$ ,  $PLRG-1^{flox/+}$  and wild type)) and  $PLRG-1^{\Delta CNS}$  ( $n = 12$ ) mice at days 1, 3, and 9.

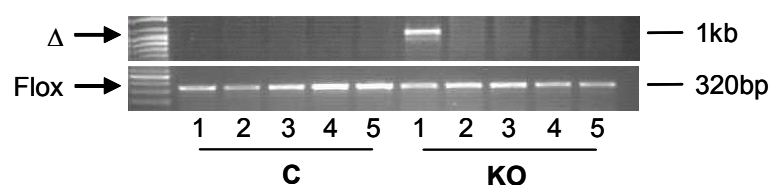


**Figure 3.22: Analysis of neuron-restricted recombination of the  $PLRG-1^{flox/flox}$  allele**  
The panel shows specific deletion of  $PLRG-1$  in the brain of  $PLRG-1^{\Delta CNS}$  mice (KO). Using a primer pair flanking exon 3, the appearance of a product of 1 kb indicated excision of exon 3 ( $\Delta$ ). PCR analysis with primers flanking the 3'-loxP site was used as loading control (Flox) (1: brain, 2: skeletal muscle, 3: heart, 4: liver, 5: spleen). C stands for  $PLRG-1^{flox/flox}$  mice (control)



As PLRG-1 deficiency induced apoptosis in both MEFs and heart tissue, I also examined the occurrence of apoptosis in the CNS of control and PLRG-1<sup>ΔCNS</sup> mice. Brains from control (PLRG-1<sup>flox/flox</sup>) and PLRG-1<sup>ΔCNS</sup> mice at postnatal day 3 were dissected and used for TUNEL analysis. Investigation of control and PLRG-1<sup>ΔCNS</sup> mice revealed a dramatic increase in the number of apoptotic neurons in the dentate gyrus of PLRG-1<sup>ΔCNS</sup> mice, coinciding with the region where Synapsin Cre mice have been shown to recombine most efficiently and where neurogenesis takes place (Fig 3.23) (Zhu et al., 2001). PLRG-1<sup>ΔCNS</sup> mice showed reduced agility, trembled and were not able to roll over when turned on their back.

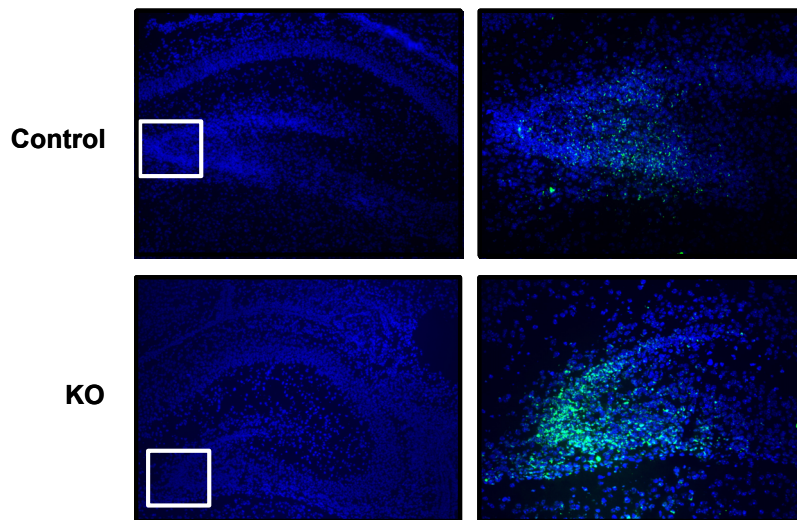


**Figure 3.23:** Immunohistochemical analysis of brains dissected from 3-day-old control and PLRG-1<sup>ΔCNS</sup> mice

Left and right panels: DAPI (nucleus) and TUNEL staining for control and KO of the same brain sections.

As in PLRG-1-deficient MEFs and PLRG-1<sup>Δmus</sup> mice, Western Blot analysis of brain tissue revealed increased p53 expression levels as well as enhanced p53 serine 15-phosphorylation in PLRG-1<sup>ΔCNS</sup> mice. Bax levels remained unaltered in brain cells, whereas PLRG-1<sup>ΔCNS</sup> mice also displayed a decrease in Bcl-2 expression (Fig. 3.24).



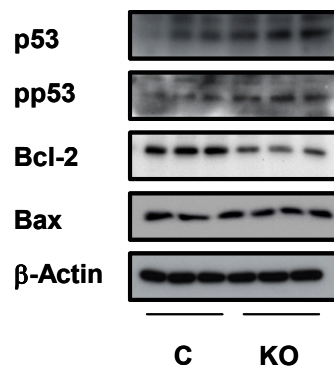


**Figure 3.24: Western blot analysis of control (C) and PLRG-1<sup>ΔCNS</sup> (KO) hearts**

Western blot analysis of total cellular protein extracts from control (WT) and PLRG-1<sup>mus</sup>-(KO) hearts showing expression of p53, S15-phospho-p53 (pp53), Bcl-2 and Bax. Anti- $\alpha$ -tubulin was used to control for equal loading.

In summary, the absence of PLRG-1 in the CNS leads to massive apoptosis in the hippocampus. Thus, deficiency of PLRG-1 in the CNS evokes a similar apoptotic response to that observed in PLRG-1-deficient MEFs or cardiomyocytes.

### 3.16 Interaction of the nuclear CDC5L-PLRG-1 complex with the p53 phosphatase WIP1 is disrupted in the absence of PLRG-1

The previous studies with heart- and neuron-specific PLRG-1 knockout mice revealed massive apoptosis in the respective tissues, responsible for the premature death of the animals. Moreover, PLRG-1-deficient MEFs failed to enter S-phase upon serum stimulation and showed increased apoptosis as a result of enhanced p53 phosphorylation and stabilization. To understand the molecular basis of the PLRG-1 deficiency phenotype, the connection between PLRG-1 and p53 was further investigated.

Mass spectrometry and affinity purification analyses of proteins associated with CDC5L, the known interaction partner of PLRG-1, identified numerous spliceosomal components including ASF/SF2, hnRNP-G, SAP145, and U2A, as well as protein phosphatases such as PP1, PP2, and WIP1. Taking this into account, the question was addressed whether the CDC5L-PLRG-1 complex interacts with known p53 phosphatases, in particular with

WIP1. To this end, nuclear extracts of wild type MEFs were immunoprecipitated with anti-WIP1 or an unrelated control followed by Western Blot analysis with anti-CDC5L. This analysis revealed the presence of CDC5L protein in WIP1 immunoprecipitates, but not in the unrelated controls (Fig. 3.25A), confirming the interaction of CDC5L and WIP1 in wild type control cells as previously reported (Ajuh 2000)

To determine whether the CDC5L-WIP1 interaction was also detectable in PLRG-1-deficient cells, co-immunoprecipitation experiments were performed using nuclear extracts from PLRG-1<sup>fl<sup>ox</sup>/fl<sup>ox</sup></sup> MEFs 48 h after Cre treatment. Surprisingly, this analysis revealed no immunoreactive CDC5L in WIP1 precipitates of PLRG-1-deficient nuclei (Fig. 3.25A).

To investigate whether this failure of CDC5L-binding to WIP1 is dependent on protein degradation or cytosolic translocation, CDC5L content was assessed in the respective fractions using Western Blot analysis. No difference in the total cellular content of CDC5L between wild type and PLRG-1-deficient MEFs was observed, but strikingly, CDC5L could only be detected in the cytosol of PLRG-1-deficient cells, whereas in control cells, CDC5L was mainly located in the nucleus (Fig. 3.25B). These data indicate that CDC5L interacts with WIP1 in the nucleus and that this complex fails to form in the absence of PLRG-1, which presumably results in cytosolic relocalization of CDC5L.

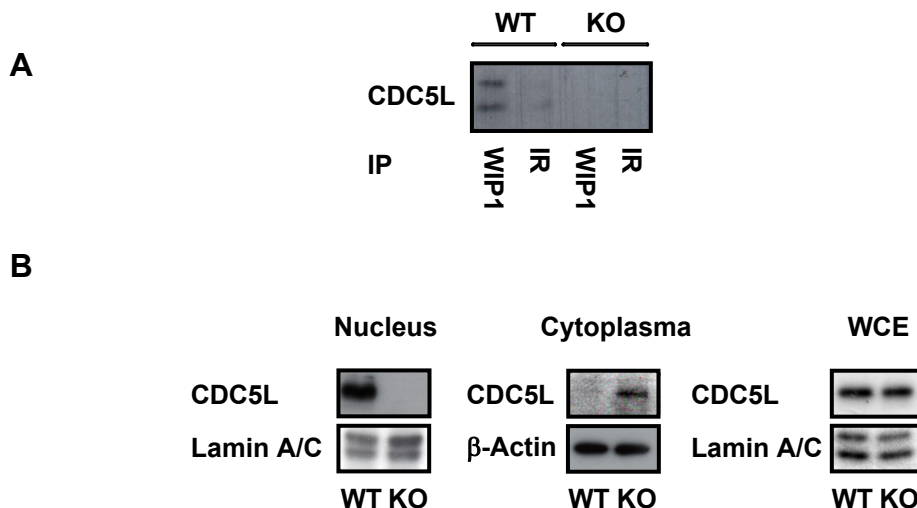


**Figure 3.25: CDC5L and WIP1 fail to form complexes in the nucleus of PLRG-1-deficient MEFs**

(A) Control and PLRG-1<sup>fllox/fllox</sup> MEFs were treated with cell-permeable Cre protein overnight, lysed after 48 h, and subjected to immunoprecipitation with either an anti-WIP1 or an insulin receptor (IR) antibody (negative control), followed by Western Blot analysis with anti-CDC5L.

(B) Western Blot analysis of immunoreactive CDC5L in nuclear, cytosolic, and whole cell extracts (WCE) of control (WT) and PLRG-1-deficient (KO) MEFs. Representative results confirmed from three independent experiments. Anti- $\beta$ -actin and anti-lamin A/C were used to control for equal loading.

### 3.17 Rescue of the apoptotic PLRG-1 phenotype by knockdown of p53

To address whether stabilization of the p53 protein functionally accounts for the phenotype resulting from PLRG-1 deficiency, the effect of a downregulated p53 expression in PLRG-1-deficient cells was investigated. MEFs were either left untransfected or were transfected with siRNAs directed either against an unrelated sequence, against PLRG-1, against p53 or against PLRG-1 and p53. In this approach, I chose to knock down PLRG-1 expression using siRNAs, because HTNC-mediated deletion of PLRG-1 followed by siRNA transfection is toxic for the cells. Western Blot analyses revealed efficient siRNA-mediated silencing of PLRG-1 and p53 (Fig. 3.26).

Occurrence of apoptosis was determined performing TUNEL assays, and siRNA-mediated knockdown of PLRG-1 resulted in dramatically increased apoptosis in the presence of increased p53 expression and phosphorylation, as well as increased Bax and p21 expression, similar to the findings in PLRG-

## Results

$1^{\text{flox/flox}}$  MEFs treated with HTNC (Fig. 3.26, Fig. 3.12). MEFs treated with p53 siRNA showed a decreased p53 expression, but no apparent phenotype and changes in Bax and p21 expression (Fig. 3.26). Cells treated with PLRG-1 along with p53 siRNA reversed the PLRG-1-deficient phenotype showing no apoptosis and restoring Bax and p21 expression levels to those found in cells either left untransfected or transfected with control siRNA (Fig. 3.26).

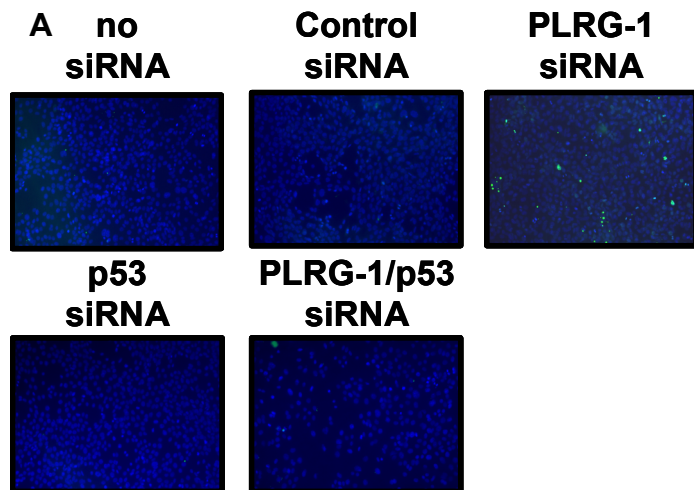
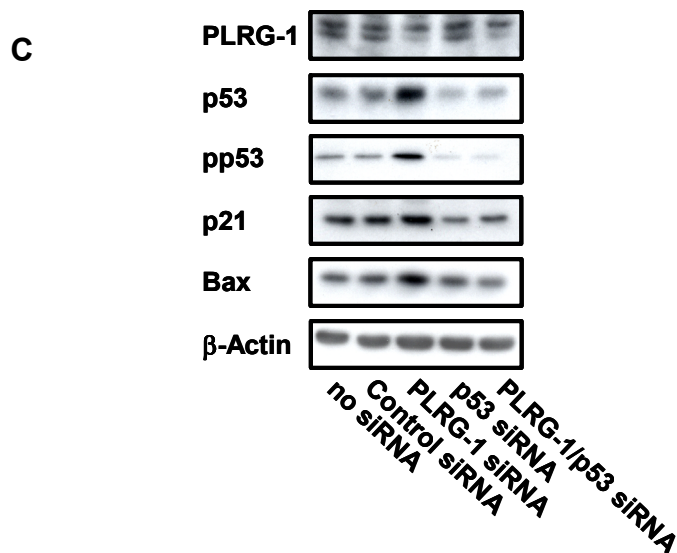
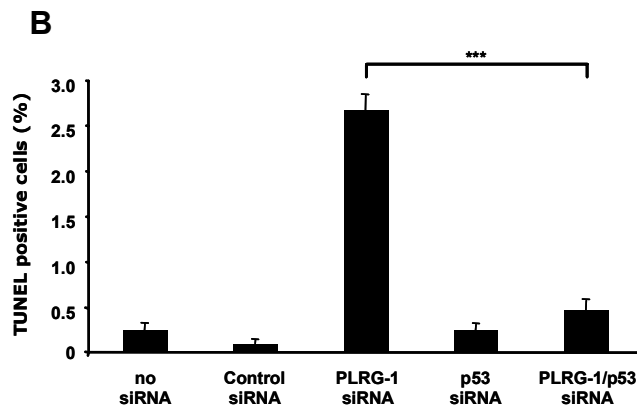


**Figure 3.26: Rescue of the apoptotic PLRG-1 phenotype by knockdown of p53**

Upper panel: Representative photomicrographs of TUNEL stained MEFs treated with the respective siRNAs. Lower panel: Percentage of TUNEL positive cells in MEFs treated with the respective siRNAs. Values represent mean  $\pm$  SEM from three independent experiments (\*\* $p < 0.001$ ).

(B) Western Blot analysis of MEFs treated with the respective siRNAs. Anti- $\beta$ -actin was used to control for equal loading.



In collaboration with the group of Prof. Hammerschmidt (University of Heidelberg), the subject was addressed whether p53 regulation accounted also for the effect of PLRG-1 deficiency *in vivo*, using a morpholino-mediated knockdown of the PLRG-1 homolog in zebrafish (*Danio rerio*).

Its deduced amino acid sequence (Genbank accession number NM\_213440) shows 77.9% identity to that of mouse *plrg-1*, indicating that this is a true ortholog. Whole-mount *in situ* hybridization analysis revealed ubiquitous distribution of zebrafish *plrg-1* transcripts during all investigated developmental stages, i.e. from one-cell through to larval stages, indicating that the gene product is both maternally and zygotically derived (see <http://zfin.org>, gene expression).

Inactivation of zebrafish *plrg-1* by Prof. Hammerschmidt's group with an antisense morpholino-oligonucleotide (MO) targeting the *plrg-1* translation initiation site led to dose-dependent severe and wide-spread apoptosis that was already apparent at early segmentation stages (12 h post-fertilization (hpf)).

Morphologically, the phenotype of MO-injected embryos was slightly stronger than that of naturally occurring zebrafish *plrg-1* mutants (Amsterdam 2004) see <http://zfin.org>, mutants). This indicated that in mutants, defects are partly rescued by maternally supplied *plrg-1* transcripts, which in this model are inactivated by MO injection. However, MO treatment did not affect maternally derived PLRG-1 protein, which would explain why the defects of zebrafish morphants develop later than those of PLRG-1-deficient mice. Importantly, concomitant inactivation of zebrafish p53 in *plrg-1* morphants via co-injection of *plrg-1* and p53 MOs (Langheinrich et al., 2002) led to a significant attenuation of apoptosis and morphological defects, adding further *in vivo* evidence that apoptosis resulting from *plrg-1* deficiency is p53-dependent.

The data described above demonstrate that by deleting PLRG-1 along with p53 it is possible to rescue the apoptotic phenotype of PLRG-1 deficiency in MEFs. The knockdown of both proteins enables the cells to survive and normalizes Bax and p21 expression to wild type levels.

Taken together, it could be demonstrated that mouse PLRG-1 serves as an important nuclear regulator of complex formation between CDC5L and the p53 phosphatase WIP1, and thus is implicated in the control of G<sub>1</sub>/S-phase progression and apoptosis, thereby providing new insight into a novel

## Results

---

mechanism by which components of the spliceosome regulate cell cycle progression and apoptosis. Moreover, rescue of the PLRG-1-deficient phenotype in MEFs clearly establishes the causal role of p53 stabilization in the observed effects, further supporting the crucial role of the CDC5L-PLRG1 spliceosome complex for nuclear targeting of p53 phosphatase complexes.

## 4 Discussion

### 4.1 Essential role for PLRG-1 in the development of the preimplantation murine embryo

The results obtained in this thesis reveal a crucial role for PLRG-1 in the development of the preimplantation murine embryo. In fact, the loss of PLRG-1 constitutes such a severe impairment to the murine embryo that it leads to its death as early as embryonic day 1.5, a rarely described phenomenon in knockout mice. Apparently maternal PLRG-1 protein from the oocyte cannot compensate for the lack of PLRG-1 as early as the first day of embryogenesis, indicating a short half-life of PLRG-1 mRNA and protein. This notion is consistent with the fact that the amount of immunodetectable PLRG-1 in PLRG-1<sup>flox/flox</sup> MEFs is already largely reduced after overnight incubation with cell-permeable Cre. This finding is specific for mammals, because although inactivation of zebrafish *plrg-1* with antisense morpholino-oligonucleotides (MO) also leads to wide-spread apoptosis, defects of zebrafish morphants develop later than those of PLRG-1-deficient mice (unpublished data, Hammerschmidt et al.).

The mechanism, by which deletion of PLRG-1 ultimately results in embryonic lethality, is based on a failure in cell cycle progression. In yeast, the mutation of the PLRG-1 homologue YPL151c (Prp46) arrests cell proliferation causing a dual block in G<sub>1</sub>/S- and M-phase progression (Albers et al., 2003; Sonnichsen et al., 2005). PLRG-1-deficient MEFs display a cell cycle arrest in G<sub>1</sub>/S phase and show an enlarged cell size. An increased cell size is typical for cells with a block in G<sub>1</sub>/S or G<sub>2</sub>/M transition due to cellular growth during gap phases (La Porta et al., 1998; Gandarillas et al., 2000). Enhanced stabilization of p53 ultimately leads to apoptosis of PLRG-1-deficient MEFs. Coinciding with the findings *in vitro*, analyses of a heart and a neuron-specific PLRG-1-deficient mouse strain display a similar severe apoptotic phenotype.

Taken together, the results gathered from experiments using PLRG-1-deficient MEFs and tissue-specific PLRG-1-deficient mouse models underline

the essential role of PLRG-1 in the regulation of cell proliferation and apoptosis independent from its postulated function in the regulation of pre-mRNA splicing.

### 4.2 Disruption of other splicing factors and their effects

To this date, only few knockout mice for components of the spliceosome have been described. Disruption of the splicing factor SRp20 was shown to result in early embryonic lethality. However, in contrast to PLRG-1-deficient embryos, SRp20-deficient embryos are still detectable at ED 3.5, despite the fact that immunoreactive SRp20 was already absent at the eight-cell stage (Jumaa et al., 1999). These data indicate that interference with splicing *per se* results in less dramatic effects on embryogenesis than disruption of PLRG-1. Similarly, disruption of the *hnRNP C* gene, encoding an essential component of hnRNP complexes involved in the regulation of pre-mRNA processing and export, results in embryonic lethality at ED 6.5 (Choi et al., 1986; Neubauer et al., 1998; Weighardt et al., 1996; Williamson et al., 2000). These previously described findings argue strongly for a specific additional or alternative role of PLRG-1 in cell cycle control and apoptosis rather than a general involvement in pre-mRNA processing and splicing.

This was confirmed by quantitative Realtime PCR using exon-spanning primers, which, surprisingly, excluded aberrant splicing in PLRG-1-deficient MEFs. This stands in contrast to a previously published role for PLRG-1 in splicing reactions (Ajuh et al., 2001; Ajuh and Lamond, 2003). However, all published splicing defects in mammals caused by PLRG-1 deficiency were postulated using an adeno-pre-mRNA-vector, an artificial splicing assay system. In contrast, the data obtained indicates no or merely a redundant role for PLRG-1 in splicing, showing that the functional role for PLRG-1 in mammals has diversified. In addition, the aberrant splicing for the TUB1  $\alpha$ -tubulin gene caused by the CDC5L mutation, the interaction partner of PLRG-1, did not occur in PLRG-1-deficient MEFs (Burns et al., 2002). PLRG-1-deleted cells showed an even higher expression of  $\alpha$ -tubulin, which is consistent with the enlarged cell size.



The *in vitro* studies on PLRG-1 interaction partners demonstrate that mouse PLRG-1 serves as an important nuclear regulator of complex formation between CDC5L and the p53 phosphatase WIP1, and thus is implicated in the control of G<sub>1</sub>/S phase progression. This provides the first insight into a novel mechanism by which components of the spliceosome regulate cell cycle progression and apoptosis (Fig. 4.2). The results also highlight the possibility that mammalian and human PLRG-1 orthologues function analogously in this pathway, whereas their duplicated plant orthologues have probably diverged functionally throughout evolution.

### 4.3 Function of PLRG-1 orthologues

In contrast to eukaryotic species, which only have one PLRG-1 orthologue, *Arabidopsis* and other plants employ two PLRG-1 orthologues (Nemeth et al., 1998). *Arabidopsis* PRL1 and PRL2 exhibit a high degree of conservation in the C-terminal WD40 repeat domain, whereas their N-terminal sequences differ significantly (Nemeth et al., 1998). PRL1 has been initially identified as a transcriptional repressor in the regulation of glucose, sucrose and some plant hormone signaling pathways (Nemeth et al., 1998). Subsequent experiments showed that PRL1 interacts via its N-terminus with the  $\alpha$ -subunits of *Arabidopsis* AMP-activated kinase orthologues AKIN10 and AKIN11 and inhibits the activity of these kinases *in vitro* (Bhalerao et al., 1999). The fact that no viable *prl2* mutant could be isolated so far, suggests that PRL1 and PRL2 perform only partly overlapping functions and that, similarly to mouse PLRG-1, homozygous *Arabidopsis* PRL2 mutants are not viable (Csaba Koncz, unpublished). Given the fact that yeast and mammalian orthologues (Prp46p and PLRG-1) of *Arabidopsis* PRL proteins play a critical role in pre-mRNA splicing and that mouse and human PLRG-1 does not interact with AMPKs (Andrea Mesaros, unpublished), it is possible that plant members of the Pleiotropic Regulator WD40 domain family play somewhat divergent roles in signaling compared to other members of this family. This is consistent with the findings, that splicing is unaltered in PLRG-1-deficient MEFs.

In yeast, it has been demonstrated that the PLRG-1 orthologue Prp46p is essential for pre-mRNA splicing (Albers et al., 2003). Moreover, *prp46* mutants exhibit a defect in cell cycle progression. While PLRG-1 deficiency in mouse leads to an arrest in G<sub>1</sub>/S phase transition (Fig. 3.11 and 12 in results), inactivation of yeast Prp46p results in impaired mitosis with a G<sub>2</sub>/M block (Albers et al., 2003). Biochemical and genetic studies demonstrate that Prp46p interacts with other components of the spliceosome, such as Prp45p, Prp19 (Pso4) and Cef1p/Cdc5p (Ohi and Gould, 2002). Mutations of these spliceosomal components results in pleiotropic defects, including temperature sensitivity, enhanced sensitivity to mutagens and radiation and accumulation of pre-mRNA (Ohi and Gould, 2002). Although the molecular mechanisms resulting in cell cycle defects as a consequence of deletion of spliceosomal components have not been fully characterized, previous experiments in yeast demonstrate that defective pre-mRNA splicing directly blocks mitosis. Thus, altered splicing of a single intron from TUB1  $\alpha$ -tubulin gene, caused by the CDC5 mutation, results in the G<sub>2</sub>/M cell cycle defect in fission yeast (Burns et al., 2002). These data indicate that splicing of a critical component in cell cycle regulation may account for the defect present in mutants of yeast spliceosomal components. Nevertheless, deficiency for Prp17, another splicing factor, results in defects both in G<sub>1</sub>/S and G<sub>2</sub>/M progression, only the latter of which can be partially rescued by introducing an intronless tubulin gene (Chawla et al., 2003), indicating the presence of multiple pathways by which spliceosomal components can regulate cell cycle progression.

#### **4.4 PLRG-1 in control of cell cycle and apoptosis**

PLRG-1-deficient MEFs displayed a G<sub>1</sub>/S-phase block, resulting in decreased Cyclin D1 and Cyclin E expression and enhanced phosphorylated and thus stabilized p53 and increased p21 expression. Cyclin D1 expression is already reduced before serum stimulation, followed by a reduction in Cyclin E expression 6 h after serum stimulation of PLRG-1-deficient MEFs. This is consistent with findings that activated Cyclin D1/CDK4 complex

hyperphosphorylates Rb enabling E2F to act as a transcription factor (Schulze et al., 1994), which subsequently activates transcription of Cyclin E, forcing the progression into S-phase (Fig. 4.1).

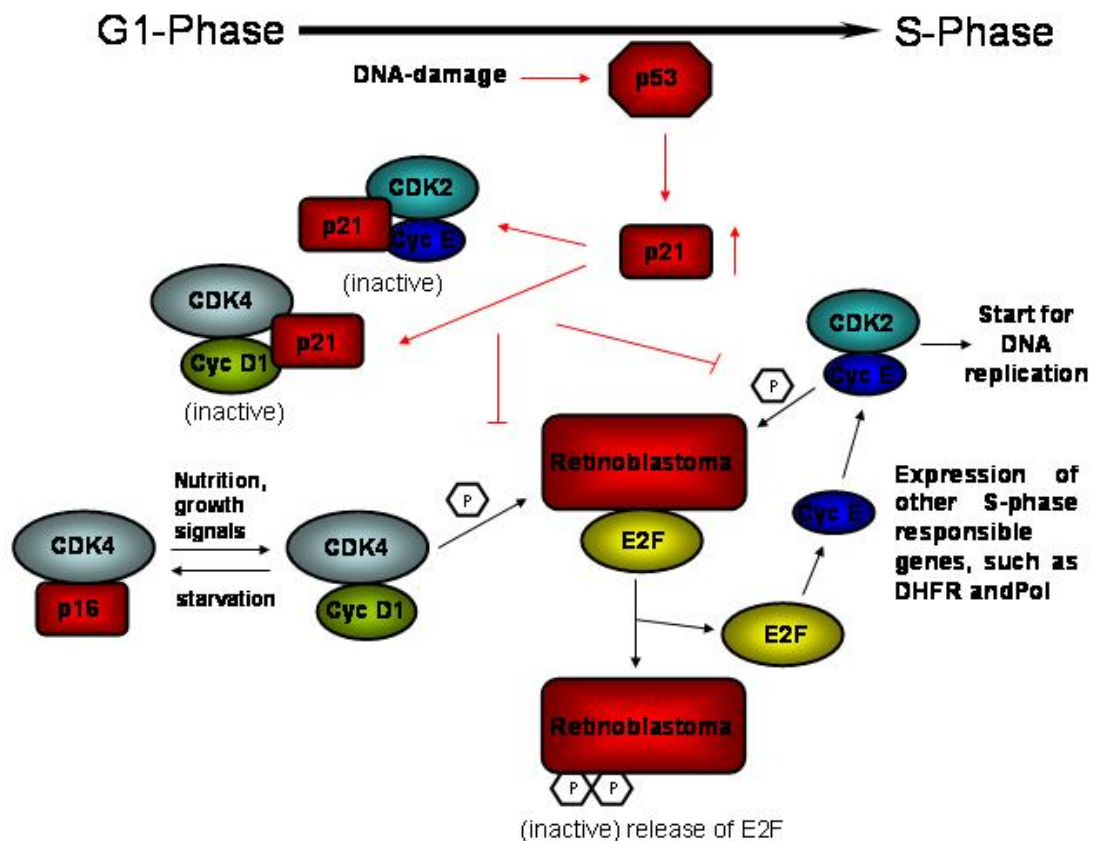


**Figure 4.1: Schematic representation of G<sub>1</sub>/S-phase progression and block**  
Signaltransduction for G<sub>1</sub>/S-phase progression are depicted by black arrows. p53 induction and block in progression are highlighted by red arrows. P represent phosphogroups

The diminished expression of Cyclin D1 was not due to a general alteration in pre-mRNA splicing, as seen in Fig. 3.13, but rather as a result from enhanced p53 stabilization. As published by Guardavaccaro and colleagues, the p53-inducible gene *PC3* induces the accumulation of hypophosphorylated Rb, thereby leading to an arrest in G<sub>1</sub>-phase. In addition, *PC3* inhibits Cyclin D1 transcription, thus further contributing to the G<sub>1</sub> arrest (Guardavaccaro et al., 2000). The findings of unaltered general pre-mRNA splicing were contradictory to data published by Ajuh et al., who postulated a role for PLRG-1 in pre-mRNA

splicing in mammals (Ajuh et al., 2001; Ajuh and Lamond, 2003). As mentioned earlier, pre-mRNA splicing was investigated using an adeno-pre-mRNA-vector, a confirmed, yet artificial system.

Up to now, pre-mRNA splicing and expression of endogenous genes had not been studied in vivo. These data obtained is contradictory to published findings in yeast showing the importance for Prp46p (PLRG-1) in pre-mRNA splicing (Albers et al., 2003). Deletion of CDC5L in yeast leads to a G<sub>2</sub>/M block and the phenotype was rescued by introducing intronless  $\alpha$ -tubulin cDNA into *Saccharomyces cerevisiae*, showing that removal of a single  $\alpha$ -tubulin gene intron suppresses the cell cycle arrest phenotype (Burns et al., 2002). PLRG-1-deficient MEFs exhibit a 1.5fold increase in  $\alpha$ -tubulin expression, indicating that PLRG-1 deficiency does not impair its expression. The enhanced expression of  $\alpha$ -tubulin is consistent with the observation of the enlarged cell size of PLRG-1-deficient MEFs, indicating an enlarged cytoskeleton. The appearance of the knockout cells resembles the phenotype of senescent cells, which are characterized by enlargement and flattening of the cell (Bayreuther et al., 1992).

In terms of apoptosis, PLRG-1 deficiency resulted in enhanced p53 phosphorylation and stabilization, leading to a cell cycle block and apoptosis. This is consistent with findings, where wild type MEFs were irradiated with UV as an exogenous damage reagent. UV treatment led to enhanced p53 phosphorylation promoting p21 expression and to a decline in Bcl-2, resulting in apoptosis (Tomicic et al., 2005). PLRG-1-deficient MEFs and PLRG-1 <sup>$\Delta$ mus</sup> mice showed increased Bax levels, due to p53 stabilization, whereas PLRG-1 <sup>$\Delta$ CNS</sup> mice exhibited no difference in Bax expression compared to controls. Miyashita *et al.* showed that the tumour suppressor p53 is a direct transcriptional activator of the human *Bax* gene, further confirming the enhanced Bax expression observed in cell culture experiments and investigation of PLRG-1 <sup>$\Delta$ mus</sup> mice (Miyashita et al., 1995). However, Morris *et al.* could show p53-mediated Bax activation in neurons after DNA damage by translocation of Bax from the cytoplasm to the mitochondria and not by enhanced expression (Morris et al., 2001). Wang *et al.*, showed a similar phenotype in terms of apoptosis in heart by knockdown of Tfam using the MCK-Cre mouse strain. The mice died 2-4 weeks after birth due to respiratory chain deficiency, dilated cardiomyopathy and atrioventricular heart conduction blocks (Wang et al., 1999). Contrary to our

findings that no deletion of PLRG-1 occurred in skeletal muscle using the MCK-Cre strain, they confirmed deletion of Tfam in this tissue. However, deletion of Tfam was investigated at day 32, a time point at which all PLRG-1<sup>Δmus</sup> mice had already died. This indicates that MCK-Cre is potentially active from day 10 on, when considering the existence of PLRG-1 in skeletal muscle in the first days after birth.

The early postnatal death of the PLRG-1<sup>ΔCNS</sup> mice was a result of enhanced apoptosis in the dentate gyrus. Kim *et al.*, showed that apoptosis in the dentate gyrus occurred in anorexia mice. These mice died during the third or fourth postnatal week, a similar strong phenotype as observed in PLRG-1<sup>ΔCNS</sup> mice. In addition, these mice displayed neurological defects, such as body tremors, a feature monitored in PLRG-1<sup>ΔCNS</sup> mice (Kim *et al.*, 2001).

Taken together, these data indicate the importance of PLRG-1 in mitotic cells.

#### **4.5 Impaired DNA damage repair as a consequence of PLRG-1 deficiency**

PLRG-1-deficient MEFs exhibit no spontaneously detectable DNA double-strand breaks, but showed impaired DNA damage repair after UV treatment, indicating that PLRG-1 deficiency results in UV hypersensitivity. Mutation of ERCC1, a protein involved in nucleotide exchange repair, also results in UV hypersensitivity, supplying a possible connection to the DNA damage repair pathway (Johansson *et al.*, 2004; Melton *et al.*, 1998).

The enhanced appearance of  $\gamma$ -H2AX foci in PLRG-1-deficient MEFs indicates that these cells are sensitive to stalled replication forks without the ability to repair these. It was shown that pulse-field gel electrophoresis as a method for detection of DNA double-strand breaks reveals a sensitivity in detection of DNA double-strand breaks of a minimum of 100 lesions per cell (Johansson *et al.*, 2004). The appearance of more than 100  $\gamma$ -H2AX foci per cell (PLRG-1-deficient nuclei exhibit a complete accumulation of the foci), without detectable DNA double-strand breaks via pulse-field gel electrophoresis indicates that DNA lesions rather represent stalled replication forks than DNA

double-strand breaks. These findings were unexpected, because of previous data obtained that cells are arrested in the G<sub>1</sub>-phase prior to the start of DNA replication in the S-phase. Possibly, when PLRG-1 is deleted in MEFs currently in the beginning of the S-phase, stalled replication forks occur leading to the observed phenotype. In addition, FACS analysis showed that the percentage of cells in S-phase was raised from 2.3 to 3.2% in PLRG-1-deficient MEFs indicating that these cells either do not show a complete deletion of PLRG-1 or a small proportion of cells enter the S-phase and directly stop progressing throughout the cell cycle due to spontaneously occurring DNA lesions. Replication forks, bulky DNA lesions or interstrand crosslinks are often spontaneously generated. Bulky DNA lesions are constantly produced by endogenously generated oxidative damage in mammalian cells (Melton et al., 2004). Furthermore, metabolic byproducts, such as malonyldialdehyde, cause interstrand crosslinks (Chaudhary et al., 1994) and DNA secondary structures, such as hairpins or G4-tetraplex structure at telomeres, cause stalled replication forks (Cromie et al., 2000; Samadashwily et al., 1997). Hence, naturally occurring stalled replication forks are common in mammalian cells and result in  $\gamma$ -H2AX foci, also observed in untreated PLRG-1<sup>flox/flox</sup> MEFs. The increase in  $\gamma$ -H2AX foci in PLRG-1-deficient MEFs seems to occur from such lesions, because these cells did not exhibit enhanced DNA double-strand breaks. When encountering interstrand crosslinks, the cell uses the NER pathway followed by homologous recombination to repair this DNA damage (Niedernhofer et al., 2004). Because PLRG-1-deficient cells cannot progress in cell cycle, it seems impossible for these cells to repair these lesions.

ATR, a member of the PIKK-family, controls the integrity of DNA replication in unstressed cells (Shechter et al., 2004, Shechter et al., 2004). Thus, future experiments will have to address the role of ATR in mediating the PLRG-1-deficient phenotype.

The appearance of PLRG-1-deficient MEFs resembles that of senescent cells, displaying larger cell size and a flattened cell shape (Bayreuther et al., 1992). Another senescent-specific feature is an increase in telomere-dysfunction-induced foci, resulting in enhanced recruitment of  $\gamma$ -H2AX and other DNA damage response factors to telomeres (Takai et al., 2003). Herbig *et al.* could show that telomere shortening triggers senescence of human cells

through a pathway involving p53 and p21, an upregulation of proteins also observed in PLRG-1-deficient MEFs, and resulting in a G<sub>1</sub> arrest (Herbig et al., 2004). However, deletion of PLRG-1 in MEFs showed this senescence-like phenotype for a maximum of 4-7 days due to p53-induced apoptosis. Whether PLRG-1 deficiency has an effect on senescent cells, despite their inability to divide and the accumulation of DNA double-strand breaks (Sedelnikova et al., 2004), remains unknown.

It remains elusive, whether PLRG-1 is recruited to DNA lesions with the Pso4-complex. Further investigation will show, if ATM or ATR plays the important role in phosphorylating p53 at serine 15 in this context.

#### **4.6 Proposed model for PLRG-1, linking DNA repair, control of cell cycle progression and apoptosis via the Pso4-complex**

This thesis demonstrated that murine PLRG-1 serves as an important regulator of complex formation between CDC5L and the p53 phosphatase WIP1 and is implicated in the control of G<sub>1</sub>/S-phase progression and apoptosis; thereby, providing new insight into a novel mechanism by which members of the Pso4-complex are involved in the regulation of cell cycle progression, DNA damage repair and apoptosis (Fig. 4.2). This cell cycle defect is accompanied by increased p53 phosphorylation and expression, which results from failure of CDC5L to interact with the p53 phosphatase WIP1 in PLRG-1-deficient cells. Unlike the PLRG-1 mutants, WIP1-deficient mice are viable to adulthood, indicating that additional p53 phosphatases are associated with CDC5L (Anton et al., 2002). Thus, in addition to WIP1, PP-1 phosphatase was also detected in CDC5L-associated protein complexes by mass spectrometry. Furthermore, active PP1 co-purifies with CDC5L and CDC5L directly interacts with the PP1-binding nuclear-scaffold protein NIPP1 (Boudrez et al., 2000). Interestingly, disruption of the *NIPP1* gene also results in early embryonic lethality although at a later stage (ED 6.5) (Van Eynde et al., 2004). Therefore, it is proposed that CDC5L interacts with multiple p53 phosphatases including WIP1 and PP-1 $\alpha$  and that cytosolic relocation of CDC5L as a consequence of PLRG-1 deficiency

has a more severe effect than individual deletion or inhibition of these phosphatases. Moreover, rescue of the PLRG-1-deficient phenotype in both MEFs and zebrafish *in vivo* clearly establishes the causal role of p53 stabilization in the observed effects, thereby further supporting the crucial role of the CDC5L-PLRG-1 spliceosome complex for nuclear targeting of p53 phosphatase complexes.

The WRN/Pso4-CDC5L-PLRG-1 complex interaction is essential for uncoupling of DNA interstrand crosslinks (Zhang et al., 2005). The findings, that PLRG-1 deficiency results in enhanced appearance of  $\gamma$ -H2AX foci and impaired DNA damage repair, lead to the assumption that PLRG-1 is crucial for stabilizing the multiprotein-complex implicated in DNA damage repair. Therefore, these data extend the role of the Pso4-CDC5L-PLRG-1 complex beyond the regulation of pre-mRNA splicing to DNA repair (Zhang et al., 2005). Thus, direct integration of interstrand crosslink uncoupling in the regulation of p53 stability through Pso4-CDC5L-PLRG-1-regulated phosphorylation provides a new working model (Fig. 4.2). Namely, cell cycle arrest initiated upon stalled replication forks or double-strand break could be resolved by the final steps of interstrand crosslink uncoupling to signal successful repair to the cell and allow further cell cycle progression. In this model, DNA double-strand breaks as intermediates of interstrand crosslink (ICL) repair result in the activation of the ATM kinase family, stimulating p53 phosphorylation and stabilization. This subsequently leads to increased Cdk-inhibitor p21 expression and ultimately to stimulation of expression of the pro-apoptotic Bax protein. If ICL repair proceeds successfully, the Pso4-CDC5L-PLRG-1 complex recruited to the ICL site, promoting interaction of CDC5L with the p53 phosphatase, allows for dephosphorylation and subsequent degradation of p53. This stimulates re-entry into the cell cycle and inhibits apoptosis (Fig. 4.2).



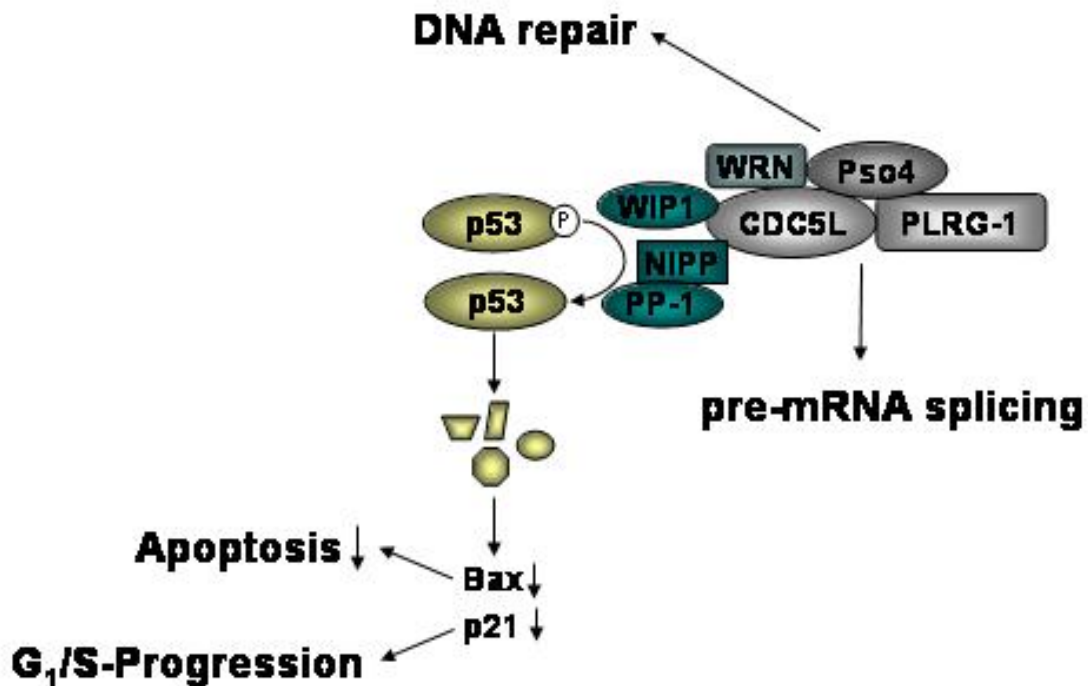


**Figure 4.2: Proposed model for novel integration of pre-mRNA splicing components linking DNA repair, and control of cell cycle progression and apoptosis via CDC5L-PLRG-1 interaction**

The Pso4-CDC5L-PLRG-1 complex in cooperation with the Werner protein (WRN) helicase and RPA (not shown) regulates DNA interstrand crosslinks and is thus required for DNA repair. The CDC5L-PLRG-1 complex was also identified as a critical component of the spliceosome and the interaction of both proteins was demonstrated to be crucial for pre-mRNA splicing. The data presented here reveal that the same CDC5L-PLRG-1 complex interacts with p53 phosphatases and that lack of PLRG-1 disrupts the interaction of these phosphatases with CDC5L, thus resulting in p53 phosphorylation and stabilization leading to induction of G<sub>1</sub>/S arrest and apoptosis.

Although in the present experiments, the role of Pso4-CDC5L-PLRG-1-mediated p53 regulation in ICL repair was not directly investigated, further studies are in progress to clarify the role of Pso4-CDC5L-PLRG-1-mediated p53 regulation in ICL repair.

This novel link between spliceosomal and DNA-repair components and the regulation of cell cycle progression and apoptosis appears particularly interesting as in many mammalian tumors CDC5L and/or PLRG-1 are overexpressed (Fenske et al., 2006; Geigl et al., 2004; Groenen et al., 1998). Hence, the interaction of overexpressed CDC5L with p53 phosphatases may provide a new mechanism for p53 suppression in tumorigenesis. Further characterization of the signaling network including additional partners of PLRG-

1, CDC5L, and the p53 phosphatase WIP1 is therefore expected to help in further deciphering regulatory links between common components of splicing and DNA repair pathways and may yet uncover functions in malignant transformation.

## 5 Summary

Mammalian Pleiotropic Regulator PLRG-1 was initially identified as a component of the spliceosome and belongs to a highly conserved family of seven WD40 domain containing proteins in eukaryotes (Ajuh et al., 2000; Ajuh et al., 2001). Founding members of this WD40-repeat protein family, PRL1 and PRL2, were first identified by T-DNA tagging in *Arabidopsis thaliana* (Nemeth et al., 1998). Whereas in plants the *PRL* genes are uniquely duplicated, in yeast, *C. elegans* and mammals there are only single orthologues of the Pleiotropic Regulator family which play important roles in the control of cellular homeostasis by forming at least in mammals, a complex with Pso4 and the cell division and cycle 5 homolog (CDC5L), that regulates both pre-mRNA splicing and DNA repair.

To characterize the role of PLRG-1 *in vivo*, in the present study, I inactivated its gene both conventionally and conditionally in mice. Here, it is shown that inactivation of PLRG-1 results in embryonic lethality 1.5 days post-fertilization in mice, indicating a fundamental role for PLRG-1 in early cell cycle events. Studies on heart- and neuron-specific PLRG-1 knockout mice revealed that massive apoptosis was responsible for their premature death. Moreover, PLRG-1-deficient mouse embryonic fibroblasts (MEFs) fail to enter S-phase upon serum stimulation and show increased apoptosis resulting from enhanced p53 phosphorylation and stabilization. Interestingly, p53-phosphatase WIP1 was seen to interact with CDC5L in wild-type, but not in PLRG-1-deficient MEFs due to cytosolic translocation of CDC5L. p53 downregulation rescues lethality in PLRG-1-deficient MEFs, showing that apoptosis resulting from PLRG-1-deficiency is p53 dependent. Taken together, it is shown that the Pso4-CDC5L-PLRG-1 complex controls cell proliferation and apoptosis by novel integration of pre-mRNA splicing and DNA repair via a p53-phosphorylation-dependent pathway, thus providing the first evidence for Pso4-complex regulation of p53.

## 6 Zusammenfassung

PLRG-1 gehört zu einer hoch konservierten Proteinfamilie in Eukaryoten, welche sich durch wiederholende WD40 Domänen auszeichnet und wurde in Säugern als Bestandteil des Spliceosoms identifiziert (Ajuh et al., 2000; Ajuh et al., 2001). Die ersten Mitglieder dieser Familie, PRL1 und PRL2, wurden durch T-DNA Markierung in *Arabidopsis thaliana* gefunden (Nemeth et al., 1998). Während in Pflanzen die *PRL* Gene dupliziert sind, gibt es in Hefe, *C.elegans* und Säugern jeweils nur ein Ortholog der pleiotropen Regulatorfamilie, welche eine wichtige Rolle in der Kontrolle der Zellhomöostase innehaben. Zumindest in Säugern formt PLRG-1 einen Komplex mit Pso4 und dem cell division and cycle 5 homolog (CDC5L), welcher sowohl an der Regulation des pre-mRNA Spleißens und auch an der DNA Reparatur beteiligt ist.

Um die Funktion von PLRG-1 in Säugern *in vivo* zu charakterisieren, habe ich im Rahmen der vorliegenden Arbeit des PLRG-1-Gen in Mäusen sowohl konventionell, als auch konditionell inaktiviert. Es konnte gezeigt werden, dass die Inaktivierung von PLRG-1 in Mäusen embryonale Lethalität an Tag 1,5 nach Befruchtung der Eizelle zur Folge hat, welches für eine fundamentale Rolle von PLRG-1 in der ersten Zellteilung spricht. Herz- und Neuron-spezifischen Knockout Mäuse weisen eine massive Apoptose in diesen Organen auf, welche zu deren frühzeitigem Tod führt. Außerdem verlieren PLRG-1-defiziente Mausembryofibroblasten (MEFs) die Fähigkeit, nach Serumstimulation in die S-Phase einzutreten und weisen eine erhöhte Apoptose auf, welche aus vermehrter p53 Phosphorylierung und Stabilisierung resultiert. Interessanterweise interagiert die p53-Phosphatase WIP1 mit CDC5L in Wildtypenzellen, nicht jedoch, aufgrund der cytosolischen Translokation von CDC5L, in PLRG-1-defizienten MEFs. Die Herunterregulierung von p53 rettet die Lethalität sowohl in PLRG-1 defizienten MEFs als auch in Zebrafisch *in vivo*, und verdeutlicht, dass die durch PLRG-1 Defizienz hervorgerufene Apoptose p53 abhängig ist. Zusammenfassend konnte gezeigt werden, dass der Pso4-CDC5L-PLRG-1 Komplex Zellproliferation und Apoptose, durch p53-Regulation kontrolliert.

## 7 Kurzzusammenfassung

In dieser Arbeit wurde die Rolle von PLRG-1 *in vitro* und *in vivo* untersucht. Die Erzeugung und Untersuchung von PLRG-1-defizienten Mausembryofibroblasten und Mäusen ergab, dass die Inaktivierung von PLRG-1 in Säugern einen G<sub>1</sub>/S Zellzyklusarrest und massive Apoptose induziert. Der Zellzyklusarrest, sowie die Apoptose resultieren aus einer Stabilisierung des p53 Proteins, sowie des Fehlens der Interaktion der p53 Phosphatase WIP1 mit CDC5L. Die Herunterregulierung von p53 rettet die Lethalität PLRG-1-defizienter Zellen und verdeutlicht, dass die Apoptose, hervorgerufen durch PLRG-1 Defizienz, p53 abhängig ist. Es konnte gezeigt werden, dass der Pso4-CDC5L-PLRG-1 Komplex Zellproliferation und Apoptose, durch eine neue Integration von DNA Reparatur über einen p53-Phosphorylierung-abhängigen Signalweges kontrolliert.

## 8 References

Aboussekhra, A., Biggerstaff, M., Shivji, M. K., Vilpo, J. A., Moncollin, V., Podust, V. N., Protic, M., Hubscher, U., Egly, J. M., and Wood, R. D. (1995). Mammalian DNA nucleotide excision repair reconstituted with purified protein components. *Cell* 80, 859-868.

Adams, J. M., and Cory, S. (1998). The Bcl-2 protein family: arbiters of cell survival. *Science* 281, 1322-1326.

Adrain, C., Slee, E. A., Harte, M. T., and Martin, S. J. (1999). Regulation of apoptotic protease activating factor-1 oligomerization and apoptosis by the WD-40 repeat region. *J Biol Chem* 274, 20855-20860.

Agarwal, M. K., Agarwal, M. L., Athar, M., and Gupta, S. (2004). Tocotrienol-rich fraction of palm oil activates p53, modulates Bax/Bcl2 ratio and induces apoptosis independent of cell cycle association. *Cell Cycle* 3, 205-211.

Ajuh, P., Kuster, B., Panov, K., Zomerdijk, J. C., Mann, M., and Lamond, A. I. (2000). Functional analysis of the human CDC5L complex and identification of its components by mass spectrometry. *Embo J* 19, 6569-6581.

Ajuh, P., and Lamond, A. I. (2003). Identification of peptide inhibitors of pre-mRNA splicing derived from the essential interaction domains of CDC5L and PLRG1. *Nucleic Acids Res* 31, 6104-6116.

Ajuh, P., Sleeman, J., Chusainow, J., and Lamond, A. I. (2001). A direct interaction between the carboxyl-terminal region of CDC5L and the WD40 domain of PLRG1 is essential for pre-mRNA splicing. *J Biol Chem* 276, 42370-42381.

Akkari, Y. M., Bateman, R. L., Reifsteck, C. A., Olson, S. B., and Grompe, M. (2000). DNA replication is required To elicit cellular responses to psoralen-induced DNA interstrand cross-links. *Mol Cell Biol* 20, 8283-8289.

Alarcon, R., Koumenis, C., Geyer, R. K., Maki, C. G., and Giaccia, A. J. (1999). Hypoxia induces p53 accumulation through MDM2 down-regulation and inhibition of E6-mediated degradation. *Cancer Res* 59, 6046-6051.

Albers, M., Diment, A., Muraru, M., Russell, C. S., and Beggs, J. D. (2003). Identification and characterization of Prp45p and Prp46p, essential pre-mRNA splicing factors. *Rna* 9, 138-150.

Alnemri, E. S. (1997). Mammalian cell death proteases: a family of highly conserved aspartate specific cysteine proteases. *J Cell Biochem* 64, 33-42.

Anderson, H., and Roberge, M. (1996). Topoisomerase II inhibitors affect entry into mitosis and chromosome condensation in BHK cells. *Cell Growth Differ* 7,

83-90.

Anton, I. M., de la Fuente, M. A., Sims, T. N., Freeman, S., Ramesh, N., Hartwig, J. H., Dustin, M. L., and Geha, R. S. (2002). WIP deficiency reveals a differential role for WIP and the actin cytoskeleton in T and B cell activation. *Immunity* *16*, 193-204.

Aoki, M., Morishita, R., Matsushita, H., Nakano, N., Hayashi, S., Tomita, N., Yamamoto, K., Moriguchi, A., Higaki, J., and Ogihara, T. (1997). Serum deprivation-induced apoptosis accompanied by up-regulation of p53 and bax in human aortic vascular smooth muscle cells. *Heart Vessels Suppl* *12*, 71-75.

Baer, M., and Sancar, G. B. (1989). Photolyases from *Saccharomyces cerevisiae* and *Escherichia coli* recognize common binding determinants in DNA containing pyrimidine dimers. *Mol Cell Biol* *9*, 4777-4788.

Balmano, K., and Cook, S. J. (1999). Sustained MAP kinase activation is required for the expression of cyclin D1, p21Cip1 and a subset of AP-1 proteins in CCL39 cells. *Oncogene* *18*, 3085-3097.

Banin, S., Moyal, L., Shieh, S., Taya, Y., Anderson, C. W., Chessa, L., Smorodinsky, N. I., Prives, C., Reiss, Y., Shiloh, Y., and Ziv, Y. (1998). Enhanced phosphorylation of p53 by ATM in response to DNA damage. *Science* *281*, 1674-1677.

Bartek, J., Lukas, C., and Lukas, J. (2004). Checking on DNA damage in S phase. *Nat Rev Mol Cell Biol* *5*, 792-804.

Bayreuther, K., Francz, P. I., Gogol, J., and Kontermann, K. (1992). Terminal differentiation, aging, apoptosis, and spontaneous transformation in fibroblast stem cell systems in vivo and in vitro. *Ann N Y Acad Sci* *663*, 167-179.

Berardini, M., Foster, P. L., and Loechler, E. L. (1999). DNA polymerase II (polB) is involved in a new DNA repair pathway for DNA interstrand cross-links in *Escherichia coli*. *J Bacteriol* *181*, 2878-2882.

Berardini, M., Mackay, W., and Loechler, E. L. (1997). Evidence for a recombination-independent pathway for the repair of DNA interstrand cross-links based on a site-specific study with nitrogen mustard. *Biochemistry* *36*, 3506-3513.

Bernards, R. (2004). Wip-ing out cancer. *Nat Genet* *36*, 319-320.

Bessho, T. (2003). Induction of DNA replication-mediated double strand breaks by psoralen DNA interstrand cross-links. *J Biol Chem* *278*, 5250-5254.

Bhalerao, R. P., Salchert, K., Bako, L., Okresz, L., Szabados, L., Muranaka, T., Machida, Y., Schell, J., and Koncz, C. (1999). Regulatory interaction of PRL1 WD protein with Arabidopsis SNF1-like protein kinases. *Proc Natl Acad Sci U S A* *96*, 5322-5327.

## References

---

- Bonura, T., Smith, K. C., and Kaplan, H. S. (1975). Enzymatic induction of DNA double-strand breaks in gamma-irradiated *Escherichia coli* K-12. *Proc Natl Acad Sci U S A* 72, 4265-4269.
- Boudrez, A., Beullens, M., Groenen, P., Van Eynde, A., Vulsteke, V., Jagiello, I., Murray, M., Krainer, A. R., Stalmans, W., and Bollen, M. (2000). NIPP1-mediated interaction of protein phosphatase-1 with CDC5L, a regulator of pre-mRNA splicing and mitotic entry. *J Biol Chem* 275, 25411-25417.
- Boulton, S. J., and Jackson, S. P. (1996). Identification of a *Saccharomyces cerevisiae* Ku80 homologue: roles in DNA double strand break rejoining and in telomeric maintenance. *Nucleic Acids Res* 24, 4639-4648.
- Boulton, S. J., and Jackson, S. P. (1998). Components of the Ku-dependent non-homologous end-joining pathway are involved in telomeric length maintenance and telomeric silencing. *Embo J* 17, 1819-1828.
- Brown, J. D., and Beggs, J. D. (1992). Roles of PRP8 protein in the assembly of splicing complexes. *Embo J* 11, 3721-3729
- Bruning, J. C., Michael, M. D., Winnay, J. N., Hayashi, T., Horsch, D., Accili, D., Goodyear, L. J., and Kahn, C. R. (1998). A muscle-specific insulin receptor knockout exhibits features of the metabolic syndrome of NIDDM without altering glucose tolerance. *Mol Cell* 2, 559-569.
- Burma, S., Chen, B. P., Murphy, M., Kurimasa, A., and Chen, D. J. (2001). ATM phosphorylates histone H2AX in response to DNA double-strand breaks. *J Biol Chem* 276, 42462-42467.
- Burns, C. G., Ohi, R., Krainer, A. R., and Gould, K. L. (1999). Evidence that Myb-related CDC5 proteins are required for pre-mRNA splicing. *Proc Natl Acad Sci U S A* 96, 13789-13794.
- Burns, C. G., Ohi, R., Mehta, S., O'Toole, E. T., Winey, M., Clark, T. A., Sugnet, C. W., Ares, M., Jr., and Gould, K. L. (2002). Removal of a single alpha-tubulin gene intron suppresses cell cycle arrest phenotypes of splicing factor mutations in *Saccharomyces cerevisiae*. *Mol Cell Biol* 22, 801-815.
- Canman, C. E., Lim, D. S., Cimprich, K. A., Taya, Y., Tamai, K., Sakaguchi, K., Appella, E., Kastan, M. B., and Siliciano, J. D. (1998). Activation of the ATM kinase by ionizing radiation and phosphorylation of p53. *Science* 281, 1677-1679.
- Chan, T. A., Hermeking, H., Lengauer, C., Kinzler, K. W., and Vogelstein, B. (1999). 14-3-3Sigma is required to prevent mitotic catastrophe after DNA damage. *Nature* 401, 616-620.
- Chaudhary, A. K., Nokubo, M., Reddy, G. R., Yeola, S. N., Morrow, J. D., Blair, I. A., and Marnett, L. J. (1994). Detection of endogenous malondialdehyde-deoxyguanosine adducts in human liver. *Science* 265, 1580-1582.



- Chawla, G., Sapra, A. K., Surana, U., and Vijayraghavan, U. (2003). Dependence of pre-mRNA introns on PRP17, a non-essential splicing factor: implications for efficient progression through cell cycle transitions. *Nucleic Acids Res* 31, 2333-2343.
- Chen, C. H., Tsai, W. Y., Chen, H. R., Wang, C. H., and Cheng, S. C. (2001). Identification and characterization of two novel components of the Prp19p-associated complex, Ntc30p and Ntc20p. *J Biol Chem* 276, 488-494.
- Chittenden, T., Harrington, E. A., O'Connor, R., Flemington, C., Lutz, R. J., Evan, G. I., and Guild, B. C. (1995). Induction of apoptosis by the Bcl-2 homologue Bak. *Nature* 374, 733-736.
- Choi, Y. D., Grabowski, P. J., Sharp, P. A., and Dreyfuss, G. (1986). Heterogeneous nuclear ribonucleoproteins: role in RNA splicing. *Science* 231, 1534-1539.
- Cole, R. S. (1973). Repair of DNA containing interstrand crosslinks in *Escherichia coli*: sequential excision and recombination. *Proc Natl Acad Sci U S A* 70, 1064-1068.
- Cook, S. A., Sugden, P. H., and Clerk, A. (1999). Regulation of bcl-2 family proteins during development and in response to oxidative stress in cardiac myocytes: association with changes in mitochondrial membrane potential. *Circ Res* 85, 940-949.
- Costanzo, V., Shechter, D., Lupardus, P. J., Cimprich, K. A., Gottesman, M., and Gautier, J. (2003). An ATR- and Cdc7-dependent DNA damage checkpoint that inhibits initiation of DNA replication. *Mol Cell* 11, 203-213.
- Coulonval, K., Bockstaele, L., Paternot, S., and Roger, P. P. (2003). Phosphorylations of cyclin-dependent kinase 2 revisited using two-dimensional gel electrophoresis. *J Biol Chem* 278, 52052-52060.
- Cromie, G. A., Millar, C. B., Schmidt, K. H., and Leach, D. R. (2000). Palindromes as substrates for multiple pathways of recombination in *Escherichia coli*. *Genetics* 154, 513-522.
- Den Haese, G. J., Walworth, N., Carr, A. M., and Gould, K. L. (1995). The Wee1 protein kinase regulates T14 phosphorylation of fission yeast Cdc2. *Mol Biol Cell* 6, 371-385.
- Desai, D., Gu, Y., and Morgan, D. O. (1992). Activation of human cyclin-dependent kinases in vitro. *Mol Biol Cell* 3, 571-582.
- DiBiase, S. J., Zeng, Z. C., Chen, R., Hyslop, T., Curran, W. J., Jr., and Iliakis, G. (2000). DNA-dependent protein kinase stimulates an independently active, nonhomologous, end-joining apparatus. *Cancer Res* 60, 1245-1253.
- Du, C., Fang, M., Li, Y., Li, L., and Wang, X. (2000). Smac, a mitochondrial protein that promotes cytochrome c-dependent caspase activation by

## References

---

eliminating IAP inhibition. *Cell* 102, 33-42.

Duan, X., Liang, Y. Y., Feng, X. H., and Lin, X. (2006). Protein serine/threonine phosphatase PPM1A dephosphorylates Smad1 in the bone morphogenetic protein signaling pathway. *J Biol Chem* 281, 36526-36532.

Dulic, V., Stein, G. H., Far, D. F., and Reed, S. I. (1998). Nuclear accumulation of p21Cip1 at the onset of mitosis: a role at the G2/M-phase transition. *Mol Cell Biol* 18, 546-557.

el-Deiry, W. S., Harper, J. W., O'Connor, P. M., Velculescu, V. E., Canman, C. E., Jackman, J., Pietenpol, J. A., Burrell, M., Hill, D. E., Wang, Y., and et al. (1994). WAF1/CIP1 is induced in p53-mediated G1 arrest and apoptosis. *Cancer Res* 54, 1169-1174.

Emili, A. (1998). MEC1-dependent phosphorylation of Rad9p in response to DNA damage. *Mol Cell* 2, 183-189.

Evans, E., Moggs, J. G., Hwang, J. R., Egly, J. M., and Wood, R. D. (1997). Mechanism of open complex and dual incision formation by human nucleotide excision repair factors. *Embo J* 16, 6559-6573.

Fadok, V. A., Voelker, D. R., Campbell, P. A., Cohen, J. J., Bratton, D. L., and Henson, P. M. (1992). Exposure of phosphatidylserine on the surface of apoptotic lymphocytes triggers specific recognition and removal by macrophages. *J Immunol* 148, 2207-2216.

Fan, T. J., Han, L. H., Cong, R. S., and Liang, J. (2005). Caspase family proteases and apoptosis. *Acta Biochim Biophys Sin (Shanghai)* 37, 719-727.

Fattaey, A., and Booher, R. N. (1997). Myt1: a Wee1-type kinase that phosphorylates Cdc2 on residue Thr14. *Prog Cell Cycle Res* 3, 233-240.

Fiscella, M., Zhang, H., Fan, S., Sakaguchi, K., Shen, S., Mercer, W. E., Vande Woude, G. F., O'Connor, P. M., and Appella, E. (1997). Wip1, a novel human protein phosphatase that is induced in response to ionizing radiation in a p53-dependent manner. *Proc Natl Acad Sci U S A* 94, 6048-6053.

Ford, J. M., and Hanawalt, P. C. (1997). Expression of wild-type p53 is required for efficient global genomic nucleotide excision repair in UV-irradiated human fibroblasts. *J Biol Chem* 272, 28073-28080.

Frosina, G., Fortini, P., Rossi, O., Carrozzino, F., Raspaglio, G., Cox, L. S., Lane, D. P., Abbondandolo, A., and Dogliotti, E. (1996). Two pathways for base excision repair in mammalian cells. *J Biol Chem* 271, 9573-9578.

Frutos, S., Moscat, J., and Diaz-Meco, M. T. (1999). Cleavage of zetaPKC but not lambda/iotaPKC by caspase-3 during UV-induced apoptosis. *J Biol Chem* 274, 10765-10770.

Fulda, S., Meyer, E., Friesen, C., Susin, S. A., Kroemer, G., and Debatin, K. M.

- (2001). Cell type specific involvement of death receptor and mitochondrial pathways in drug-induced apoptosis. *Oncogene* 20, 1063-1075.
- Furman, E., and Glitz, D. G. (1995). Purification of the spliceosome A-complex and its visualization by electron microscopy. *J Biol Chem* 270, 15515-15522.
- Gandarillas, A., Davies, D., and Blanchard, J. M. (2000). Normal and c-Myc-promoted human keratinocyte differentiation both occur via a novel cell cycle involving cellular growth and endoreplication. *Oncogene* 19, 3278-3289.
- Gardner, R., Putnam, C. W., and Weinert, T. (1999). RAD53, DUN1 and PDS1 define two parallel G2/M checkpoint pathways in budding yeast. *Embo J* 18, 3173-3185.
- Gerson, S. L., Trey, J. E., Miller, K., and Benjamin, E. (1987). Repair of O6-alkylguanine during DNA synthesis in murine bone marrow hematopoietic precursors. *Cancer Res* 47, 89-95.
- Goldberg, M., Stucki, M., Falck, J., D'Amours, D., Rahman, D., Pappin, D., Bartek, J., and Jackson, S. P. (2003). MDC1 is required for the intra-S-phase DNA damage checkpoint. *Nature* 421, 952-956.
- Grawunder, U., Zimmer, D., Fugmann, S., Schwarz, K., and Lieber, M. R. (1998). DNA ligase IV is essential for V(D)J recombination and DNA double-strand break repair in human precursor lymphocytes. *Mol Cell* 2, 477-484.
- Grinberg, M., Schwarz, M., Zaltsman, Y., Eini, T., Niv, H., Pietrokovski, S., and Gross, A. (2005). Mitochondrial carrier homolog 2 is a target of tBID in cells signaled to die by tumor necrosis factor alpha. *Mol Cell Biol* 25, 4579-4590.
- Gross, A., Jockel, J., Wei, M. C., and Korsmeyer, S. J. (1998). Enforced dimerization of BAX results in its translocation, mitochondrial dysfunction and apoptosis. *Embo J* 17, 3878-3885.
- Gu, Y., Rosenblatt, J., and Morgan, D. O. (1992). Cell cycle regulation of CDK2 activity by phosphorylation of Thr160 and Tyr15. *Embo J* 11, 3995-4005.
- Guadagno, T. M., and Newport, J. W. (1996). Cdk2 kinase is required for entry into mitosis as a positive regulator of Cdc2-cyclin B kinase activity. *Cell* 84, 73-82.
- Guardavaccaro, D., Corrente, G., Covone, F., Micheli, L., D'Agnano, I., Starace, G., Caruso, M., and Tirone, F. (2000). Arrest of G(1)-S progression by the p53-inducible gene PC3 is Rb dependent and relies on the inhibition of cyclin D1 transcription. *Mol Cell Biol* 20, 1797-1815.
- Guo, Z., Kumagai, A., Wang, S. X., and Dunphy, W. G. (2000). Requirement for Atr in phosphorylation of Chk1 and cell cycle regulation in response to DNA replication blocks and UV-damaged DNA in *Xenopus* egg extracts. *Genes Dev* 14, 2745-2756.

## References

---

- Hastings, M. L., and Krainer, A. R. (2001). Pre-mRNA splicing in the new millennium. *Curr Opin Cell Biol* 13, 302-309.
- Haupt, S., Berger, M., Goldberg, Z., and Haupt, Y. (2003). Apoptosis - the p53 network. *J Cell Sci* 116, 4077-4085.
- Herbig, U., Jobling, W. A., Chen, B. P., Chen, D. J., and Sedivy, J. M. (2004). Telomere shortening triggers senescence of human cells through a pathway involving ATM, p53, and p21(CIP1), but not p16(INK4a). *Mol Cell* 14, 501-513.
- Hirao, A., Kong, Y. Y., Matsuoka, S., Wakeham, A., Ruland, J., Yoshida, H., Liu, D., Elledge, S. J., and Mak, T. W. (2000). DNA damage-induced activation of p53 by the checkpoint kinase Chk2. *Science* 287, 1824-1827.
- Hoffmann, I., Clarke, P. R., Marcote, M. J., Karsenti, E., and Draetta, G. (1993). Phosphorylation and activation of human cdc25-C by cdc2--cyclin B and its involvement in the self-amplification of MPF at mitosis. *Embo J* 12, 53-63.
- Hogan, B., Constantini, F., and Lacy, I. (1987). *Manipulating the mouse embryo*, Cold Spring Harbor Laboratory Press).
- Honda, R., Tanaka, H., and Yasuda, H. (1997). Oncoprotein MDM2 is a ubiquitin ligase E3 for tumor suppressor p53. *FEBS Lett* 420, 25-27.
- Howlett, N. G., Taniguchi, T., Olson, S., Cox, B., Waisfisz, Q., De Die-Smulders, C., Persky, N., Grompe, M., Joenje, H., Pals, G., *et al.* (2002). Biallelic inactivation of BRCA2 in Fanconi anemia. *Science* 297, 606-609.
- Hsu, S. Y., Kaipia, A., McGee, E., Lomeli, M., and Hsueh, A. J. (1997). Bok is a pro-apoptotic Bcl-2 protein with restricted expression in reproductive tissues and heterodimerizes with selective anti-apoptotic Bcl-2 family members. *Proc Natl Acad Sci U S A* 94, 12401-12406.
- Inoue, H., Nojima, H., and Okayama, H. (1990). High efficiency transformation of *Escherichia coli* with plasmids. *Gene* 96, 23-28.
- Jabbur, J. R., Huang, P., and Zhang, W. (2000). DNA damage-induced phosphorylation of p53 at serine 20 correlates with p21 and Mdm-2 induction in vivo. *Oncogene* 19, 6203-6208.
- Jachymczyk, W. J., von Borstel, R. C., Mowat, M. R., and Hastings, P. J. (1981). Repair of interstrand cross-links in DNA of *Saccharomyces cerevisiae* requires two systems for DNA repair: the RAD3 system and the RAD51 system. *Mol Gen Genet* 182, 196-205.
- Jiang, P., Du, W., Heese, K., and Wu, M. (2006). The Bad guy cooperates with good cop p53: Bad is transcriptionally up-regulated by p53 and forms a Bad/p53 complex at the mitochondria to induce apoptosis. *Mol Cell Biol* 26, 9071-9082.
- Johansson, F., Lagerqvist, A., Erixon, K., and Jenssen, D. (2004). A method to monitor replication fork progression in mammalian cells: nucleotide excision

repair enhances and homologous recombination delays elongation along damaged DNA. *Nucleic Acids Res* 32, e157.

Jones, B. K., and Yeung, A. T. (1990). DNA base composition determines the specificity of UvrABC endonuclease incision of a psoralen cross-link. *J Biol Chem* 265, 3489-3496.

Jumaa, H., Wei, G., and Nielsen, P. J. (1999). Blastocyst formation is blocked in mouse embryos lacking the splicing factor SRp20. *Curr Biol* 9, 899-902.

Jurgensmeier, J. M., Xie, Z., Deveraux, Q., Ellerby, L., Bredesen, D., and Reed, J. C. (1998). Bax directly induces release of cytochrome c from isolated mitochondria. *Proc Natl Acad Sci U S A* 95, 4997-5002.

Jurica, M. S., Sousa, D., Moore, M. J., and Grigorieff, N. (2004). Three-dimensional structure of C complex spliceosomes by electron microscopy. *Nat Struct Mol Biol* 11, 265-269.

Karni, R., de Stanchina, E., Lowe, S. W., Sinha, R., Mu, D., and Krainer, A. R. (2007). The gene encoding the splicing factor SF2/ASF is a proto-oncogene. *Nat Struct Mol Biol* 14, 185-193.

Kaufman, R. J. (1999). Stress signaling from the lumen of the endoplasmic reticulum: coordination of gene transcriptional and translational controls. *Genes Dev* 13, 1211-1233.

Kelekar, A., and Thompson, C. B. (1998). Bcl-2-family proteins: the role of the BH3 domain in apoptosis. *Trends Cell Biol* 8, 324-330.

Kelly-Spratt, K. S., Gurley, K. E., Yasui, Y., and Kemp, C. J. (2004). p19Arf suppresses growth, progression, and metastasis of Hras-driven carcinomas through p53-dependent and -independent pathways. *PLoS Biol* 2, E242.

Kerr, J. F., Wyllie, A. H., and Currie, A. R. (1972). Apoptosis: a basic biological phenomenon with wide-ranging implications in tissue kinetics. *Br J Cancer* 26, 239-257.

Kim, M. J., Kim, Y., Kim, S. A., Lee, H. J., Choe, B. K., Nam, M., Kim, B. S., Kim, J. W., Yim, S. V., Kim, C. J., and Chung, J. H. (2001). Increases in cell proliferation and apoptosis in dentate gyrus of anorexia (anx/anx) mice. *Neurosci Lett* 302, 109-112.

Kim, S. T., Xu, B., and Kastan, M. B. (2002). Involvement of the cohesin protein, Smc1, in Atm-dependent and independent responses to DNA damage. *Genes Dev* 16, 560-570.

Kim, T. H., Zhao, Y., Barber, M. J., Kuharsky, D. K., and Yin, X. M. (2000). Bid-induced cytochrome c release is mediated by a pathway independent of mitochondrial permeability transition pore and Bax. *J Biol Chem* 275, 39474-39481.

## References

---

- Kischkel, F. C., Hellbardt, S., Behrmann, I., Germer, M., Pawlita, M., Krammer, P. H., and Peter, M. E. (1995). Cytotoxicity-dependent APO-1 (Fas/CD95)-associated proteins form a death-inducing signaling complex (DISC) with the receptor. *Embo J* 14, 5579-5588.
- Kitajima, T. S., Sakuno, T., Ishiguro, K., Iemura, S., Natsume, T., Kawashima, S. A., and Watanabe, Y. (2006). Shugoshin collaborates with protein phosphatase 2A to protect cohesin. *Nature* 441, 46-52.
- Kluck, R. M., Esposti, M. D., Perkins, G., Renken, C., Kuwana, T., Bossy-Wetzel, E., Goldberg, M., Allen, T., Barber, M. J., Green, D. R., and Newmeyer, D. D. (1999). The pro-apoptotic proteins, Bid and Bax, cause a limited permeabilization of the mitochondrial outer membrane that is enhanced by cytosol. *J Cell Biol* 147, 809-822.
- Knockaert, M., Sapkota, G., Alarcon, C., Massague, J., and Brivanlou, A. H. (2006). Unique players in the BMP pathway: small C-terminal domain phosphatases dephosphorylate Smad1 to attenuate BMP signaling. *Proc Natl Acad Sci U S A* 103, 11940-11945.
- Korsmeyer, S. J. (1992). Bcl-2 initiates a new category of oncogenes: regulators of cell death. *Blood* 80, 879-886.
- Korsmeyer, S. J., Wei, M. C., Saito, M., Weiler, S., Oh, K. J., and Schlesinger, P. H. (2000). Pro-apoptotic cascade activates BID, which oligomerizes BAK or BAX into pores that result in the release of cytochrome c. *Cell Death Differ* 7, 1166-1173.
- Kramer, A. (1996). The structure and function of proteins involved in mammalian pre-mRNA splicing. *Annu Rev Biochem* 65, 367-409.
- Kuraoka, I., Kobertz, W. R., Ariza, R. R., Biggerstaff, M., Essigmann, J. M., and Wood, R. D. (2000). Repair of an interstrand DNA cross-link initiated by ERCC1-XPF repair/recombination nuclease. *J Biol Chem* 275, 26632-26636.
- La Porta, C. A., Porro, D., and Comolli, R. (1998). Opposite effects of TPA on G1/S transition and on cell size in the low metastatic B16F1 with respect to high metastatic BL6 murine melanoma cells. *Cancer Lett* 132, 159-164.
- Lakin, N. D., Hann, B. C., and Jackson, S. P. (1999). The ataxia-telangiectasia related protein ATR mediates DNA-dependent phosphorylation of p53. *Oncogene* 18, 3989-3995.
- Lambert, P. F., Kashanchi, F., Radonovich, M. F., Shiekhattar, R., and Brady, J. N. (1998). Phosphorylation of p53 serine 15 increases interaction with CBP. *J Biol Chem* 273, 33048-33053.
- Lammer, C., Wagerer, S., Saffrich, R., Mertens, D., Ansorge, W., and Hoffmann, I. (1998). The cdc25B phosphatase is essential for the G2/M phase transition in human cells. *J Cell Sci* 111 ( Pt 16), 2445-2453.

- Landesman-Bollag, E., Channavajhala, P. L., Cardiff, R. D., and Seldin, D. C. (1998). p53 deficiency and misexpression of protein kinase CK2alpha collaborate in the development of thymic lymphomas in mice. *Oncogene* 16, 2965-2974.
- Langheinrich, U., Hennen, E., Stott, G., and Vacun, G. (2002). Zebrafish as a model organism for the identification and characterization of drugs and genes affecting p53 signaling. *Curr Biol* 12, 2023-2028.
- Larochelle, S., Merrick, K. A., Terret, M. E., Wohlbold, L., Barboza, N. M., Zhang, C., Shokat, K. M., Jallepalli, P. V., and Fisher, R. P. (2007). Requirements for Cdk7 in the assembly of Cdk1/cyclin B and activation of Cdk2 revealed by chemical genetics in human cells. *Mol Cell* 25, 839-850.
- Lee, J. E., Sohn, J., Lee, J. H., Lee, K. C., Son, C. S., and Tockgo, Y. C. (2000). Regulation of bcl-2 family in hydrogen peroxide-induced apoptosis in human leukemia HL-60 cells. *Exp Mol Med* 32, 42-46.
- Levine, A. J. (1997). p53, the cellular gatekeeper for growth and division. *Cell* 88, 323-331.
- Li, H., Zhu, H., Xu, C. J., and Yuan, J. (1998). Cleavage of BID by caspase 8 mediates the mitochondrial damage in the Fas pathway of apoptosis. *Cell* 94, 491-501.
- Li, J., Lee, B., and Lee, A. S. (2006). Endoplasmic reticulum stress-induced apoptosis: multiple pathways and activation of p53-up-regulated modulator of apoptosis (PUMA) and NOXA by p53. *J Biol Chem* 281, 7260-7270.
- Li, J., Meyer, A. N., and Donoghue, D. J. (1997). Nuclear localization of cyclin B1 mediates its biological activity and is regulated by phosphorylation. *Proc Natl Acad Sci U S A* 94, 502-507.
- Li, L. Y., Luo, X., and Wang, X. (2001). Endonuclease G is an apoptotic DNase when released from mitochondria. *Nature* 412, 95-99.
- Li, P., Nijhawan, D., Budihardjo, I., Srinivasula, S. M., Ahmad, M., Alnemri, E. S., and Wang, X. (1997). Cytochrome c and dATP-dependent formation of Apaf-1/caspase-9 complex initiates an apoptotic protease cascade. *Cell* 91, 479-489.
- Lin, D., Shields, M. T., Ullrich, S. J., Appella, E., and Mercer, W. E. (1992). Growth arrest induced by wild-type p53 protein blocks cells prior to or near the restriction point in late G1 phase. *Proc Natl Acad Sci U S A* 89, 9210-9214.
- Lin, X., Duan, X., Liang, Y. Y., Su, Y., Wrighton, K. H., Long, J., Hu, M., Davis, C. M., Wang, J., Brunicardi, F. C., *et al.* (2006). PPM1A functions as a Smad phosphatase to terminate TGFbeta signaling. *Cell* 125, 915-928.
- Liu, C. W., Wang, R. H., Dohadwala, M., Schonthal, A. H., Villa-Moruzzi, E., and Berndt, N. (1999). Inhibitory phosphorylation of PP1alpha catalytic subunit

## References

---

during the G(1)/S transition. *J Biol Chem* 274, 29470-29475.

Liu, Q., Guntuku, S., Cui, X. S., Matsuoka, S., Cortez, D., Tamai, K., Luo, G., Carattini-Rivera, S., DeMayo, F., Bradley, A., *et al.* (2000). Chk1 is an essential kinase that is regulated by Atr and required for the G(2)/M DNA damage checkpoint. *Genes Dev* 14, 1448-1459.

Liu, X., Kim, C. N., Yang, J., Jemmerson, R., and Wang, X. (1996). Induction of apoptotic program in cell-free extracts: requirement for dATP and cytochrome c. *Cell* 86, 147-157.

Lou, Z., Chini, C. C., Minter-Dykhouse, K., and Chen, J. (2003). Mediator of DNA damage checkpoint protein 1 regulates BRCA1 localization and phosphorylation in DNA damage checkpoint control. *J Biol Chem* 278, 13599-13602.

Lu, X., Nannenga, B., and Donehower, L. A. (2005). PPM1D dephosphorylates Chk1 and p53 and abrogates cell cycle checkpoints. *Genes Dev* 19, 1162-1174.

Lu, X., Nguyen, T. A., Appella, E., and Donehower, L. A. (2004). Homeostatic regulation of base excision repair by a p53-induced phosphatase: linking stress response pathways with DNA repair proteins. *Cell Cycle* 3, 1363-1366.

Madeo, F., Frohlich, E., Ligr, M., Grey, M., Sigrist, S. J., Wolf, D. H., and Frohlich, K. U. (1999). Oxygen stress: a regulator of apoptosis in yeast. *J Cell Biol* 145, 757-767.

Mahajan, K. N., and Mitchell, B. S. (2003). Role of human Pso4 in mammalian DNA repair and association with terminal deoxynucleotidyl transferase. *Proc Natl Acad Sci U S A* 100, 10746-10751.

Mailand, N., Falck, J., Lukas, C., Syljuasen, R. G., Welcker, M., Bartek, J., and Lukas, J. (2000). Rapid destruction of human Cdc25A in response to DNA damage. *Science* 288, 1425-1429.

Makarov, E. M., Makarova, O. V., Urlaub, H., Gentzel, M., Will, C. L., Wilm, M., and Luhrmann, R. (2002). Small nuclear ribonucleoprotein remodeling during catalytic activation of the spliceosome. *Science* 298, 2205-2208.

Mandal, M., Bandyopadhyay, D., Goepfert, T. M., and Kumar, R. (1998). Interferon-induces expression of cyclin-dependent kinase-inhibitors p21WAF1 and p27Kip1 that prevent activation of cyclin-dependent kinase by CDK-activating kinase (CAK). *Oncogene* 16, 217-225.

Margolis, S. S., Perry, J. A., Weitzel, D. H., Freel, C. D., Yoshida, M., Haystead, T. A., and Kornbluth, S. (2006). A role for PP1 in the Cdc2/Cyclin B-mediated positive feedback activation of Cdc25. *Mol Biol Cell* 17, 1779-1789.

Maroto, R., and Perez-Polo, J. R. (1997). BCL-2-related protein expression in apoptosis: oxidative stress versus serum deprivation in PC12 cells. *J Neurochem* 69, 514-523.



- Mason, S. L., Loughran, O., and La Thangue, N. B. (2002). p14(ARF) regulates E2F activity. *Oncogene* *21*, 4220-4230.
- Matsumoto, A., Vos, J. M., and Hanawalt, P. C. (1989). Repair analysis of mitomycin C-induced DNA crosslinking in ribosomal RNA genes in lymphoblastoid cells from Fanconi's anemia patients. *Mutat Res* *217*, 185-192.
- Matsuoka, S., Huang, M., and Elledge, S. J. (1998). Linkage of ATM to cell cycle regulation by the Chk2 protein kinase. *Science* *282*, 1893-1897.
- Matsuoka, S., Rotman, G., Ogawa, A., Shiloh, Y., Tamai, K., and Elledge, S. J. (2000). Ataxia telangiectasia-mutated phosphorylates Chk2 in vivo and in vitro. *Proc Natl Acad Sci U S A* *97*, 10389-10394.
- McDonald, W. H., Ohi, R., Smelkova, N., Frendewey, D., and Gould, K. L. (1999). Myb-related fission yeast cdc5p is a component of a 40S snRNP-containing complex and is essential for pre-mRNA splicing. *Mol Cell Biol* *19*, 5352-5362.
- McHugh, P. J., Sones, W. R., and Hartley, J. A. (2000). Repair of intermediate structures produced at DNA interstrand cross-links in *Saccharomyces cerevisiae*. *Mol Cell Biol* *20*, 3425-3433.
- Medema, J. P., Scaffidi, C., Kischkel, F. C., Shevchenko, A., Mann, M., Krammer, P. H., and Peter, M. E. (1997). FLICE is activated by association with the CD95 death-inducing signaling complex (DISC). *Embo J* *16*, 2794-2804.
- Medema, R. H., Klompmaker, R., Smits, V. A., and Rijksen, G. (1998). p21waf1 can block cells at two points in the cell cycle, but does not interfere with processive DNA-replication or stress-activated kinases. *Oncogene* *16*, 431-441.
- Melchionna, R., Chen, X. B., Blasina, A., and McGowan, C. H. (2000). Threonine 68 is required for radiation-induced phosphorylation and activation of Cds1. *Nat Cell Biol* *2*, 762-765.
- Melton, D. W., Ketchen, A. M., Nunez, F., Bonatti-Abbondandolo, S., Abbondandolo, A., Squires, S., and Johnson, R. T. (1998). Cells from ERCC1-deficient mice show increased genome instability and a reduced frequency of S-phase-dependent illegitimate chromosome exchange but a normal frequency of homologous recombination. *J Cell Sci* *111* ( Pt 3), 395-404.
- Memisoglu, A., and Samson, L. (2000). Base excision repair in yeast and mammals. *Mutat Res* *451*, 39-51.
- Merendino, L., Guth, S., Bilbao, D., Martinez, C., and Valcarcel, J. (1999). Inhibition of msl-2 splicing by Sex-lethal reveals interaction between U2AF35 and the 3' splice site AG. *Nature* *402*, 838-841.
- Michaud, S., and Reed, R. (1991). An ATP-independent complex commits pre-mRNA to the mammalian spliceosome assembly pathway. *Genes Dev* *5*, 2534-

## References

---

2546.

Mikhailov, V., Mikhailova, M., Degenhardt, K., Venkatachalam, M. A., White, E., and Saikumar, P. (2003). Association of Bax and Bak homo-oligomers in mitochondria. Bax requirement for Bak reorganization and cytochrome c release. *J Biol Chem* 278, 5367-5376.

Mikhailov, V., Mikhailova, M., Pulkrabek, D. J., Dong, Z., Venkatachalam, M. A., and Saikumar, P. (2001). Bcl-2 prevents Bax oligomerization in the mitochondrial outer membrane. *J Biol Chem* 276, 18361-18374.

Mirzoeva, O. K., and Petrini, J. H. (2001). DNA damage-dependent nuclear dynamics of the Mre11 complex. *Mol Cell Biol* 21, 281-288.

Miyashita, T., Krajewski, S., Krajewska, M., Wang, H. G., Lin, H. K., Liebermann, D. A., Hoffman, B., and Reed, J. C. (1994). Tumor suppressor p53 is a regulator of bcl-2 and bax gene expression in vitro and in vivo. *Oncogene* 9, 1799-1805.

Miyashita, T., and Reed, J. C. (1995). Tumor suppressor p53 is a direct transcriptional activator of the human bax gene. *Cell* 80, 293-299.

Mol, C. D., Parikh, S. S., Putnam, C. D., Lo, T. P., and Tainer, J. A. (1999). DNA repair mechanisms for the recognition and removal of damaged DNA bases. *Annu Rev Biophys Biomol Struct* 28, 101-128.

Moorhead, G. B., Trinkle-Mulcahy, L., and Ulke-Lemee, A. (2007). Emerging roles of nuclear protein phosphatases. *Nat Rev Mol Cell Biol* 8, 234-244.

Moroni, M. C., Hickman, E. S., Lazzerini Denchi, E., Caprara, G., Colli, E., Cecconi, F., Muller, H., and Helin, K. (2001). Apaf-1 is a transcriptional target for E2F and p53. *Nat Cell Biol* 3, 552-558.

Morris, E. J., Keramaris, E., Rideout, H. J., Slack, R. S., Dyson, N. J., Stefanis, L., and Park, D. S. (2001). Cyclin-dependent kinases and P53 pathways are activated independently and mediate Bax activation in neurons after DNA damage. *J Neurosci* 21, 5017-5026.

Muchmore, S. W., Sattler, M., Liang, H., Meadows, R. P., Harlan, J. E., Yoon, H. S., Nettesheim, D., Chang, B. S., Thompson, C. B., Wong, S. L., *et al.* (1996). X-ray and NMR structure of human Bcl-xL, an inhibitor of programmed cell death. *Nature* 381, 335-341.

Mueller, P. R., Coleman, T. R., Kumagai, A., and Dunphy, W. G. (1995). Myt1: a membrane-associated inhibitory kinase that phosphorylates Cdc2 on both threonine-14 and tyrosine-15. *Science* 270, 86-90.

Narita, M., Shimizu, S., Ito, T., Chittenden, T., Lutz, R. J., Matsuda, H., and Tsujimoto, Y. (1998). Bax interacts with the permeability transition pore to induce permeability transition and cytochrome c release in isolated mitochondria. *Proc Natl Acad Sci U S A* 95, 14681-14686.

- Natarajan, A. T., Darroudi, F., Jha, A. N., Meijers, M., and Zdzienicka, M. Z. (1993). Ionizing radiation induced DNA lesions which lead to chromosomal aberrations. *Mutat Res* 299, 297-303.
- Nemeth, K., Salchert, K., Putnoky, P., Bhalerao, R., Koncz-Kalman, Z., Stankovic-Stangeland, B., Bako, L., Mathur, J., Okresz, L., Stabel, S., *et al.* (1998). Pleiotropic control of glucose and hormone responses by PRL1, a nuclear WD protein, in Arabidopsis. *Genes Dev* 12, 3059-3073.
- Neubauer, G., King, A., Rappsilber, J., Calvio, C., Watson, M., Ajuh, P., Sleeman, J., Lamond, A., and Mann, M. (1998). Mass spectrometry and EST-database searching allows characterization of the multi-protein spliceosome complex. *Nat Genet* 20, 46-50.
- Neubauer, G., King, A., Rappsilber, J., Calvio, C., Watson, M., Ajuh, P., Sleeman, J., Lamond, A., and Mann, M. (1998). Mass spectrometry and EST-database searching allows characterization of the multi-protein spliceosome complex. *Nat Genet* 20, 46-50.
- Niedernhofer, L. J., Odijk, H., Budzowska, M., van Drunen, E., Maas, A., Theil, A. F., de Wit, J., Jaspers, N. G., Beverloo, H. B., Hoeijmakers, J. H., and Kanaar, R. (2004). The structure-specific endonuclease Ercc1-Xpf is required to resolve DNA interstrand cross-link-induced double-strand breaks. *Mol Cell Biol* 24, 5776-5787.
- Nilsen, T. W. (2002). The spliceosome: no assembly required? *Mol Cell* 9, 8-9.
- Nunez, G., Benedict, M. A., Hu, Y., and Inohara, N. (1998). Caspases: the proteases of the apoptotic pathway. *Oncogene* 17, 3237-3245.
- O'Reilly, L. A., Cullen, L., Visvader, J., Lindeman, G. J., Print, C., Bath, M. L., Huang, D. C., and Strasser, A. (2000). The proapoptotic BH3-only protein bim is expressed in hematopoietic, epithelial, neuronal, and germ cells. *Am J Pathol* 157, 449-461.
- Ohi, M. D., Vander Kooi, C. W., Rosenberg, J. A., Ren, L., Hirsch, J. P., Chazin, W. J., Walz, T., and Gould, K. L. (2005). Structural and functional analysis of essential pre-mRNA splicing factor Prp19p. *Mol Cell Biol* 25, 451-460.
- Ohki, R., Nemoto, J., Murasawa, H., Oda, E., Inazawa, J., Tanaka, N., and Taniguchi, T. (2000). Reprimo, a new candidate mediator of the p53-mediated cell cycle arrest at the G2 phase. *J Biol Chem* 275, 22627-22630.
- Oltvai, Z. N., Milliman, C. L., and Korsmeyer, S. J. (1993). Bcl-2 heterodimerizes in vivo with a conserved homolog, Bax, that accelerates programmed cell death. *Cell* 74, 609-619.
- Osoegawa, K., Tateno, M., Woon, P. Y., Frengen, E., Mammoser, A. G., Catanese, J. J., Hayashizaki, Y., and de Jong, P. J. (2000). Bacterial artificial chromosome libraries for mouse sequencing and functional analysis. *Genome Res* 10, 116-128.

## References

---

- Park, E. J., Chan, D. W., Park, J. H., Oettinger, M. A., and Kwon, J. (2003). DNA-PK is activated by nucleosomes and phosphorylates H2AX within the nucleosomes in an acetylation-dependent manner. *Nucleic Acids Res* 31, 6819-6827.
- Pasman, Z., and Garcia-Blanco, M. A. (1996). The 5' and 3' splice sites come together via a three dimensional diffusion mechanism. *Nucleic Acids Res* 24, 1638-1645.
- Patil, C., and Walter, P. (2001). Intracellular signaling from the endoplasmic reticulum to the nucleus: the unfolded protein response in yeast and mammals. *Curr Opin Cell Biol* 13, 349-355.
- Peitz, M., Pfannkuche, K., Rajewsky, K., and Edenhofer, F. (2002). Ability of the hydrophobic FGF and basic TAT peptides to promote cellular uptake of recombinant Cre recombinase: a tool for efficient genetic engineering of mammalian genomes. *Proc Natl Acad Sci U S A* 99, 4489-4494.
- Peng, C. Y., Graves, P. R., Thoma, R. S., Wu, Z., Shaw, A. S., and Piwnicka-Worms, H. (1997). Mitotic and G2 checkpoint control: regulation of 14-3-3 protein binding by phosphorylation of Cdc25C on serine-216. *Science* 277, 1501-1505.
- Petit, P. X., Goubern, M., Diolez, P., Susin, S. A., Zamzami, N., and Kroemer, G. (1998). Disruption of the outer mitochondrial membrane as a result of large amplitude swelling: the impact of irreversible permeability transition. *FEBS Lett* 426, 111-116.
- Pikielny, C. W., Rymond, B. C., and Rosbash, M. (1986). Electrophoresis of ribonucleoproteins reveals an ordered assembly pathway of yeast splicing complexes. *Nature* 324, 341-345.
- Priebe, S. D., Westmoreland, J., Nilsson-Tillgren, T., and Resnick, M. A. (1994). Induction of recombination between homologous and diverged DNAs by double-strand gaps and breaks and role of mismatch repair. *Mol Cell Biol* 14, 4802-4814.
- Rappsilber, J., Ryder, U., Lamond, A. I., and Mann, M. (2002). Large-scale proteomic analysis of the human spliceosome. *Genome Res* 12, 1231-1245.
- Reed, J. C., Jurgensmeier, J. M., and Matsuyama, S. (1998). Bcl-2 family proteins and mitochondria. *Biochim Biophys Acta* 1366, 127-137.
- Reed, R. (1989). The organization of 3' splice-site sequences in mammalian introns. *Genes Dev* 3, 2113-2123.
- Reed, R., and Maniatis, T. (1988). The role of the mammalian branchpoint sequence in pre-mRNA splicing. *Genes Dev* 2, 1268-1276.
- Rempe, D., Vangeison, G., Hamilton, J., Li, Y., Jepson, M., and Federoff, H. J.

- (2006). Synapsin I Cre transgene expression in male mice produces germline recombination in progeny. *Genesis* 44, 44-49.
- Rich, T., Allen, R. L., and Wyllie, A. H. (2000). Defying death after DNA damage. *Nature* 407, 777-783.
- Rodriguez, C. I., Buchholz, F., Galloway, J., Sequerra, R., Kasper, J., Ayala, R., Stewart, A. F., and Dymecki, S. M. (2000). High-efficiency deleter mice show that FLPe is an alternative to Cre-loxP. *Nat Genet* 25, 139-140.
- Rothfuss, A., and Grompe, M. (2004). Repair kinetics of genomic interstrand DNA cross-links: evidence for DNA double-strand break-dependent activation of the Fanconi anemia/BRCA pathway. *Mol Cell Biol* 24, 123-134.
- Saiki, R. K., Bugawan, T. L., Horn, G. T., Mullis, K. B., and Erlich, H. A. (1986). Analysis of enzymatically amplified beta-globin and HLA-DQ alpha DNA with allele-specific oligonucleotide probes. *Nature* 324, 163-166.
- Saiki, R. K., Scharf, S., Faloona, F., Mullis, K. B., Horn, G. T., Erlich, H. A., and Arnheim, N. (1985). Enzymatic amplification of beta-globin genomic sequences and restriction site analysis for diagnosis of sickle cell anemia. *Science* 230, 1350-1354.
- Sakaguchi, K., Sakamoto, H., Lewis, M. S., Anderson, C. W., Erickson, J. W., Appella, E., and Xie, D. (1997). Phosphorylation of serine 392 stabilizes the tetramer formation of tumor suppressor protein p53. *Biochemistry* 36, 10117-10124.
- Sakahira, H., Enari, M., and Nagata, S. (1998). Cleavage of CAD inhibitor in CAD activation and DNA degradation during apoptosis. *Nature* 391, 96-99.
- Samadashwily, G. M., Raca, G., and Mirkin, S. M. (1997). Trinucleotide repeats affect DNA replication in vivo. *Nat Genet* 17, 298-304.
- Sambrook, J., E: F., F., and Maniatis, T. (1989) *Molecular Cloning*, Cold Spring Harbor Laboratory Press).
- Sancar, A. (1996). DNA excision repair. *Annu Rev Biochem* 65, 43-81.
- Sancar, A., Lindsey-Boltz, L. A., Unsal-Kacmaz, K., and Linn, S. (2004). Molecular mechanisms of mammalian DNA repair and the DNA damage checkpoints. *Annu Rev Biochem* 73, 39-85.
- Sancar, G. B. (1990). DNA photolyases: physical properties, action mechanism, and roles in dark repair. *Mutat Res* 236, 147-160.
- Sanchez, Y., Bachant, J., Wang, H., Hu, F., Liu, D., Tetzlaff, M., and Elledge, S. J. (1999). Control of the DNA damage checkpoint by chk1 and rad53 protein kinases through distinct mechanisms. *Science* 286, 1166-1171.
- Sanchez, Y., Wong, C., Thoma, R. S., Richman, R., Wu, Z., Piwnica-Worms,

## References

---

- H., and Elledge, S. J. (1997). Conservation of the Chk1 checkpoint pathway in mammals: linkage of DNA damage to Cdk regulation through Cdc25. *Science* 277, 1497-1501.
- Sandri, M. I., Isaacs, R. J., Ongkeko, W. M., Harris, A. L., Hickson, I. D., Broggin, M., and Vihanskaya, F. (1996). p53 regulates the minimal promoter of the human topoisomerase II $\alpha$  gene. *Nucleic Acids Res* 24, 4464-4470.
- Sanger, F., Nicklen, S., and Coulson, A. R. (1977). DNA sequencing with chain-terminating inhibitors. *Proc Natl Acad Sci U S A* 74, 5463-5467.
- Sanz, C., Benito, A., Inohara, N., Ekhterae, D., Nunez, G., and Fernandez-Luna, J. L. (2000). Specific and rapid induction of the proapoptotic protein Hrk after growth factor withdrawal in hematopoietic progenitor cells. *Blood* 95, 2742-2747.
- Sawa, H., Ohno, M., Sakamoto, H., and Shimura, Y. (1988). Requirement of ATP in the second step of the pre-mRNA splicing reaction. *Nucleic Acids Res* 16, 3157-3164.
- Scaffidi, C., Fulda, S., Srinivasan, A., Friesen, C., Li, F., Tomaselli, K. J., Debatin, K. M., Krammer, P. H., and Peter, M. E. (1998). Two CD95 (APO-1/Fas) signaling pathways. *Embo J* 17, 1675-1687.
- Scarlett, J. L., and Murphy, M. P. (1997). Release of apoptogenic proteins from the mitochondrial intermembrane space during the mitochondrial permeability transition. *FEBS Lett* 418, 282-286.
- Schneider, E., Montenarh, M., and Wagner, P. (1998). Regulation of CAK kinase activity by p53. *Oncogene* 17, 2733-2741.
- Schultz, L. B., Chehab, N. H., Malikzay, A., and Halazonetis, T. D. (2000). p53 binding protein 1 (53BP1) is an early participant in the cellular response to DNA double-strand breaks. *J Cell Biol* 151, 1381-1390.
- Schulze, A., Zerfass, K., Spitkovsky, D., Henglein, B., and Jansen-Durr, P. (1994). Activation of the E2F transcription factor by cyclin D1 is blocked by p16INK4, the product of the putative tumor suppressor gene MTS1. *Oncogene* 9, 3475-3482.
- Scully, R., Chen, J., Ochs, R. L., Keegan, K., Hoekstra, M., Feunteun, J., and Livingston, D. M. (1997). Dynamic changes of BRCA1 subnuclear location and phosphorylation state are initiated by DNA damage. *Cell* 90, 425-435.
- Sedelnikova, O. A., Horikawa, I., Zimonjic, D. B., Popescu, N. C., Bonner, W. M., and Barrett, J. C. (2004). Senescing human cells and ageing mice accumulate DNA lesions with unreparable double-strand breaks. *Nat Cell Biol* 6, 168-170.
- Shechter, D., Costanzo, V., and Gautier, J. (2004). ATR and ATM regulate the timing of DNA replication origin firing. *Nat Cell Biol* 6, 648-655.

- Shechter, D., Costanzo, V., and Gautier, J. (2004). Regulation of DNA replication by ATR: signaling in response to DNA intermediates. *DNA Repair (Amst)* 3, 901-908.
- Shieh, S. Y., Ahn, J., Tamai, K., Taya, Y., and Prives, C. (2000). The human homologs of checkpoint kinases Chk1 and Cds1 (Chk2) phosphorylate p53 at multiple DNA damage-inducible sites. *Genes Dev* 14, 289-300.
- Shimizu, S., Narita, M., and Tsujimoto, Y. (1999). Bcl-2 family proteins regulate the release of apoptogenic cytochrome c by the mitochondrial channel VDAC. *Nature* 399, 483-487.
- Shiraishi, J., Tatsumi, T., Keira, N., Akashi, K., Mano, A., Yamanaka, S., Matoba, S., Asayama, J., Yaoi, T., Fushiki, S., *et al.* (2001). Important role of energy-dependent mitochondrial pathways in cultured rat cardiac myocyte apoptosis. *Am J Physiol Heart Circ Physiol* 281, H1637-1647.
- Silver, L. M. (1995). *Mouse genetics: concepts and practice*, Oxford University Press).
- Sladek, F. M., Munn, M. M., Rupp, W. D., and Howard-Flanders, P. (1989). In vitro repair of psoralen-DNA cross-links by RecA, UvrABC, and the 5'-exonuclease of DNA polymerase I. *J Biol Chem* 264, 6755-6765.
- Slee, E. A., Harte, M. T., Kluck, R. M., Wolf, B. B., Casiano, C. A., Newmeyer, D. D., Wang, H. G., Reed, J. C., Nicholson, D. W., Alnemri, E. S., *et al.* (1999). Ordering the cytochrome c-initiated caspase cascade: hierarchical activation of caspases-2, -3, -6, -7, -8, and -10 in a caspase-9-dependent manner. *J Cell Biol* 144, 281-292.
- Smith, C. W., Porro, E. B., Patton, J. G., and Nadal-Ginard, B. (1989). Scanning from an independently specified branch point defines the 3' splice site of mammalian introns. *Nature* 342, 243-247.
- Sonnichsen, B., Koski, L. B., Walsh, A., Marschall, P., Neumann, B., Brehm, M., Alleaume, A. M., Artelt, J., Bettencourt, P., Cassin, E., *et al.* (2005). Full-genome RNAi profiling of early embryogenesis in *Caenorhabditis elegans*. *Nature* 434, 462-469.
- Soulier, J., and Lowndes, N. F. (1999). The BRCT domain of the *S. cerevisiae* checkpoint protein Rad9 mediates a Rad9-Rad9 interaction after DNA damage. *Curr Biol* 9, 551-554.
- Srinivasula, S. M., Ahmad, M., Fernandes-Alnemri, T., and Alnemri, E. S. (1998). Autoactivation of procaspase-9 by Apaf-1-mediated oligomerization. *Mol Cell* 1, 949-957.
- Staley, J. P., and Guthrie, C. (1998). Mechanical devices of the spliceosome: motors, clocks, springs, and things. *Cell* 92, 315-326.

## References

---

Stephens, R. M., and Schneider, T. D. (1992). Features of spliceosome evolution and function inferred from an analysis of the information at human splice sites. *J Mol Biol* 228, 1124-1136.

Stevens, S. W., Ryan, D. E., Ge, H. Y., Moore, R. E., Young, M. K., Lee, T. D., and Abelson, J. (2002). Composition and functional characterization of the yeast spliceosomal penta-snRNP. *Mol Cell* 9, 31-44.

Stevnsner, T., May, A., Petersen, L. N., Larminat, F., Pirsell, M., and Bohr, V. A. (1993). Repair of ribosomal RNA genes in hamster cells after UV irradiation, or treatment with cisplatin or alkylating agents. *Carcinogenesis* 14, 1591-1596.

Stewart, G. S., Wang, B., Bignell, C. R., Taylor, A. M., and Elledge, S. J. (2003). MDC1 is a mediator of the mammalian DNA damage checkpoint. *Nature* 421, 961-966.

Sun, Z., Hsiao, J., Fay, D. S., and Stern, D. F. (1998). Rad53 FHA domain associated with phosphorylated Rad9 in the DNA damage checkpoint. *Science* 281, 272-274.

Susin, S. A., Lorenzo, H. K., Zamzami, N., Marzo, I., Brenner, C., Larochette, N., Prevost, M. C., Alzari, P. M., and Kroemer, G. (1999). Mitochondrial release of caspase-2 and -9 during the apoptotic process. *J Exp Med* 189, 381-394.

Susin, S. A., Lorenzo, H. K., Zamzami, N., Marzo, I., Snow, B. E., Brothers, G. M., Mangion, J., Jacotot, E., Costantini, P., Loeffler, M., *et al.* (1999).

Molecular characterization of mitochondrial apoptosis-inducing factor. *Nature* 397, 441-446.

Takai, H., Smogorzewska, A., and de Lange, T. (2003). DNA damage foci at dysfunctional telomeres. *Curr Biol* 13, 1549-1556.

Takata, M., Sasaki, M. S., Sonoda, E., Morrison, C., Hashimoto, M., Utsumi, H., Yamaguchi-Iwai, Y., Shinohara, A., and Takeda, S. (1998). Homologous recombination and non-homologous end-joining pathways of DNA double-strand break repair have overlapping roles in the maintenance of chromosomal integrity in vertebrate cells. *Embo J* 17, 5497-5508.

Takekawa, M., Adachi, M., Nakahata, A., Nakayama, I., Itoh, F., Tsukuda, H., Taya, Y., and Imai, K. (2000). p53-inducible wip1 phosphatase mediates a negative feedback regulation of p38 MAPK-p53 signaling in response to UV radiation. *Embo J* 19, 6517-6526.

Takekawa, M., Adachi, M., Nakahata, A., Nakayama, I., Itoh, F., Tsukuda, H., Taya, Y., and Imai, K. (2000). p53-inducible wip1 phosphatase mediates a negative feedback regulation of p38 MAPK-p53 signaling in response to UV radiation. *Embo J* 19, 6517-6526.

Tewari, M., Quan, L. T., O'Rourke, K., Desnoyers, S., Zeng, Z., Beidler, D. R., Poirier, G. G., Salvesen, G. S., and Dixit, V. M. (1995). Yama/CPP32 beta, a



mammalian homolog of CED-3, is a CrmA-inhibitable protease that cleaves the death substrate poly(ADP-ribose) polymerase. *Cell* **81**, 801-809.

Thornborrow, E. C., Patel, S., Mastropietro, A. E., Schwartzfarb, E. M., and Manfredi, J. J. (2002). A conserved intronic response element mediates direct p53-dependent transcriptional activation of both the human and murine bax genes. *Oncogene* **21**, 990-999.

Tomicic, M. T., Christmann, M., and Kaina, B. (2005). Apoptosis in UV-C light irradiated p53 wild-type, apaf-1 and p53 knockout mouse embryonic fibroblasts: Interplay of receptor and mitochondrial pathway. *Apoptosis* **10**, 1295-1304.

Trinkle-Mulcahy, L., and Lamond, A. I. (2006). Mitotic phosphatases: no longer silent partners. *Curr Opin Cell Biol* **18**, 623-631.

Umen, J. G., and Guthrie, C. (1995). A novel role for a U5 snRNP protein in 3' splice site selection. *Genes Dev* **9**, 855-868.

Umen, J. G., and Guthrie, C. (1995). Prp16p, Slu7p, and Prp8p interact with the 3' splice site in two distinct stages during the second catalytic step of pre-mRNA splicing. *Rna* **1**, 584-597.

Unger, T., Juven-Gershon, T., Moallem, E., Berger, M., Vogt Sionov, R., Lozano, G., Oren, M., and Haupt, Y. (1999). Critical role for Ser20 of human p53 in the negative regulation of p53 by Mdm2. *Embo J* **18**, 1805-1814.

Utrera, R., Collavin, L., Lazarevic, D., Delia, D., and Schneider, C. (1998). A novel p53-inducible gene coding for a microtubule-localized protein with G2-phase-specific expression. *Embo J* **17**, 5015-5025.

Vagnarelli, P., Hudson, D. F., Ribeiro, S. A., Trinkle-Mulcahy, L., Spence, J. M., Lai, F., Farr, C. J., Lamond, A. I., and Earnshaw, W. C. (2006). Condensin and Repo-Man-PP1 co-operate in the regulation of chromosome architecture during mitosis. *Nat Cell Biol* **8**, 1133-1142.

Van de Craen, M., Declercq, W., Van den brande, I., Fiers, W., and Vandenameele, P. (1999). The proteolytic procaspase activation network: an in vitro analysis. *Cell Death Differ* **6**, 1117-1124.

Van Eynde, A., Nuytten, M., Dewerchin, M., Schoonjans, L., Keppens, S., Beullens, M., Moons, L., Carmeliet, P., Stalmans, W., and Bollen, M. (2004). The nuclear scaffold protein NIPP1 is essential for early embryonic development and cell proliferation. *Mol Cell Biol* **24**, 5863-5874.

Verhagen, A. M., Ekert, P. G., Pakusch, M., Silke, J., Connolly, L. M., Reid, G. E., Moritz, R. L., Simpson, R. J., and Vaux, D. L. (2000). Identification of DIABLO, a mammalian protein that promotes apoptosis by binding to and antagonizing IAP proteins. *Cell* **102**, 43-53.

Vialard, J. E., Gilbert, C. S., Green, C. M., and Lowndes, N. F. (1998). The budding yeast Rad9 checkpoint protein is subjected to Mec1/Tel1-dependent

## References

---

hyperphosphorylation and interacts with Rad53 after DNA damage. *Embo J* 17, 5679-5688.

Wada, M., Hosotani, R., Lee, J. U., Doi, R., Koshiba, T., Fujimoto, K., Miyamoto, Y., Tsuji, S., Nakajima, S., Okuyama, A., and Imamura, M. (1998). An exogenous cdk inhibitor, butyrolactone-I, induces apoptosis with increased Bax/Bcl-2 ratio in p53-mutated pancreatic cancer cells. *Anticancer Res* 18, 2559-2566.

Walter, B. N., Huang, Z., Jakobi, R., Tuazon, P. T., Alnemri, E. S., Litwack, G., and Traugh, J. A. (1998). Cleavage and activation of p21-activated protein kinase gamma-PAK by CPP32 (caspase 3). Effects of autophosphorylation on activity. *J Biol Chem* 273, 28733-28739.

Walworth, N., Davey, S., and Beach, D. (1993). Fission yeast chk1 protein kinase links the rad checkpoint pathway to cdc2. *Nature* 363, 368-371.

Wang, B., Matsuoka, S., Carpenter, P. B., and Elledge, S. J. (2002). 53BP1, a mediator of the DNA damage checkpoint. *Science* 298, 1435-1438.

Wang, H., Zeng, Z. C., Bui, T. A., DiBiase, S. J., Qin, W., Xia, F., Powell, S. N., and Iliakis, G. (2001). Nonhomologous end-joining of ionizing radiation-induced DNA double-stranded breaks in human tumor cells deficient in BRCA1 or BRCA2. *Cancer Res* 61, 270-277.

Wang, J., Wilhelmsson, H., Graff, C., Li, H., Oldfors, A., Rustin, P., Bruning, J. C., Kahn, C. R., Clayton, D. A., Barsh, G. S., *et al.* (1999). Dilated cardiomyopathy and atrioventricular conduction blocks induced by heart-specific inactivation of mitochondrial DNA gene expression. *Nat Genet* 21, 133-137.

Wang, Q., Zambetti, G. P., and Suttle, D. P. (1997). Inhibition of DNA topoisomerase II alpha gene expression by the p53 tumor suppressor. *Mol Cell Biol* 17, 389-397.

Ward, I. M., and Chen, J. (2001). Histone H2AX is phosphorylated in an ATR-dependent manner in response to replicational stress. *J Biol Chem* 276, 47759-47762.

Wei, M. C., Lindsten, T., Mootha, V. K., Weiler, S., Gross, A., Ashiya, M., Thompson, C. B., and Korsmeyer, S. J. (2000). tBID, a membrane-targeted death ligand, oligomerizes BAK to release cytochrome c. *Genes Dev* 14, 2060-2071.

Weighardt, F., Biamonti, G., and Riva, S. (1996). The roles of heterogeneous nuclear ribonucleoproteins (hnRNP) in RNA metabolism. *Bioessays* 18, 747-756.

Williamson, D. J., Banik-Maiti, S., DeGregori, J., and Ruley, H. E. (2000). hnRNP C is required for postimplantation mouse development but is dispensable for cell viability. *Mol Cell Biol* 20, 4094-4105.

- Wilson, S. H. (1998). Mammalian base excision repair and DNA polymerase beta. *Mutat Res* 407, 203-215.
- Winters, Z. E., Ongkeko, W. M., Harris, A. L., and Norbury, C. J. (1998). p53 regulates Cdc2 independently of inhibitory phosphorylation to reinforce radiation-induced G2 arrest in human cells. *Oncogene* 17, 673-684.
- Woo, M., Hakem, R., Soengas, M. S., Duncan, G. S., Shahinian, A., Kagi, D., Hakem, A., McCurrach, M., Khoo, W., Kaufman, S. A., *et al.* (1998). Essential contribution of caspase 3/ CPP32 to apoptosis and its associated nuclear changes. *Genes Dev* 12, 806-819.
- Wood, R. D. (1997). Nucleotide excision repair in mammalian cells. *J Biol Chem* 272, 23465-23468.
- Wu, S., Romfo, C. M., Nilsen, T. W., and Green, M. R. (1999). Functional recognition of the 3' splice site AG by the splicing factor U2AF35. *Nature* 402, 832-835.
- Xiao, Z., Chen, Z., Gunasekera, A. H., Sowin, T. J., Rosenberg, S. H., Fesik, S., and Zhang, H. (2003). Chk1 mediates S and G2 arrests through Cdc25A degradation in response to DNA-damaging agents. *J Biol Chem* 278, 21767-21773.
- Xu, D., Wilson, T. J., Chan, D., De Luca, E., Zhou, J., Hertzog, P. J., and Kola, I. (2002). Ets1 is required for p53 transcriptional activity in UV-induced apoptosis in embryonic stem cells. *Embo J* 21, 4081-4093.
- Yazdi, P. T., Wang, Y., Zhao, S., Patel, N., Lee, E. Y., and Qin, J. (2002). SMC1 is a downstream effector in the ATM/NBS1 branch of the human S-phase checkpoint. *Genes Dev* 16, 571-582.
- Yean, S. L., and Lin, R. J. (1991). U4 small nuclear RNA dissociates from a yeast spliceosome and does not participate in the subsequent splicing reaction. *Mol Cell Biol* 11, 5571-5577.
- Zamore, P. D., Patton, J. G., and Green, M. R. (1992). Cloning and domain structure of the mammalian splicing factor U2AF. *Nature* 355, 609-614.
- Zhan, Q., Antinore, M. J., Wang, X. W., Carrier, F., Smith, M. L., Harris, C. C., and Fornace, A. J., Jr. (1999). Association with Cdc2 and inhibition of Cdc2/Cyclin B1 kinase activity by the p53-regulated protein Gadd45. *Oncogene* 18, 2892-2900.
- Zhan, Q., Fan, S., Bae, I., Guillouf, C., Liebermann, D. A., O'Connor, P. M., and Fornace, A. J., Jr. (1994). Induction of bax by genotoxic stress in human cells correlates with normal p53 status and apoptosis. *Oncogene* 9, 3743-3751.
- Zhan, Q., Kontny, U., Iglesias, M., Alamo, I., Jr., Yu, K., Hollander, M. C., Woodworth, C. D., and Fornace, A. J., Jr. (1999). Inhibitory effect of Bcl-2 on p53-mediated transactivation following genotoxic stress. *Oncogene* 18, 297-

## References

---

304.

Zhang, L., Yu, D., Hu, M., Xiong, S., Lang, A., Ellis, L. M., and Pollock, R. E. (2000). Wild-type p53 suppresses angiogenesis in human leiomyosarcoma and synovial sarcoma by transcriptional suppression of vascular endothelial growth factor expression. *Cancer Res* 60, 3655-3661.

Zhang, N., Kaur, R., Lu, X., Shen, X., Li, L., and Legerski, R. J. (2005). The Pso4 mRNA splicing and DNA repair complex interacts with WRN for processing of DNA interstrand cross-links. *J Biol Chem* 280, 40559-40567.

Zhang, Y., and Xiong, Y. (2001). A p53 amino-terminal nuclear export signal inhibited by DNA damage-induced phosphorylation. *Science* 292, 1910-1915.

Zhao, H., and Piwnica-Worms, H. (2001). ATR-mediated checkpoint pathways regulate phosphorylation and activation of human Chk1. *Mol Cell Biol* 21, 4129-4139.

Zhao, H., Watkins, J. L., and Piwnica-Worms, H. (2002). Disruption of the checkpoint kinase 1/cell division cycle 25A pathway abrogates ionizing radiation-induced S and G2 checkpoints. *Proc Natl Acad Sci U S A* 99, 14795-14800.

Zhou, B. B., and Elledge, S. J. (2000). The DNA damage response: putting checkpoints in perspective. *Nature* 408, 433-439.

Zhou, C., Yang, Y., and Jong, A. Y. (1990). Mini-prep in ten minutes. *Biotechniques* 8, 172-173.

Zhou, Z., Licklider, L. J., Gygi, S. P., and Reed, R. (2002). Comprehensive proteomic analysis of the human spliceosome. *Nature* 419, 182-185.

Zhu, J., and Chen, X. (2000). MCG10, a novel p53 target gene that encodes a KH domain RNA-binding protein, is capable of inducing apoptosis and cell cycle arrest in G(2)-M. *Mol Cell Biol* 20, 5602-5618.

Zhu, Y., Romero, M. I., Ghosh, P., Ye, Z., Charnay, P., Rushing, E. J., Marth, J. D., and Parada, L. F. (2001). Ablation of NF1 function in neurons induces abnormal development of cerebral cortex and reactive gliosis in the brain. *Genes Dev* 15, 859-876.

Zorio, D. A., and Blumenthal, T. (1999). Both subunits of U2AF recognize the 3' splice site in *Caenorhabditis elegans*. *Nature* 402, 835-838.

Zuscik, M. J., Sands, S., Ross, S. A., Waugh, D. J., Gaivin, R. J., Morilak, D., and Perez, D. M. (2000). Overexpression of the alpha1B-adrenergic receptor causes apoptotic neurodegeneration: multiple system atrophy. *Nat Med* 6, 1388-1394.

## 9 Acknowledgements

My sincere thanks to Prof. Dr. Jens Brüning for giving me the opportunity to join his research group, for supporting and giving me advice in all ways.

I want to thank Prof. Dr. Thomas Langer, Prof. Dr. Siegfried Roth and Dr. Ursula Lichtenberg for agreeing to form my thesis committee.

I want to thank my family and Tina Baumeister for their love and support.

I wish to express my gratefulness to Sigrid Irlenbusch for being a perfect technician and friend. I thank the lab 3.45 and Gabi for being a fruitful place to work in.

I would like to express my sincere gratitude to all the members of the Brüning lab for creating a friendly and productive environment.

In particular I thank, Béatrice Bailly-Maitre, Stephanie Baudler, Nadine Hövelmeyer, Linda Koch, and Thomas Wunderlich for critical proofreading the manuscript.

Furthermore I thank Christoph Göttliger, Sonja Becker, Brigitte Hampel and Julia Baumgartl for technical assistance.

I thank Carsten Merkwirth and Dr. Paul Ajuh for supply of HTN-Cre protein and PLRG-1 antibody.

I thank Miriam Große Hovest and Tobias Heinen for technical advice in  $\gamma$ -H2AX staining and pulse-field gel electrophoresis.

## **10 Versicherung**

Ich versichere, dass ich die von mir vorgelegte Dissertation selbständig angefertigt, die benutzten Quellen und Hilfsmittel vollständig angegeben und die Stellen der Arbeit – einschließlich der Tabellen, Karten und Abbildungen –, die anderen Werken im Wortlaut oder dem Sinn nach entnommen sind, in jedem Einzelfall als Entlehnung kenntlich gemacht habe; dass diese Dissertation noch keiner anderen Fakultät oder Universität zur Prüfung vorgelegen hat; dass sie – abgesehen von unten angegebenen Teilpublikationen – noch nicht veröffentlicht worden ist sowie, dass ich eine solche Veröffentlichung vor Abschluss des Promotionsverfahrens nicht vornehmen werde. Die Bestimmungen dieser Promotionsordnung sind mir bekannt. Die von mir vorgelegte Dissertation ist von Prof. Dr. Jens C. Brüning betreut worden.

Köln, im Mai 2007

André Kleinridders

### **Teilpublikationen**

Kleinridders, A., Pogoda, H. M., Irlenbusch S., Smyth N., Koncz C., Hammerschmidt M. and Brüning, J. C. (2007) Inactivation of Pleiotropic Regulator 1 reveals p53-dependent Control of Cell Proliferation and Apoptosis by the Pso4-complex. (submitted)

---

## 11 Lebenslauf

### Persönliche Angaben:

Name: André Kleinridders  
Adresse: Moerser Str. 144  
47803 Krefeld  
Telefon: 02151 20 63 30  
Email: [andrekleinridders@web.de](mailto:andrekleinridders@web.de)  
Geburtsdatum: 14. Juni 1978  
Geburtsort: Krefeld – Hüls  
Familienstand: Ledig  
Nationalität: Deutsch

### Schulische Ausbildung:

1984 – 1988 Grundschule Kempener Allee, Krefeld  
1988 – 1997 Gymnasium Horkesgath, Krefeld mit  
dem Abschluss der Allgemeinen  
Hochschulreife

### Wehrdienst:

1997 – 1998 Wehrdienst bei der Luftwaffe der  
Bundeswehr

### Akademische Ausbildung:

1998 – 2003 Studium der Biologie an der  
Mathematisch –  
Naturwissenschaftlichen Fakultät der  
Universität zu Köln

2002

Diplomprüfungen

Hauptfach: Genetik

Nebenfächer: Biochemie &

Pharmakologie

2002 – 2003

Diplomarbeit am Institut für Genetik  
der Universität zu Köln zum Thema:  
„Inaktivierung des Maus PLRG-1-  
Gens“

**Promotion:**

Seit 07/2003

Dissertation am Institut für Genetik der  
Universität zu Köln zum Thema:  
„Inactivation of Pleiotropic Regulator 1  
reveals p53-dependent Control of Cell  
Proliferation and Apoptosis by the  
Pso4-complex

**Publikationen:**

Seibler, J., Kleinridders, A., Kuter-Luks, B., Niehaves, S., Bruning, J. C., and Schwenk, F. (2007). Reversible gene knockdown in mice using a tight, inducible shRNA expression system. *Nucleic Acids Res.* 35, No.7 e54